UMTRI-84-18

RELATIONSHIP OF TRUCK TIRE/WHEEL NONUNIFORMITIES TO CYCLIC FORCE GENERATION

Final Report

MVMA Project #1162

T.D. Gillespie

April 1984

Technical Report Documentation Page

1. Report No.	2. Government Accession No.	3. Recipient's Catalog No.
UMTRI-84-18		

4. Title and Subtitle	5. Report Date
RELATIONSHIP OF TRUCK TIRE/WHEEL NONUNIFORMITIES TO CYCLIC FORCE GENERATION	April 1984
	6. Performing Organization Code: 361858
7. Author(s): T. D. Gillespie	8. Performing Organization Report No.: UMTRI-84-18
9. Performing Organization Name and Address: The University of Michigan, Transportation Research Institute, 2901 Baxter Road, Ann Arbor, Michigan 48109	10. Work Unit No.
	11. Contract or Grant No.: MVMA #1162
12. Sponsoring Agency Name and Address: Motor Vehicle Manufacturers Association, 300 New Center Building, Detroit, Michigan 48202	13. Type of Report and Period Covered: Final, 4/79 - 12/82
	14. Sponsoring Agency Code

15. Supplementary Notes

16. Abstract

Nonuniformities in the tire/wheel assemblies of heavy trucks, such as mass imbalance or dimensional runout, add to the ride vibrations on the road at the rotational frequency of the wheel and harmonics thereof. The relationships between nonuniformities in the individual components and the excitation forces produced by the overall assembly are largely unknown.

An experimental research program was conducted in which nonuniformities in tire and wheel components and the force variations of the overall assembly were measured on a tire uniformity test machine. The testing covered radial and bias-ply truck tires of the tubeless- and tube-type, disc and cast-spoke wheels, single and dual configurations, and variations in load, pressure, and speed.

For tires, the various measures of nonuniformities are related to force variations in the radial, lateral, and tractive force directions. Runouts in the wheel/hub assembly are shown to influence radial force variations directly. Mounting practice is shown to have a significant influence on radial force variations of dual cast-spoke wheels.

17. Key Words	18. Distribution Statement
truck ride, tire and wheel nonuniformities, imbalance, runout tire modeling	UNLIMITED

19. Security Classif. (of this report)	20. Security Classif. (of this page)	21. No. of Pages	22. Price
NONE	NONE		

TABLE OF CONTENTS

ACKNOWLEDGEMENTS

The author wishes to acknowledge the contributions of the following organizations and persons in the work reported herein:

The Motor Vehicle Manufacturers Association and its member companies for funding the research.

The Rubber Manufacturers Association and its member companies for providing a tire nonuniformity test machine and samples of tire and wheel components.

Mr. Michael Sayers of UMTRI for his help in developing computer programs and procedures for the experimental testing. Mr. Sayers was also responsible for conduct of the flat-bed testing and authored the report on that work in Appendix C.

EXECUTIVE SUMMARY

"RELATIONSHIP OF TRUCK TIRE/WHEEL NONUNIFORMITIES TO CYCLIC FORCE GENERATION" by T.D. Gillespie

Report No. UMTRI-84-18

The nonuniformities in truck tire and wheel components (runouts, imbalances and stiffness variations) contribute to ride vibrations on the road. Yet the excitation forces arising from nonuniformities in the individual components are not well known.

An experimental research program was conducted on a tire uniformity test machine to determine relationships between nonuniformities and excitation forces for the radial, lateral and tractive force directions. The tests covered radial and bias-ply truck tires of the tubeless- and tube-type, disc and cast spoke wheels, single and dual configurations, and variations in load, pressure, and speed. Though dynamic problems in the test machine limited its validity, tentative conclusions were reached in the research.

Radial force variations (RFV) are the largest, and are not strongly influenced by speed. Loaded radial runout is closely related to RFV for both tires and tire/wheel assemblies. Bead seat radial runout of a wheel assembly is responsible for contributing to first harmonic RFV. Free radial runouts (on the tire centerline, shoulders or a combination thereof) are lower quality indicators of RFV, and even then only apply to the first harmonic. Lateral runout in the tire or wheel does not contribute to RFV; however, poor mounting practice with dual (but not single) cast spoke wheels contributes significantly to RFV. Imbalance in a tire or wheel assembly will contribute to RFV.

Lateral force variations (LFV) are unrelated to lateral runout in either the tires or the wheel assemblies. The LFV does not show strong speed sensitivity, therefore low-speed measurements are closely related to high-speed performance. Poor mounting practice does not contribute to LFV with any type of wheel.

Tractive force variations (TFV) vary dramatically with speed and high-speed magnitudes are not predictable from low-speed measurements. Poor mounting practice with dual (but not single) cast spoke wheels can contribute significantly to TFV. Imbalance in a tire or wheel assembly also contributes to the TFV.

CHAPTER 1

INTRODUCTION

1.1 Background

Heavy trucks and tractor-trailers used for transporting goods must be designed for efficiency and durability. Meeting these goals constrains designers in their efforts to provide a good ride environment for the truck driver [1].* As a consequence, the U.S. truck and truck component manufacturers are constantly seeking means to improve truck ride quality consistent with the truck's mission. Vehicle vibrations, the primary ingredient in ride quality, are caused by the combination of road roughness and vibration sources on-board the vehicle. Of the on-board sources, nonuniformities (mass imbalances, runouts, etc.) in the rotating tire/wheel assemblies are an important source, causing excitation to the vehicle at their rotational frequencies and multiples thereof (harmonics). Especially on smooth roads, the tire/wheel excitations may become more noticeable and perceptible as a cause of ride degradation.

In 1979, the Motor Vehicle Manufacturers Association (MVMA) in cooperation with the Rubber Manufacturers Association (RMA) initiated a research program at the University of Michigan Transportation Research Institute (formerly the Highway Safety Research Institute) to investigate the truck ride effects resulting from tire and wheel nonuniformities. The research program, entitled "Truck Tire/Wheel Systems Research Program," was organized into two concurrent phases.

-Phase I was an experimental investigation of the cyclic force variations produced by truck tire/wheel assemblies on the axle of a tire uniformity test machine to relate them to specific nonuniformities in each of the rotating components. This information is intended to provide direction for manufacturers to make coordinated improvements in the individual components to reduce the force variations of the rolling wheel, that affect vehicle ride.

---

*Numbers in brackets indicate References in Chapter 6.

-Phase II looked at how force variations on the wheels of a heavy truck cause degradations in the ride in order to identify which force variations and harmonics are most critical.

This report documents the findings and results obtained in the Phase I work. The Phase II work is reported in a separate document [2].

1.2 Problem Statement

The wheel assembly on a heavy truck may consist of upwards of 30 individual components—tires, tubes, wheels, hubs, drums, spacers, nuts, studs, etc. Each of these components incorporates irregularities in its manufacture which may potentially contribute to nonuniformities in the total assembly. Mal-assembly and/or nonuniformities of new or worn components in the tire/wheel assembly may, in turn, cause cyclic force variations as the wheel rolls, exciting truck ride vibrations. Ride excitation due to tire/wheel nonuniformities may be perceptible to the driver, especially on smooth roads.

The term "nonuniformity" as used here implies those irregularities in a component that can be observed by the manufacturer, as for example, imbalance of tires or runout of a wheel. The extent to which a given nonuniformity contributes to ride vibration on a truck, however, is several steps removed. On the one hand, it may be only one of many components contributing that type of nonuniformity in the wheel assembly. On the other hand, the extent to which one component contributes excitation may depend on the other components with which it is mated in the overall wheel assembly. Because of the complexity of the interactions, research is needed to identify and measure the nonuniformities in the rotating wheel components and relate these to the excitation forces produced by the tire/wheel assembly. Only when the mechanisms and relationships are understood, is it possible to judge the significance of a given component nonuniformity and determine means for coordinated improvements in all components.

1.3 Approach and Method

In approaching the project in a systematic fashion, certain specific tasks are in order. Those tasks are as follows:

•Literature Review - Some understandings relevant to this problem are available in the literature. Empirical information is available to characterize some of the types and magnitudes of tire/wheel nonuniformities affecting vehicle ride. The literature is also fairly rich in publications on the topic of vehicle ride. All these constitute appropriate background for this research, but have not been collected and assessed. Thus, a literature review was included, with the special provision for its publication as a document of interest to the industry [3].

•Identifying Components - Truck wheels consist of numerous rotating components, used in various combinations. As a preliminary step in the research, a formalized identification of all the components that are used on truck wheels was called for as a basis for defining the scope of the experimental program.

•Experimental Measurements - The primary question to be answered in the research program is what relationship exists between nonuniformities in individual components and the force variations produced by the overall tire/wheel assembly. The answers must be based on experimental evidence. Thus experimental measurements of nonuniformities and force variations on typical hardware are needed as a basis for developing the quantitative relationships of interest.

Experimental measurements of the above nature are most commonly obtained on tire uniformity test machines. Such machines consist of a rigid drum against which a tire is loaded and rolled. While the tire is held in a fixed position, the force and/or moment variations produced as the wheel is rolled are measured. A standard method for measuring uniformity is defined by the SAE [4]. In this research project, the interest lies in measurement of all forces that may contribute significant excitation to a truck. Exactly which forces or moments these may be are not known. However, it can be hypothesized that the relevant force directions are:

-Radial force direction (vertical with respect to the wheel)

-Lateral force direction (sideways with respect to the wheel)

-Tractive force direction (in the direction of travel)

-Aligning moment direction (about the vertical axis of the wheel)

Further, within the original scope of the project, each of these variations are of interest over a range of harmonics at least to 50 Hz in frequency.

Test equipment of the capabilities listed above, especially with capacity to handle truck tires and wheels, in single and dual configurations, is not commercially available. Therefore, arrangements were made for design and construction of a suitable test machine. Responsibility for obtaining this equipment was assumed by the RMA and arranged through MTS Systems Corporation of Minneapolis, Minnesota. The machine was obtained under a lease arrangement and installed in the UMTRI laboratory for the experimental test program. By special arrangement, the machine was constructed so as to accept truck spindle adapters as the mounting point for the wheel hardware. The Institute prepared adapters for the Rockwell FF-931 front spindle and the Rockwell R-170 rear axle. The front spindle is a popular design for single wheels, while the rear axle accepts dual wheel arrangements.

Hardware for testing was provided by many member companies of the MVMA and RMA. The tires (see Appendix D for listing) were provided by:

-Armstrong Rubber Company

-B. F. Goodrich Company

-Firestone Tire and Rubber Company

-General Tire and Rubber Company

-Goodyear Tire and Rubber Company

-Uniroyal Tire Company

A large sample of truck tires was screened by these companies for radial force variations (composite and first harmonic), lateral force variations (composite), and free radial runout on the centerline (composite). An RMA committee then selected a total of 140 tires which were shipped to UMTRI for use in testing. The samples were divided among bias and radial, tubeless and tube-type (sizes 10.00 x 20 and 11.00 x 22.5); and were selected by the RMA committee to provide samples that had high and low values of individual nonuniformities, as well as, combinations of non-uniformities. The 40 tires that were actually tested were selected on a

similar criteria, but also to provide even representation from the manufacturers. Because these tires were especially selected to cover the extremes of nonuniformities, the data presented in this report should not be considered representative of the general population of truck tires produced.

Wheel hardware was obtained from Motor Wheel Corporation, Firestone Steel Products Company and Dayton-Walther allowing a variety of combinations to be tested. The hardware included:

-Single and dual configurations
-Disc and cast spoke wheels
-Single, two, and three piece wheels and rims
-Bead seat angles of 5 and 15 degrees
-Precision wheels
-Aluminum and steel wheels
-Aluminum and steel hubs

With the exception of the precision wheels, all other wheel hardware was standard production components. Although UMTRI requested samples with high and low radial and lateral runouts in the wheels provided, no information was supplied with them to indicate that they had been selected on this basis.

The majority of tires were tested at two loads and two pressure conditions, and a minimum of three speeds. In addition, many of the tires were tested at multiple positions on the wheels so that the separate influences of the tires and wheels could be extracted. Wheels were tested separately to determine how their runout properties related to the wheel or hub components, and the way in which they mated together (mounting variations). In total, more than 5,000 individual tests were performed.

1.4 Report Organization

This report presents the results and findings of the research program outlined above. Chapter 2 documents the test methods used by describing the test machine, the procedure by which tests were performed, and how the data was treated. The relationships observed between nonuniformities and force variations in tires are presented in Chapter 3; while that for the wheels and other components are presented in Chapter 4. The conclusions from this work are presented in Chapter 5.

CHAPTER 2

TEST METHODOLOGY

2.1 The Uniformity Test Machine

At the outset of the project, the RMA assumed responsibility for providing a tire uniformity machine suitable for the planned research program. The RMA selected MTS Systems Corporation of Minneapolis to build the machine based on a reconfiguration of their Model 860 test machine. The Model 860 is a 67-inch drum machine that has been used in the trucking industry for tire and wheel component testing. The capabilities of the machine were defined in hardware specifications published by MTS [5], and by a set of Performance Specifications developed by UMTRI [6].

The machine that was built and used in the research is shown in the photograph of Figure 1. The major features are as follows:

1) The machine consists of a 67.23-inch drum, 30 inches wide to accommodate truck dual wheel assemblies. The drum is driven by a 40-horsepower motor through a tooth-belt, with the speed controlled over the range of 0-60 mph by a closed-loop control system.

2) The tire/wheel/hub/spindle assembly mates to the machine on a four-axis load transducer system. The transducer is mounted on a movable carriage to bring the assembly to load on the drum. The carriage is moved by a hydraulic servo system, allowing control of either the load or rolling radius. The transducer is instrumented for measurement of:

   -Tractive force, F_x

   -Lateral force, F_y

   -Radial force, F_z

   -Aligning moment, M_z

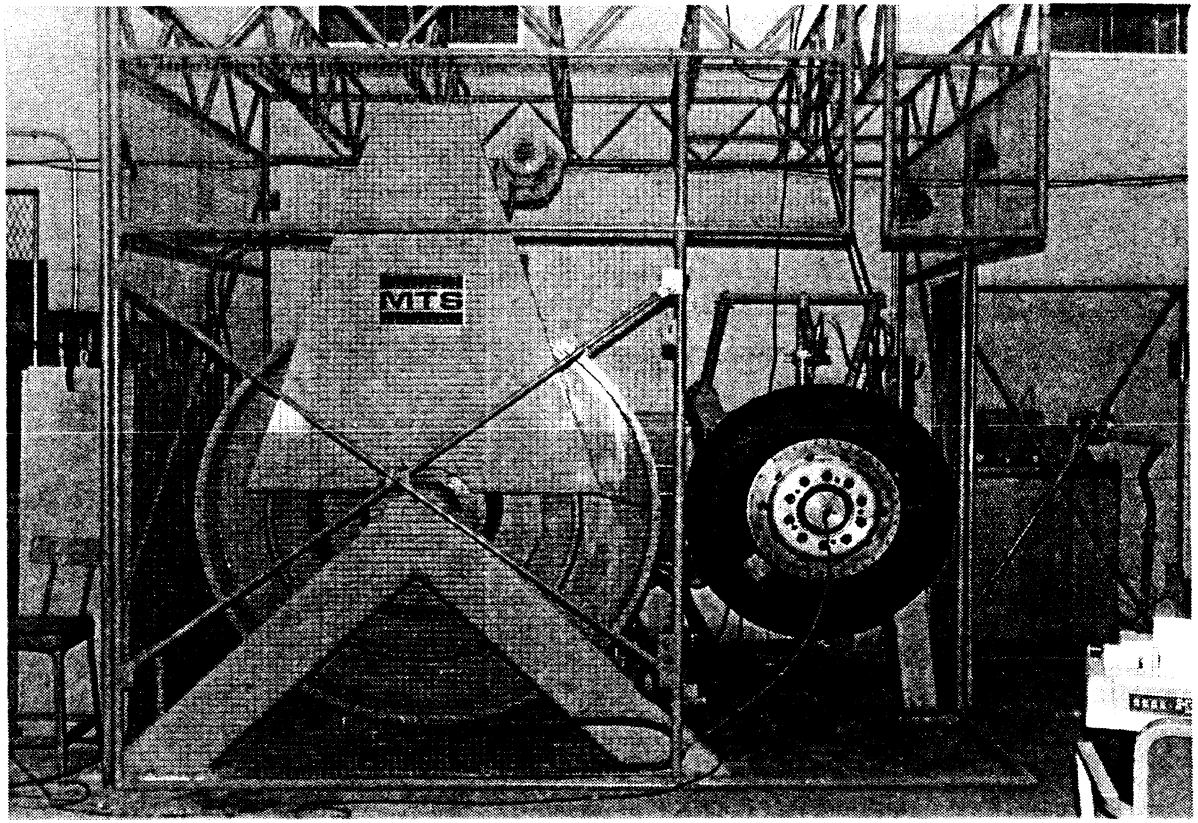

Test Machine

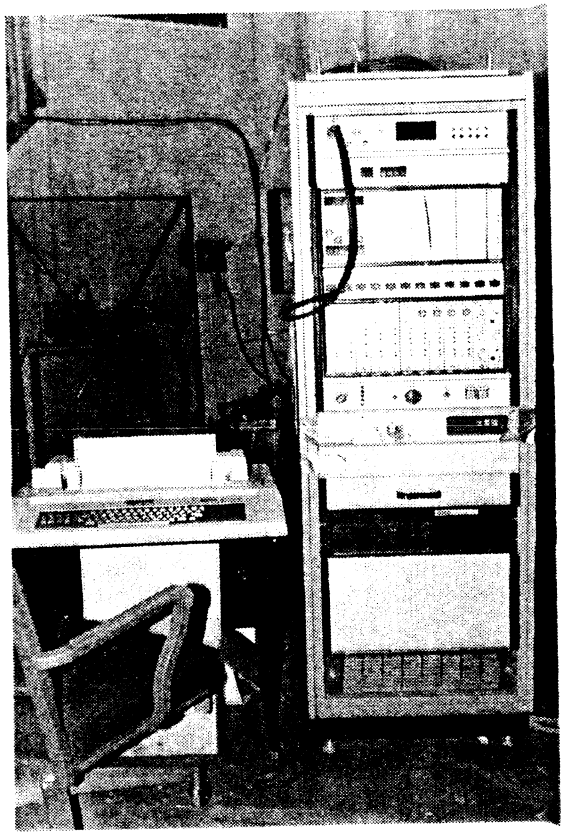

Control Console

Figure 1. Photograph of the MTS Tire Uniformity Test Machine

3) Linear Variable Displacement Transformers (LVDTs) are provided with the necessary fixtures to allow measurement of the radial and lateral runout properties of tires and wheels. A photograph of the system is shown as set up for measurement of radial runouts on a tire in Figure 2.

4) A Control Console (visible in Figure 1) provides a station from which the machine operation can be controlled.

5) A computer-based instrumentation system is incorporated within the Control Console for data acquisition and processing. The instrumentation consists of signal conditioning amplifiers for the LVDT and transducer force signals, high- and low-pass filters to remove noise and DC levels from signals where required, analog-to-digital converters (ADC), and a PDP 11/03 digital computer with 8-inch floppy disk storage mediums and a Decwriter LA36 terminal.

6) An optical wheel position sensing system is provided for detecting the exact rotational position of the tire/wheel assembly during operation. The system has two detector channels. One channel picks up a once-per-revolution reference mark (usually placed on the tire) to which the phase angles of the harmonics are referenced. The second picks up 32 marks per revolution, used to trigger the data sampling.

7) Miscellaneous support items such as a hydraulic power supply, a drive motor control system, and hardware for calibration of the transducer system are provided.

The tire test machine is designed for measurement of force and dimensional nonuniformities and transformation into harmonic values. That is, the raw force variation (or runout) signals are measured then converted to the frequency domain by the operation of a Fast Fourier Transform (FFT). The FFT is a mathematical algorithm that determines the amplitude and

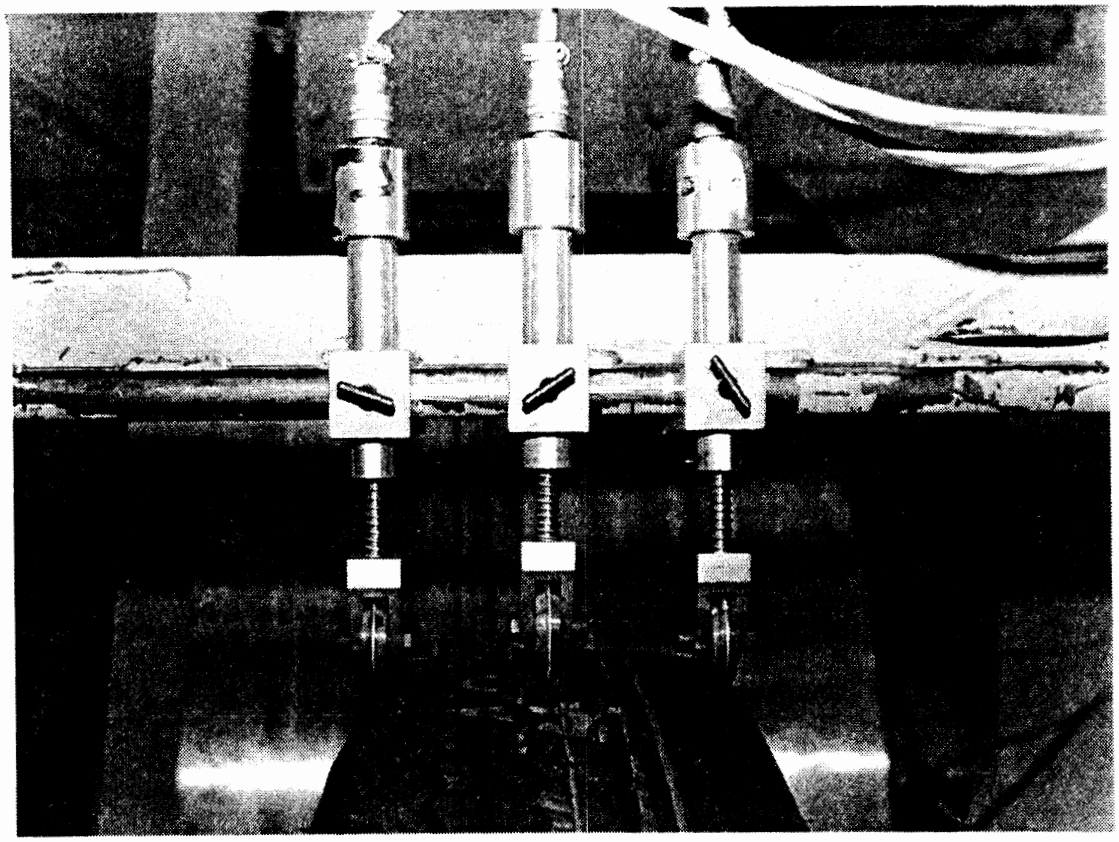

Figure 2. Photograph of the LVDT System for Measuring Tire/Wheel Assembly Runouts (in Tire Radial Runout Mode).

phase angles for a series of sine waves, which when summed together, are equivalent to the original signal. The first sine wave has a spacial frequency equal to the circumference of the tire and in this report is referred to as the "First" harmonic. The second sine wave has a frequency that is twice the first, and is hence the "Second" harmonic. The third is at three times the frequency, and so on.

2.2 Calibration and Validation of the Test Machine

When the test machine was received and installed at UMTRI, an extensive series of tests was performed to familiarize the staff with its proper use and validate the data acquired. In the process, a number of changes in the machine were necessary to make it operational for the desired research. The major pitfalls and findings discovered in that work are reported here for the benefit of those who attempt to develop or use similar equipment in the future.

2.2.1 Data Acquisition - The force and moment signals produced by the test machine are passed through an analog-to-digital converter (ADC) to the computer processing system where the FFT is performed. High-pass filters are used to remove the DC component of the signal before going to the ADC so that the converter can be used more effectively over its full dynamic range (i.e., so that maximum resolution is obtained in the conversion process). Though these filters were set to a very low roll-off frequency, they will cause significant data errors (especially in the phase angles) unless compensated. Thus it was necessary to measure the amplitude and phase response properties of the filters and develop compensation methods to correct for their influence in the digital data.

The analog signals from the force transducer are sampled 32 times with each revolution of the wheel. At very low speed (1 mph), this is equivalent to less than 5 samples/second; whereas, at 60 mph it is 280 samples/second. To validly sample analog data for frequency analysis, it is critical that the signal not contain information (or noise) at any frequency above one-half the sampling frequency. If it does, the higher frequency information appears to be at low frequency in the digital data

(a process called "aliasing"), and the digitized data is not valid. In its completed form, the machine was found to have significant transducer signal content at high frequency due to dynamic vibrations of both the machine and the tire assembly. Thus it was necessary to retrofit the machine with a system of selectable filters so that the high-frequency information (above one-half the sampling rate) could be eliminated. For these filters, it was again necessary to determine the amplitude and phase response of each of these filters, and develop algorithms whereby the processed data would be corrected for the amplitude and phase distortion introduced by the filters.

2.2.2 Transducer Compliance - The test machine (see Fig. 1) was designed with the test wheel cantilevered off of the force and moment transducer. While this is an arrangement that is very convenient for tire and wheel changes, etc., the cantilever design was discovered to be substantially more compliant than expected. As a result, three types of errors were encountered [7]:

-Static Force Attenuation - The nonuniformity forces within a tire/wheel assembly are only observed at their true magnitude on a spindle that is perfectly rigid. If the spindle is able to move freely under load, no force variation will occur (rather, the rolling radius will change as necessary to maintain the load). The observed amplitude of a force variation thus depends on the ratio of the transducer stiffness to the total for the transducer and the tire/wheel assembly. In order to obtain accurate measurements (i.e., errors < 1 percent), the transducer should be at least 100 times stiffer than the tire/wheel assembly. On the test machine, however, it is only 10 to 20 times stiffer (depending on whether single or dual wheels are mounted); hence, even the low-frequency measurements of force variation will be 5 percent to 10 percent less than the correct value.

-Dynamic Resonance Effects - When the tire/wheel assembly is mounted on a compliant transducer, it becomes a dynamic system that will resonate in different directions. Resonance in the radial (F_z) direction occurred at a frequency between 30 and 40 Hz, and in the tractive force direction (F_x)

at a frequency between 20 and 30 Hz. (Note: The exact frequency varies with the wheel mass, tire inflation pressure, load, carriage position, and other variables.) An excitation force at a frequency anywhere near the resonant frequency is artificially amplified by the increased gain on the skirts of the resonant peak. Thus the apparent amplitude of the force variation is dependent on its frequency. Figure 3 illustrates this phenomenon. The upper plot shows the machine response in the radial (F_z) direction in terms of the force measured by the transducer per unit of force input. Their ratio, the "gain," changes with frequency, reaching peak values at the machine resonant points. The lower plot shows the way in which the radial force variations in a tire as measured by the machine change with speed (frequency). From a comparison of the two plots, it is obvious that, if uncorrected, the radial force variations in a tire will erroneously appear to change with speed due to dynamics in the machine. The process of compensating for these errors is too complex to be routinely applied; therefore, only the measurements up to 20 Hz are considered to be reasonably accurate, and the results presented in this report are truncated at that limit.

-Mechanical Cross-Coupling - The compliance of the transducer is not very symmetric about the wheel. The deflections arising from force variations along one axis will cause bending on other axes (mechanically cross over onto other axes). Deflections on the other axes then generate forces on those axes. The most important of these is the radial/lateral cross-coupling; i.e., radial deflections are accompanied by rotation in the overturning moment direction producing a lateral deflection at the tire contact patch. The lateral deflection causes the tire to generate a lateral force that is picked up by the force transducer. Thus the radial force variation is mechanically cross-coupled to the lateral axis. The mechanism is quantified in the plot shown in Figure 4, which shows the output on all transducer force channels when only a radial force, F_z, is applied. Ideally, only an F_z force would be observed in this test, but because the tire was installed and loaded against the drum while an external F_z force was applied, the cross-coupling phenomenon occurred. Methods for analyzing the transducer output to determine which force variation(s) is

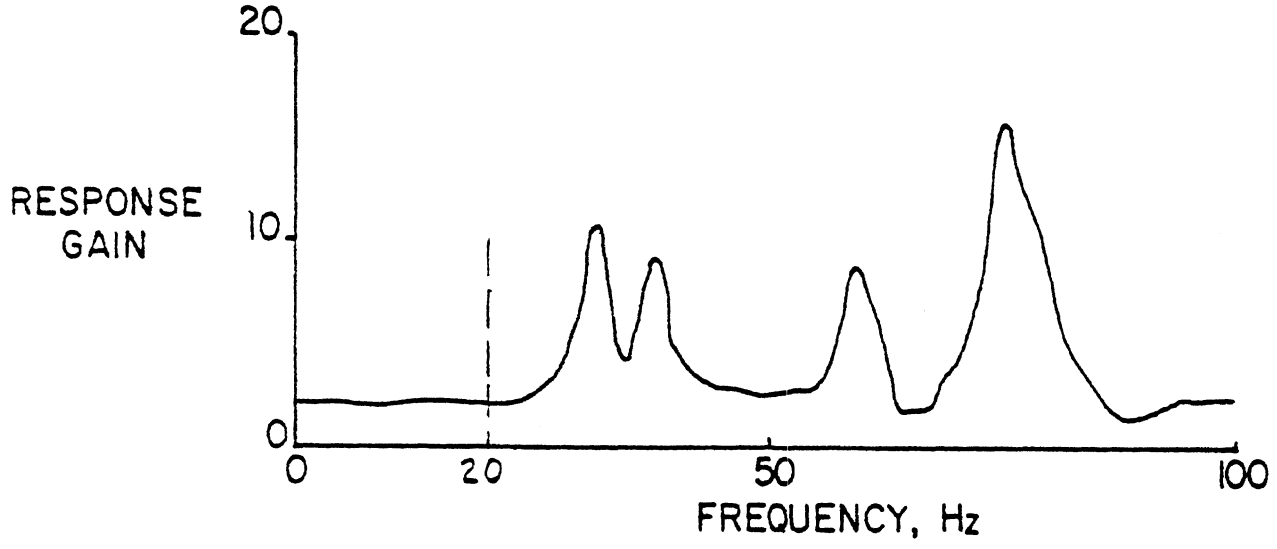

Plot of Radial Response Function Gain

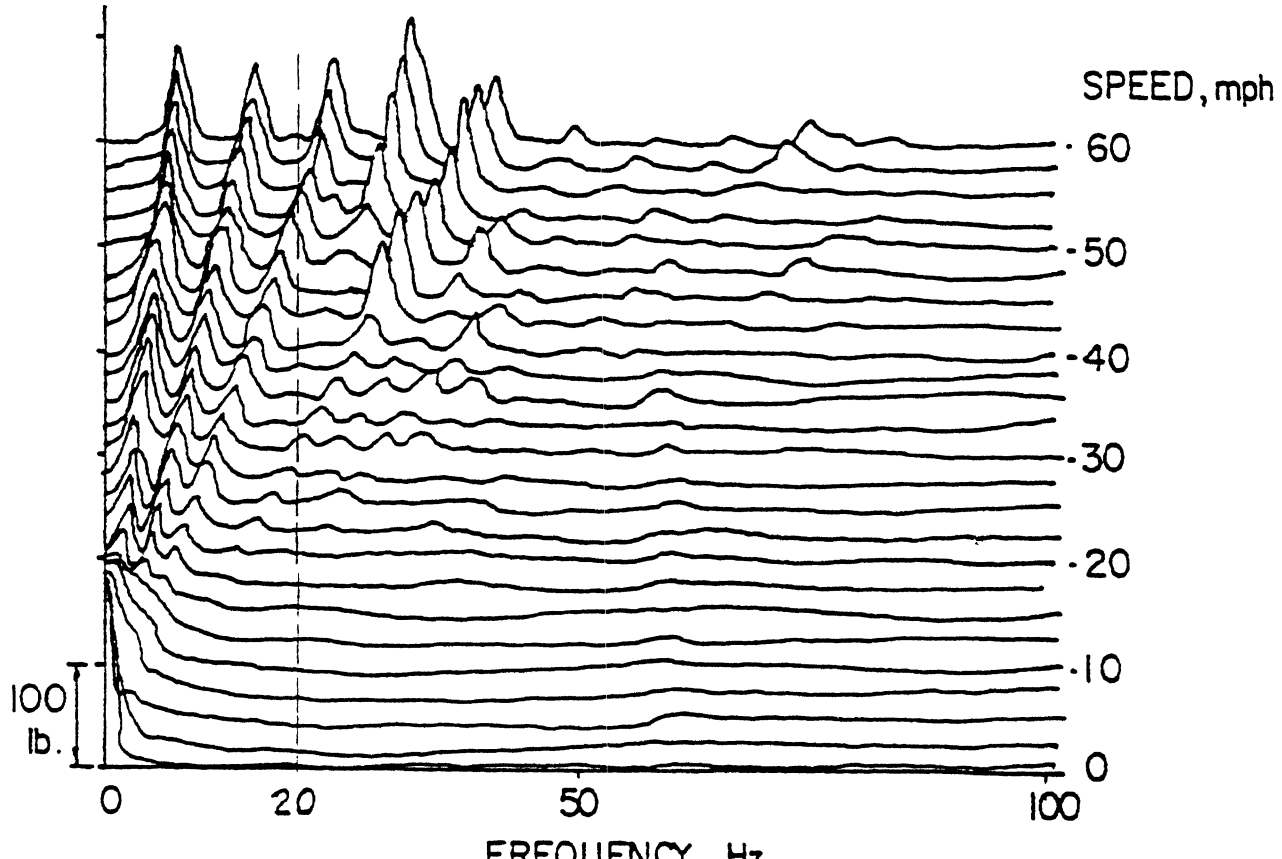

Spectral Map of Radial Force

Figure 3. Resonance Effects on Measurement Gain and Its Influence on Apparent Amplitudes of Tire Radial Harmonics.

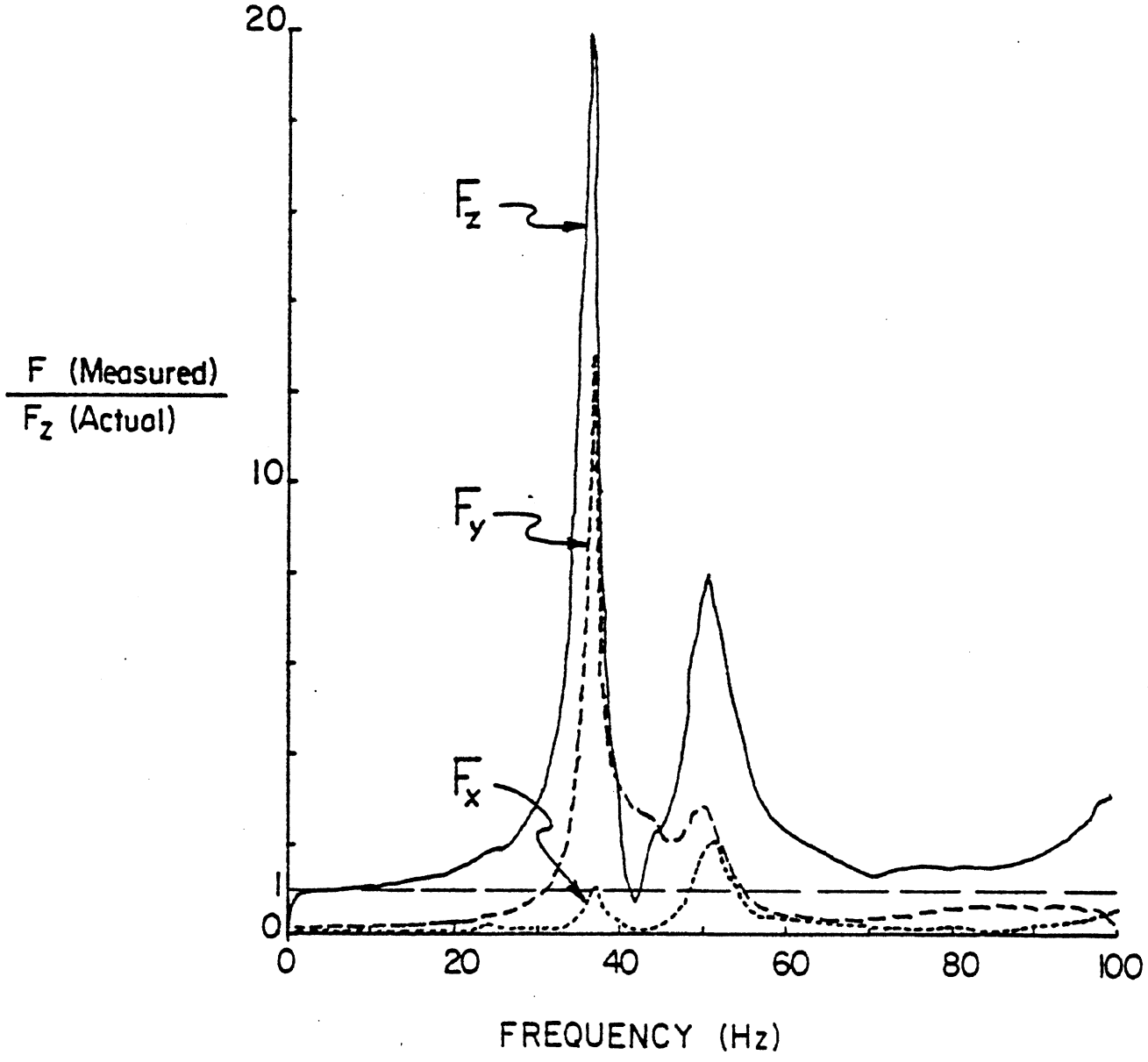

Figure 4. Mechanical Cross-Coupling of Radial Force Excitation into Other Force Directions (with Tire Loaded Against the Drum).

the source of which output(s) is a very complicated process. Though methods for correction were examined in the research, the process was found to be too complicated to be a practical step in the data reduction process.

Each of the technical problems describe above limits the accuracy of the machine measurements in one way or another. Each is a direct consequence of compliance in the machine, most of this deriving from the force and moment transducer. At least theoretically, there are engineering methods by which to measure and correct for each effect. In efforts to apply these methods, however, it was observed that the machine response in each case was critically dependent on a large number of variables. Dynamically, the amplitude and damping of each of the resonant frequencies were dependent on the configuration (single or dual wheels), load, inflation pressure, load carriage position, and even speed. Thus, a separate dynamic characterization would be required at each test condition, increasing the test effort by orders of magnitude. In lieu of data correction, the machine dynamic response has simply been measured at typical conditions to show the nature of the errors arising from these sources. Figure 5 shows the transfer function characteristics for a single-wheel configuration. The measurements in this report are not corrected for these effects, and should be treated accordingly by the reader.

The nominal magnitude of the errors in the measurements are summarized in Table 1. The values shown here are estimates for single-tire configurations, inasmuch as the majority of tests are on single wheels, and would be slightly greater for dual-wheel configurations. The first column represents the static gain errors associated with the static force attenuation mechanism described earlier. Mechanical cross-coupling errors are dependent on the relative magnitudes of force variations in the other directions and the degree to which they cross-couple. The transfer functions in Figure 5 give an indication of the extent to which forces cross-couple. The estimated errors listed in Table 1 are derived from the product of those transfer functions and the nominal level of force variations present on the other axes. Cross-coupling to the F_z axis arises primarily from the lateral and tractive axes. These forces, however, are not so large that

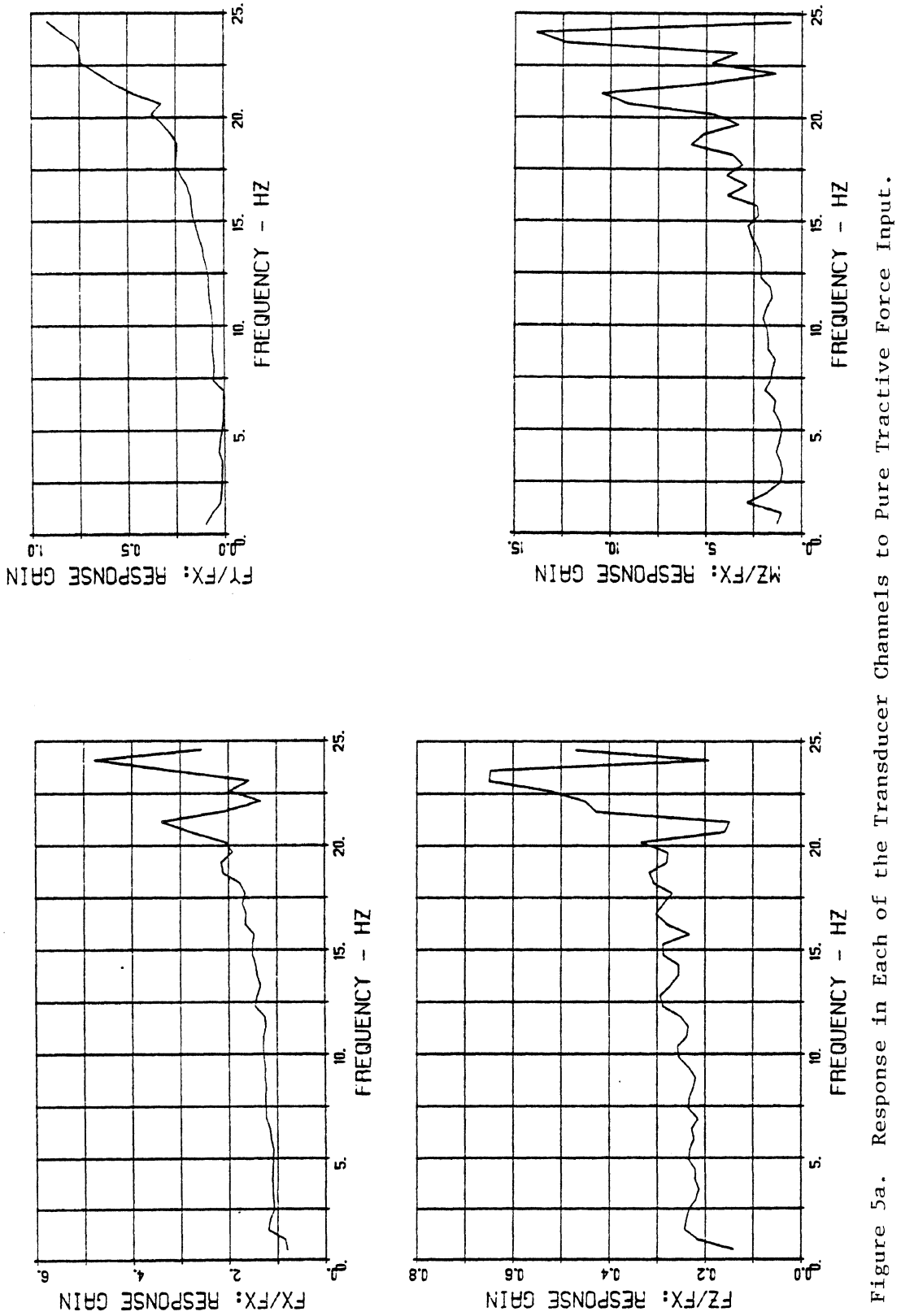

Figure 5a. Response in Each of the Transducer Channels to Pure Tractive Force Input.

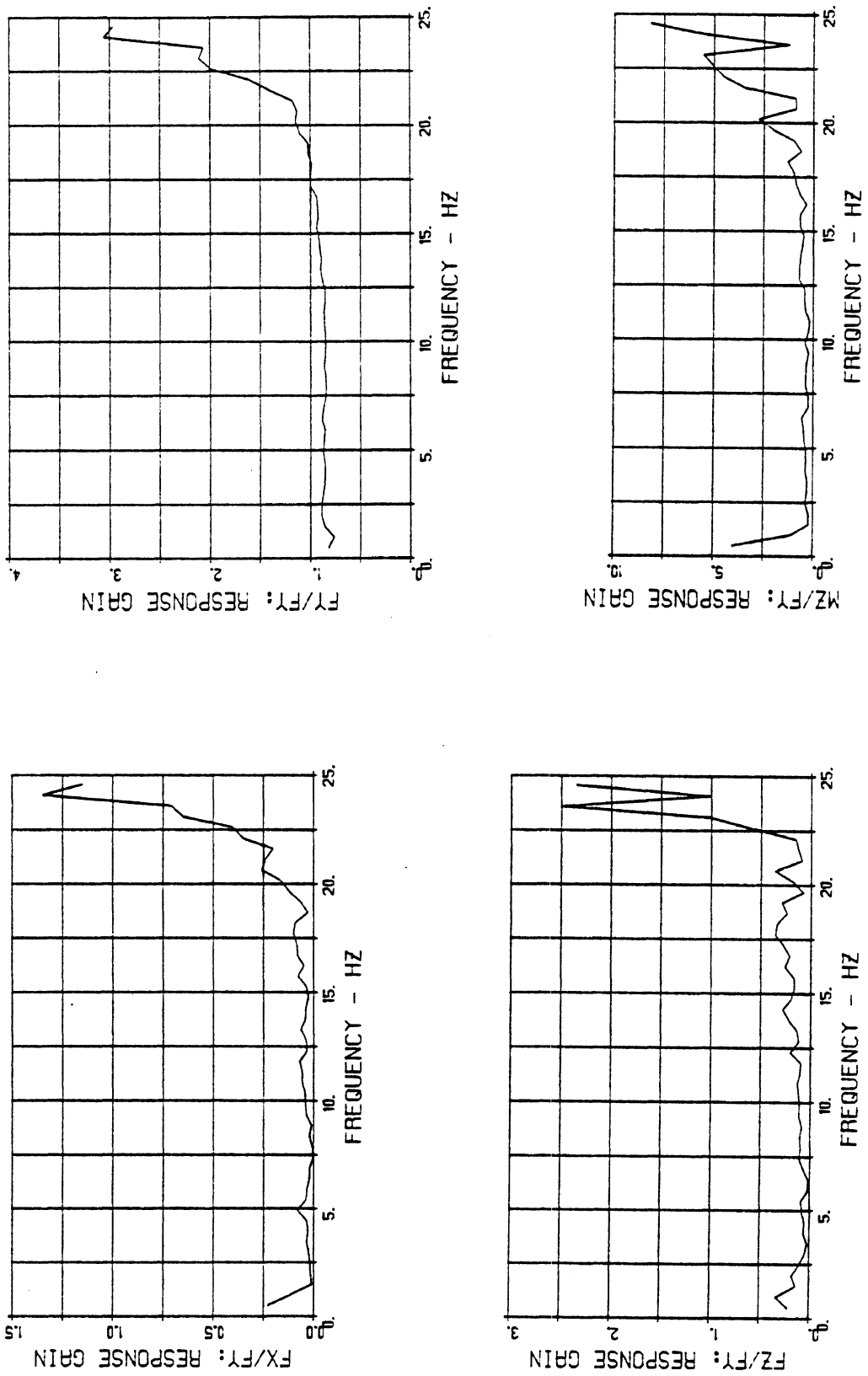

Figure 5b. Response in Each of the Transducer Channels to Pure Lateral Force Input.

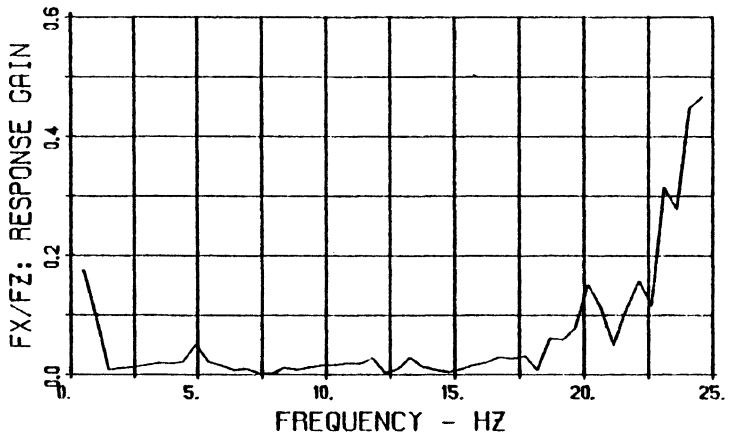

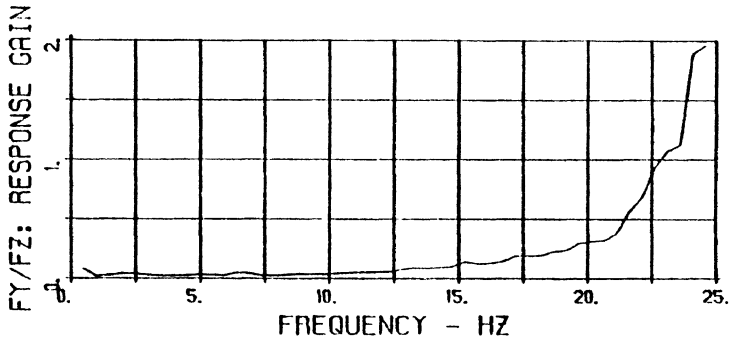

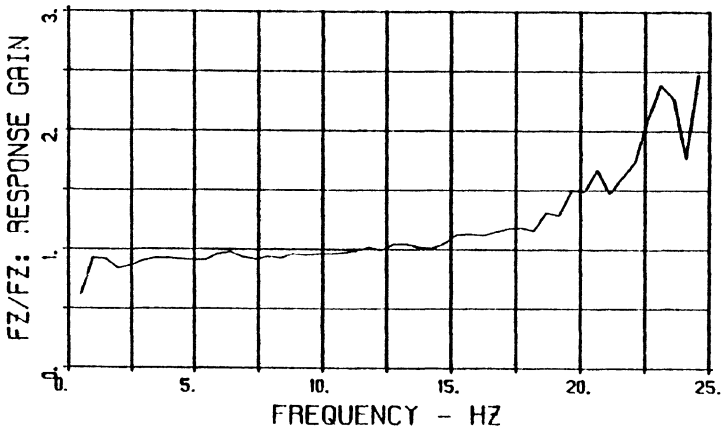

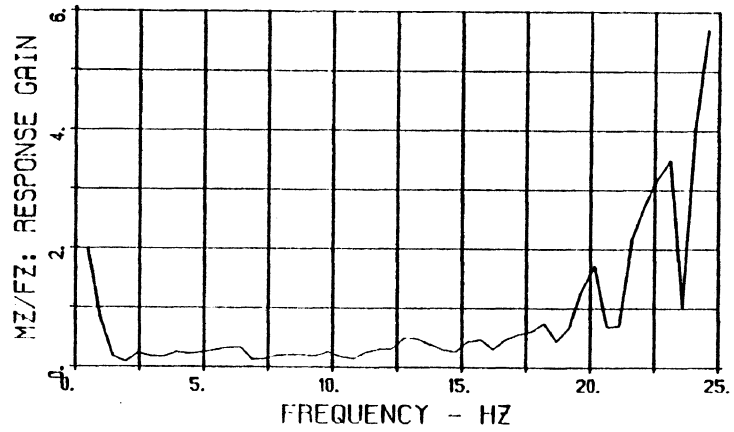

Figure 5c. Response in Each of the Transducer Channels to Pure Radial Force Input.

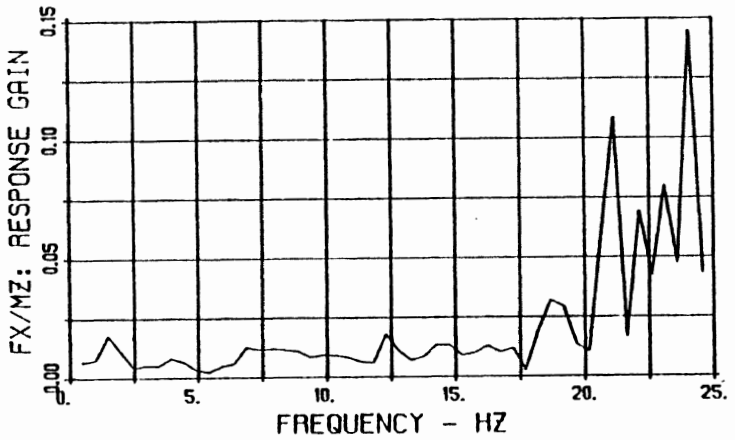

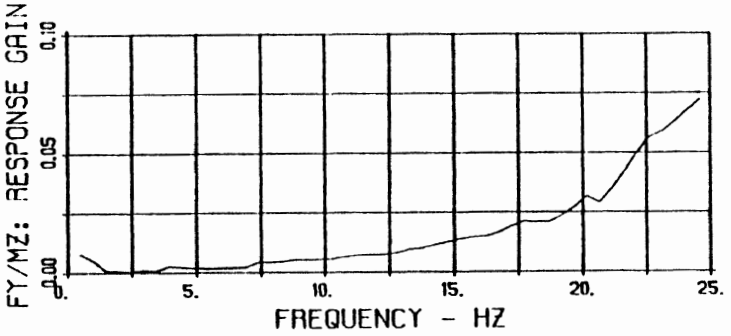

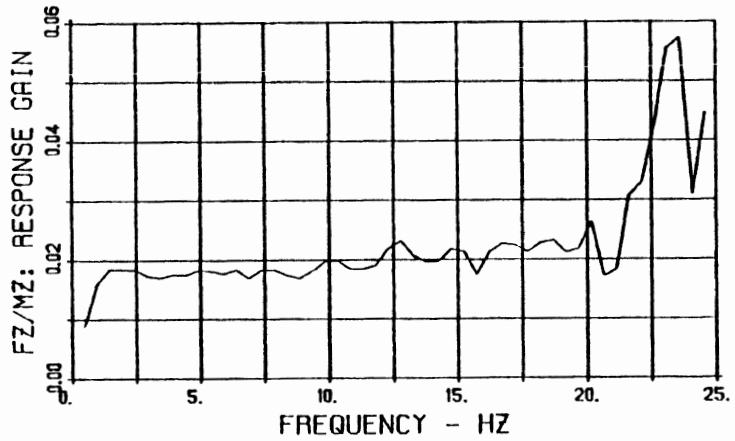

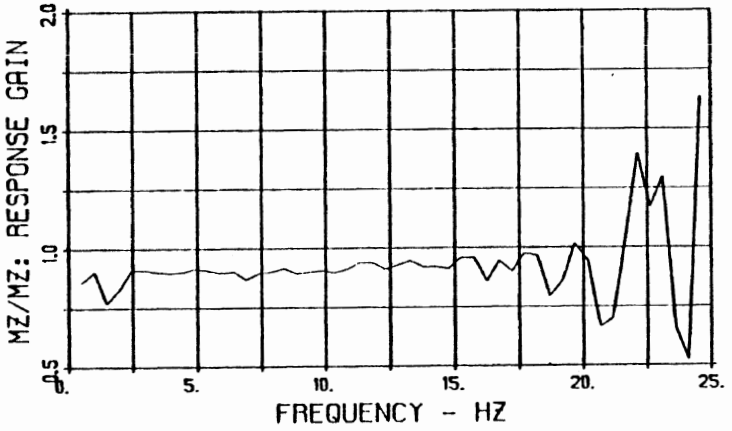

Figure 5d. Response in Each of the Transducer Channels to Pure Aligning Moment Input.

Table 1. Estimate of Error Ranges for the MTS Transducer.

	Static Gain	Low Speed (5 MPH)	High Speed (60 MPH)	
Direction		Cross-Coupling[1]	Cross-Coupling[2]	Dynamics[2]
Radial, F_z	-5%	± 6%	± 10 to 12%	+5 to 15%
Lateral, F_y	-10%	± 20%	± 20 to 30%	0%
Tractive, F_x	~0	± 70%	± 15 to 30%	+10 to 50%
Aligning Torque, M_z	-10%	± 35%	± 40 to 65%	+5 to 25%

[1]First harmonic

[2]Range for 1st and 2nd harmonics

big errors will accrue. The coupling of F_z to F_y, however, is more serious because the F_z magnitudes tend to be much greater than the F_y force magnitudes. Tractive force and aligning moment cross-coupling is more serious. The tractive force especially has errors at low speed because the tractive forces tend to be quite small such that the cross-coupled forces appear relatively large. The force magnitudes and the transfer functions each change respectively with speed and frequency, hence the typical cross-coupling errors will change with speed. Thus an estimate of cross-coupling errors are given for high-speed conditions. Finally, because the gain of each channel changes with frequency, additional errors will accrue. These errors grow with speed, and typical error magnitudes are indicated in the last column of Table 1. By and large, the values shown in this table are considered only crude estimates for purposes of illustrating potential magnitudes and should not be taken as a statement of known error magnitudes.

Aside from these technical issues related to dynamic limitations of the machine, other exercises were performed to validate the static calibration of the transducer. At the stage where the machine was considered operational, the transducer was recalibrated to ensure that the static force measurements were in agreement with a precision load cell provided with the machine. Hardware for installing and aligning the precision load cell was provided by the manufacturer, along with their assistance in performing the calibration. From this exercise it was possible to confirm that the forces measured by the transducer were indeed accurately related to the forces being imposed on the spindle in accordance with the coordinate system specified for the transducer.

2.2.3 Comparison of Machine Measurements with RMA Measurements - In the course of tire tests, it was noted that the measured force variations were significantly different than those reported by the RMA member companies that supplied the tires. Comparison of four measurements was possible—the Composite Radial Force Variation (FZ_c), the First Harmonic Force Variation (FZ_1), the Free Radial Runout on the Tire Centerline (FRROC), and the Composite Lateral Force Variation (FY_c). Comparison of the RMA values with those obtained by UMTRI for each of these parameters is shown in Figures 6, 7, 8, and 9. Though the radial force variations show poor agreement, the

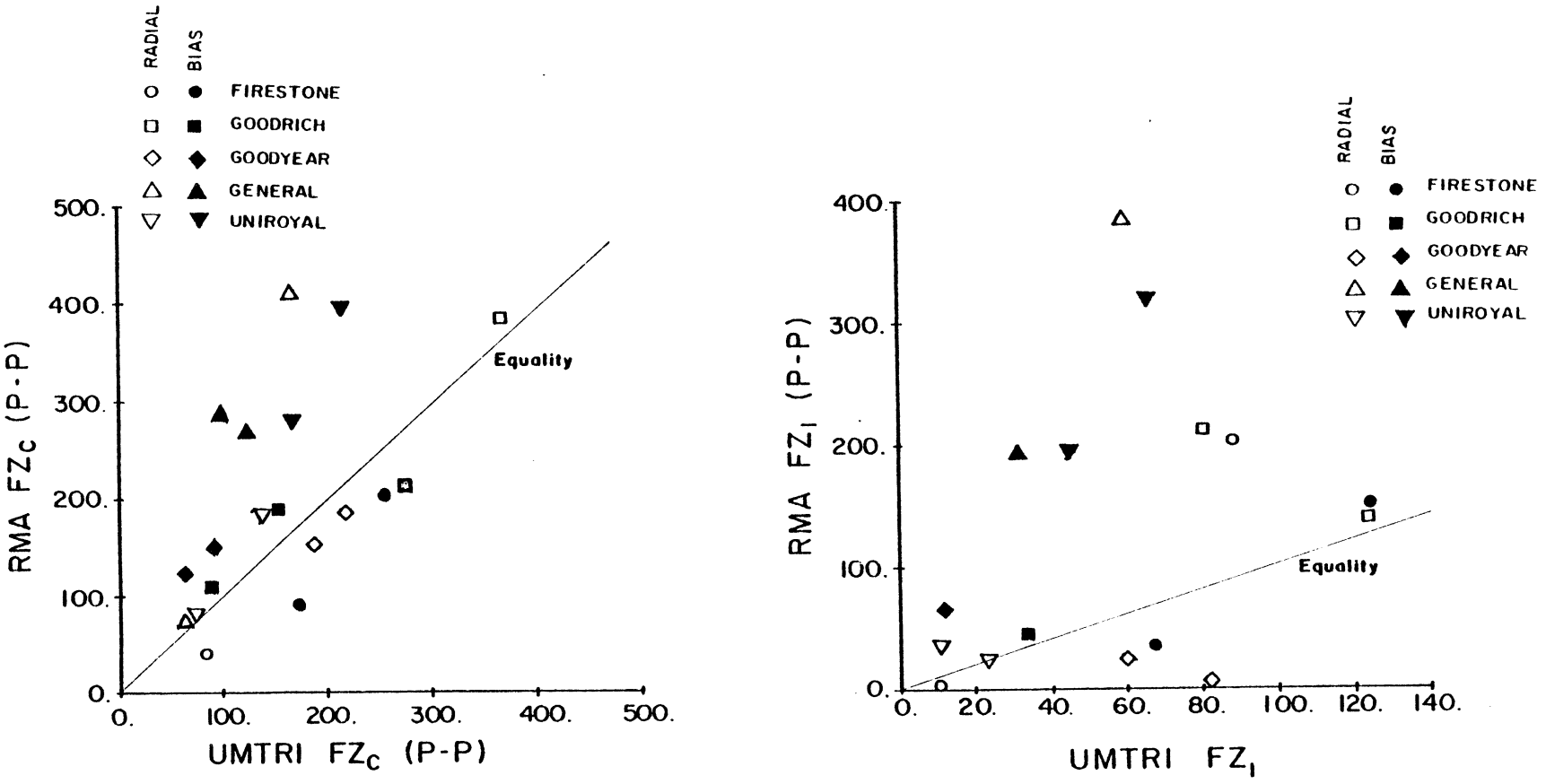

Figure 6. Comparison of RMA and UMTRI Composite Radial Force Variations (in pounds) on Tubeless Tires.

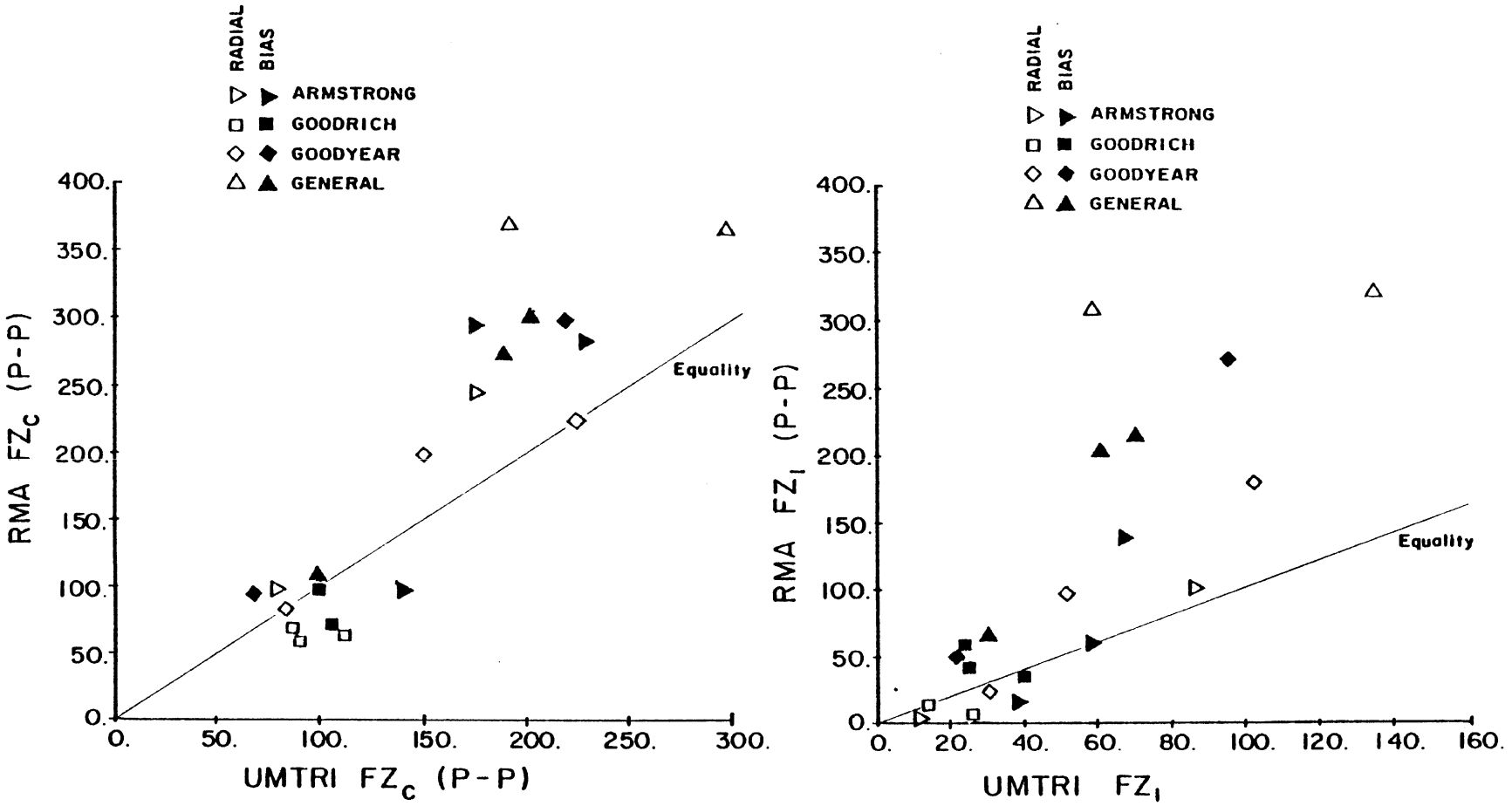

Figure 7. Comparison of RMA and UMTRI 1st Harmonic Radial Force Variations (in pounds) on Tube-Type Tires.

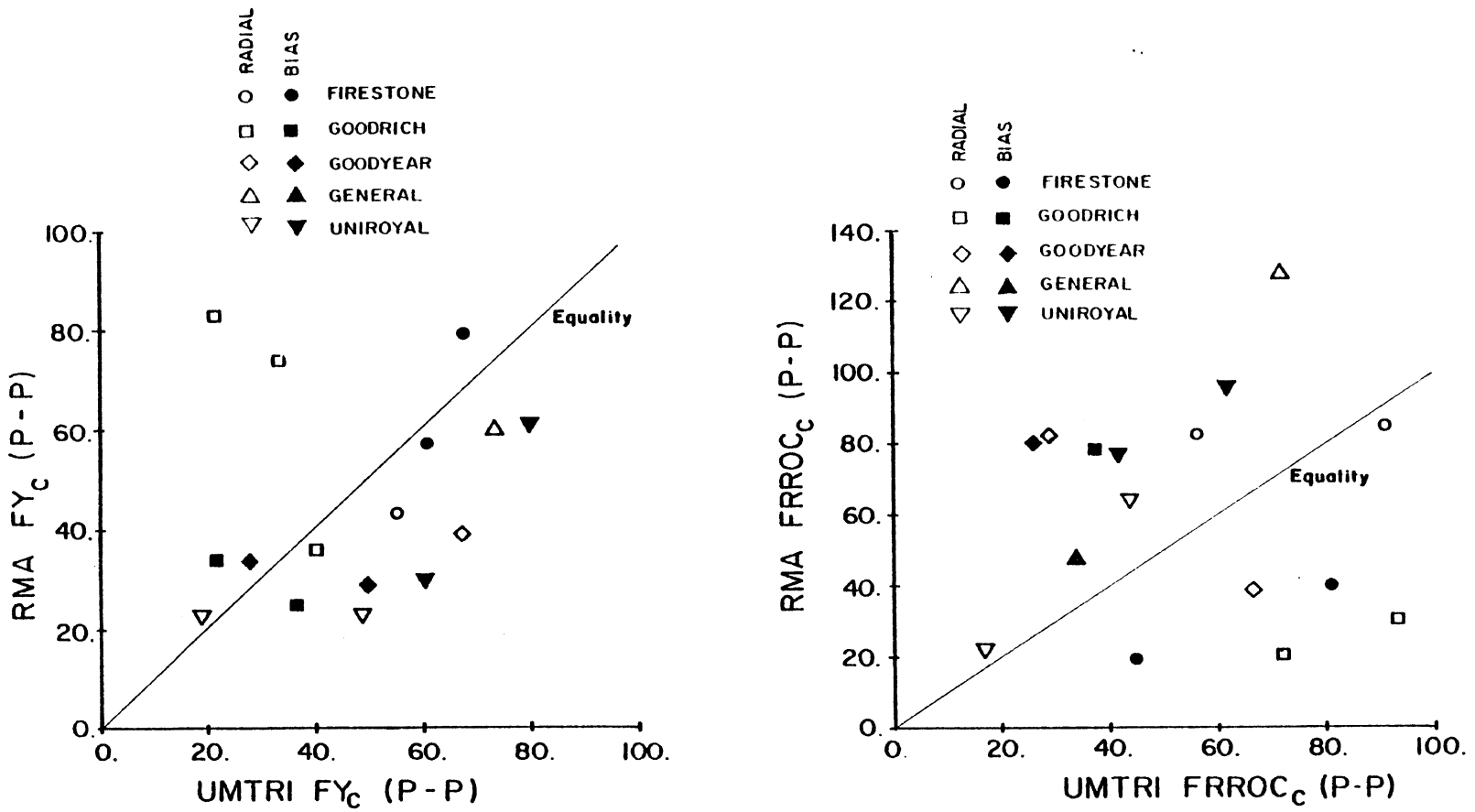

Figure 8. Comparison of RMA and UMTRI Measurements of Lateral Force Variation (in pounds) and Free Radial Runout (.001 in.) on Tubeless Tires

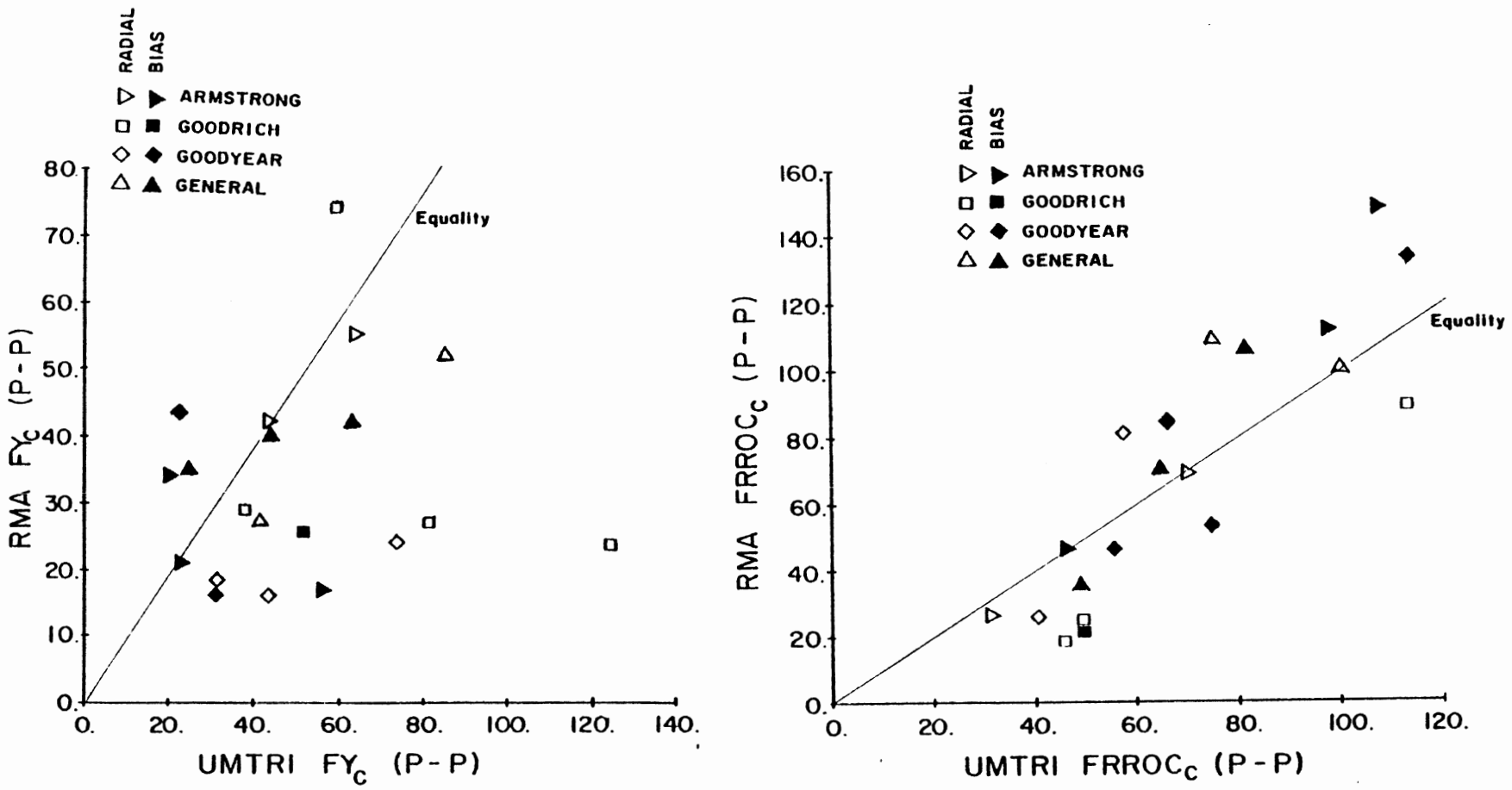

Figure 9. Comparison of RMA and UMTRI Measurements of Lateral Force Variation (in pounds) and Free Radial Runout (.001 in.) on Tube-Type Tires

fact that the radial runout measurements are comparably bad is an indication that the tires were not being mounted equivalently by both organizations, hence the force values should be different. The disparities observed here are perhaps typical of the differences between test machines of different design, operated using different procedures. At the stage in the research where this disparity was noted, a complete re-evaluation of the test machine was conducted to verify its accuracy [8]. From the exercise it was concluded that the test machine was performing as represented in the above discussions about its accuracy and error sources. Perhaps one of the more interesting observations in that report was that the correlation between the machine measures of radial runout and radial force variation was very good. Inasmuch as the measurement of radial runout was validated by comparison to measurements by a dial indicator, the good correlation was an indication that the radial force measurements being obtained are consistent. Although errors creep into the results via the above-mentioned mechanisms, the measures obtained can nonetheless reveal much about force variations present in truck tires, if the results are used knowledgeably.

Finally, out of concern that force variations measured on a drum machine might differ systematically from those produced on a flat (road) surface, tire uniformity tests were conducted on the Institute's flat-bed tire tester for comparison with the MTS machine (see App. C). From those tests it was concluded that measurements on the 67-inch drum are essentially equivalent to those on a flat surface.

2.3 Test and Data Processing Procedures

The results that are obtained in a research endeavor such as this are to some extent influenced by the procedures used in testing and data processing. Hence, the procedures that were used are described in this section.

2.3.1 General Test Procedures - The general methods characterizing the test procedures can be separated into the following topical headings.

-Tire Mounting Procedures - Throughout the experimental program, tires were repeatedly mounted on precision wheels and commercial wheels. In the mounting process, especially with tubeless tires, care was taken to

avoid bead damage as would affect bead seating on a wheel. In each mount, Murphy's Soap was used as a lubricant to aid seating. The tires were not inflated above T&RA ratings to hasten the seating.

-Tire Warmup - Prior to any tests, the tire was run at full load/pressure conditions on the drum at a speed of 60 mph for a period of 20 minutes. This procedure was found to be adequate for bringing the tire up to warm conditions, such that repeatable data was obtained.

-Load/Pressure Conditions - Many of the tires were tested at four standard load/pressure conditions. These conditions were to be defined by T&RA single-tire ratings equivalent to 100% load with 100% pressure, 75% load with 100% pressure, 75% load with 75% pressure, and 50% load with 75% pressure. However, the tires received included a mix of F-rated bias-plies and G-rated radial tires. Inasmuch as the two ratings would result in 16 load/pressure conditions, making comparisons more difficult, all tires were tested at the F-rated condition. Thus, the load/pressure conditions used for radial and bias-ply tires were as follows:

	Radial		Bias-Ply	
Load/Pressure	Load	Pressure	Load	Pressure
100%/100%	5430 lb	90 psi	5430 lb	85 psi
75%/100%	4073	90	4073	85
75%/75%	4073	67.5	4073	64
50%/75%	2715	67.5	2715	64

In the tests on tire/wheel assemblies, all hardware was tested at the full load pressure condition, which was 5430 lbs for single wheels and 9520 lbs for dual wheels. In the dual-wheel tests, radial tires were operated at 80 psi, and bias-ply tires were operated at 75 psi. In selected cases, tests at other load/pressure conditions were performed as considered necessary for the planned analysis. The conditions included both those listed above, and tests of single wheels at the dual wheel load/pressure conditions, as baseline information for their use on dual wheels in later tests.

-Test Order - No specific test order was prescribed, nor was the operator required to randomize the order. In the initial exploratory tests in which test procedures were established, the data appeared to be repeatable enough that test order was of no consequence.

-Test Length - A "test" at any specific condition is considered to be the average of data obtained over 8 revolutions of a wheel. That is, the harmonic force variations are the average for 8 revolutions, imbalance is determined from data acquired in 8 revolutions, and runout measurements are the average from 8 measurements of the tire. The choice of 8 revolutions was determined from exploratory tests in which it was established that 8 revolutions were sufficient to minimize variability of the measurements.

2.3.2 Radial Runout Measurements - Tire radial runout measurements were obtained by emplacing the LVDT fixtures against the tread band of the tire, as was illustrated in Figure 2. Two LVDTs were run on the edges of the tread band (normally in the center of the outside rib), while one was located intermediately on the centerline of the tire. Once in place, the tire/wheel assembly was rotated by hand for 8 revolutions while the computerized data acquisition system took digital samples of runout at the rate of 32 points per revolution. These data were processed through the FFT to obtain ten harmonic values which are then averaged over the eight revolutions. The data were stored as the harmonic values for the three individual measurements. The Free Radial Runout on the Centerline (FRROC) was used directly. Two-Point Free Radial Runout (FRRO2P) was determined by vector averaging the harmonic values for the inside and outside shoulders. Three-Point Free Radial Runout (FRRO3P) was obtained by vector averaging all three measurements. Runout measurements on wheels were obtained in a similar fashion, differing only in the placement of the LVDTs. For wheel runout measurement, two LVDTs are used, one placed on each bead seat. The LVDTs are located just inside the radius between the flange and the bead seat, that position representing the outer limit of the sloping bead seat. The Bead Seat Radial Runout (BSRO) was obtained by vector averaging the harmonic values for the two sides.

2.3.3 Lateral Runout Measurements - Lateral runout of both tires and wheels was measured with two LVDTs. Lateral runout of the tire was measured on the scuff band which is normally the point of maximum overall width, with the LVDT placed parallel to the wheel spin axis. Lateral runout on a wheel was measured by positioning the LVDTs to follow the inside of the wheel flanges. Because of their size, the LVDTs were not quite parallel to the spin axis but would normally have an inclination of about five degrees. No correction was made to the data for this effect. The lateral runout on each side of the tire or wheel was reduced to harmonic values. The magnitude of one was reversed to account for its opposite orientation, and the harmonics from both sides were added vectorally to obtain the overall (average) lateral runout for the tire (FLRO) or wheel (BSLRO).

2.3.4 Loaded Radial Runout - The test machine provided an operating mode for measuring the Loaded Radial Runout (LRR) for a tire/wheel assembly. The measurement was obtained by loading the assembly against the drum to the selected value which was then maintained by force feedback servo-control. The drum was then rotated slowly (equivalent to approximately 1 mph) during which the loaded radius signal was sampled. After the eight revolutions, the sampled data was processed by the FFT routines to obtain the harmonic values.

2.3.5 Imbalance Measurement - Imbalance was measured while the tire/wheel assembly was rotated in free space at high speed. The procedure was to load the tire lightly against the drum and take it up to a speed of 60 mph. The tire was then backed-off from the drum, and once contact was broken, the forces were measured for the required eight revolutions. The first harmonic values observed in the radial and tractive force directions represent the overall imbalance force. The average speed of the test wheel over the eight revolutions was measured concurrently by measuring the time required to complete the eight revolutions (via computer algorithms developed by the research staff). The imbalance magnitude was then computed from the ratio of the force to the square of the average speed over the measurement interval. The measurement of imbalance force in both the

radial and tractive force directions provided redundant measurement capability which on several occasions was helpful in detecting errors in instrumentation for the radial force direction.

2.4 Data Processing

The types of processing applied to the data obtained on the MTS tire test machine are described in this section. Two basic stages of processing were required—initial processing to correct for machine effects, and processing for purposes of analysis.

2.4.1 Initial Processing - When the electrical signals representing the runouts or force variations were received into the signal processing system, filtering and digitizing were performed. The data were then immediately processed via the FFT to obtain the harmonic magnitudes and phase angles. At this stage, several errors were still present in the data. The high- and low-pass filtering processes necessary before digitizing influence both the magnitude and phase angle values, necessitating corrections for their effects. From separate characterizations, corrections for the amplitude and phase distortions through the filters were determined as a function of frequency. By timing the period required for the eight revolutions during which data were acquired, the speed of the wheel was known and the temporal frequency of each harmonic could be determined. Knowing this frequency, appropriate corrections for the filtering could be applied.

The machine force and moment transducer incorporates crosstalk between channels due to the practical limits on the precision with which such devices can be manufactured. The crosstalk effects between the different channels were determined in the calibration prior to testing. Crosstalk is not frequency sensitive, hence corrections are simply applied by harmonic across all channels. Once these corrections were performed, the data were stored on the floppy disk storage medium along with test header data identifying the components under test, speed, load, inflation pressure, etc.

2.4.2 Processing for Analysis - In the analysis phase, data were read from the floppy disks and processed by a number of methods. The processing and analyses were performed on the University's main computer system, an Amdahl 470V/8. Processing was largely oriented toward quantifying the magnitudes of nonuniformities and force variations attributable to specific wheel components so that their functional relationship could be determined. The separation of the "sources" is conceptually illustrated in Figure 10. When we consider only one harmonic at a time for a tire/wheel assembly, the force component arising from the tire can be considered as a vector of a fixed magnitude and phase angle. Because the measurements are always made with respect to a reference mark on the tire (which is sensed by the photo-optical wheel rotation pickups), the force variation of the tire always appears at the same phase angle in the tests. The wheel nonuniformity is also represented as a vector having a magnitude and phase angle, the phase angle of the wheel, however, depending on the orientation of the wheel with respect to the tire. If the assembly is tested with the wheel oriented at four different positions with respect to the tire, the positions being 90 degrees apart, data points like those seen in the figure will be observed. Thence the magnitude of the tire force variation is obtained by finding the distance from the origin to the center of the circle, and the magnitude of the wheel contribution is determined by finding the radius of the circle.

In practice, the data may not look quite as ideal as that shown in the figure. Typically, the data points will not fall exactly on a circle. In that case, a "best fit" circle is found. The errors between each data point and the circumference of the circle represent variations due to test-to-test repeatability and variations in the way the tire mounts on the wheel. This latter effect on force variations is considered "bead seating variation."

This same type of procedure can also be used to separate the nonuniformity contributions of the hub on which the wheel is mounted. In that case, a tire/wheel assembly is mounted on a hub in multiple orientations. The tire/wheel assembly then produces the vector that locates the center of the circle, while the hub contribution corresponds to the radius

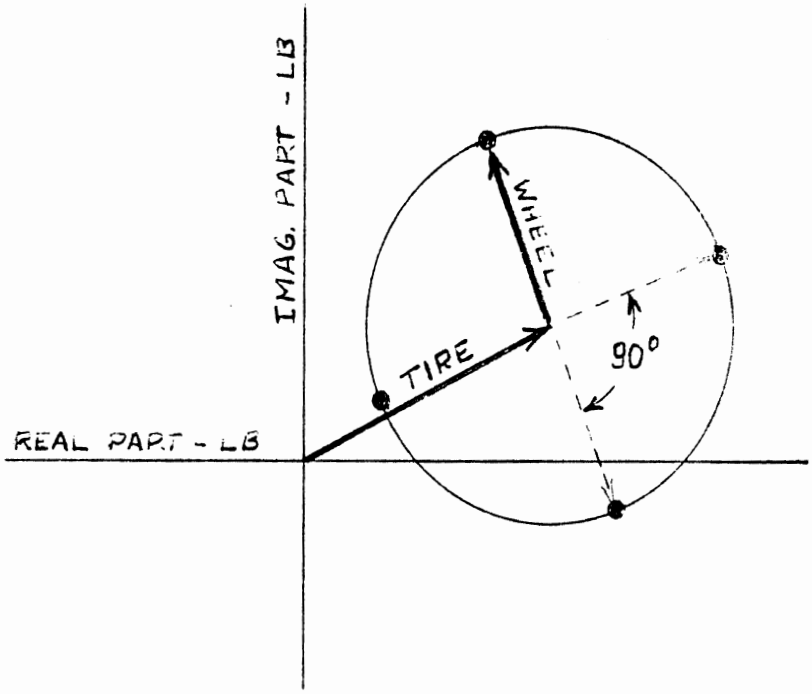

Figure 10. Vector Addition of a Nonuniformity Harmonic of a Tire and Wheel.

of the circle. The errors in the individual data points (i.e., the distance which they fall from the "best-fit" circle) represent the variations due primarily to the wheel mounting process. Thus, by tests in multiple mounting orientations, the force or runout variations due to wheel mounting could also be quantified.

The methods for reducing data in accordance with this concept were implemented on the University's computer system via specially written computer algorithms. Selected test results representing these multiple mounting cases were then processed by these programs.

CHAPTER 3

RELATIONSHIP OF TIRE NONUNIFORMITIES TO FORCE VARIATIONS

3.1 Introduction

The logical first step in presenting the findings from the Phase I research program is to examine the force variations arising from tires alone, in an effort to relate them to the measured nonuniformities. The discussion presented in this chapter reflects observations about tires obtained from experiments in which they were mounted on precision wheels. The degree to which these observations hold true when tires are mounted on commercial wheels is considered in Chapter 4.

The ultimate objective in this exercise is to identify the non-uniformity measures most closely related to the force variations produced under high-speed operating conditions. Because of the complex limitations introduced by the machine compliance properties, it is more informative to examine first the relationship of nonuniformities to low-speed force variations, then extend the examination to high-speed conditions.

The findings to be presented are multi-dimensional in nature, covering three force directions, different load and pressure conditions, and different operating speeds. In order to cover these dimensions in a systematic manner, the presentation that follows is divided up into separate and complete discussions of each force direction.

3.2 Radial Force Variations

In its simplest representation, the tire may be modeled as a toroidal-shaped pneumatic membrane. In its manufacture, the toroid may incorporate dimensional nonuniformities reflected in runout measurements. Being elastic, it may also exhibit variations in its stiffness properties around its circumference. Before actually examining the results obtained from experimental measurements, it is helpful to consider a model of the phenomenon of interest to aid in understanding and rationalizing the results observed. For this purpose, the tire may be assumed to be a linear system.

Though this is not true when one looks closely at its behavior, the linear model serves to illustrate the system in a way that helps the comprehension of the results to be seen. Such an engineering model for the tire is shown in Figure 11. The equations describing its force behavior are as follows:

$$F_z(\theta) = K(\theta) \cdot (R_o(\theta) - R(\theta)) \tag{3.1}$$

where

$F_z(\theta)$ = The radial force at any position on the circumference (θ)

$K(\theta)$ = The effective stiffness at that position (θ)

$R_o(\theta)$ = The free radius at the position (θ)

$R(\theta)$ = The actual load radius at position (θ)

The equation may be simplified by linearizing around the nominal operating point of interest. To linearize it is assumed that the force ($F_z(\theta)$ consists of a steady-state component, $\bar{F}_z$, equivalent to the nominal load, plus a cyclic component, $\tilde{F}_z$, which varies with the angle of rotation. Likewise, the stiffness, $K(\theta)$ consists of a nominal stiffness component, $\bar{K}$, plus a varying component, $\tilde{K}$; and likewise for the free and loaded radii. Only the cyclically varying component of each parameter is now a function of the position, θ, on the tire. The equation can now be rewritten in the form:

$$\bar{F}_z + \tilde{F}_z = (\bar{K}+\tilde{K})(\bar{R}_o+\tilde{R}_o-\bar{R}-\tilde{R}) = \bar{K}(\bar{R}_o-\bar{R}) + \bar{K}(\tilde{R}_o-\tilde{R}) + \tilde{K}(\tilde{R}_o-\tilde{R}) \tag{3.2}$$

Now in the steady-state:

$$\bar{F}_z = \bar{K}(\bar{R}_o-\bar{R}) \tag{3.3}$$

and can be subtracted out of the preceding equation, leaving the equation describing only the force variations:

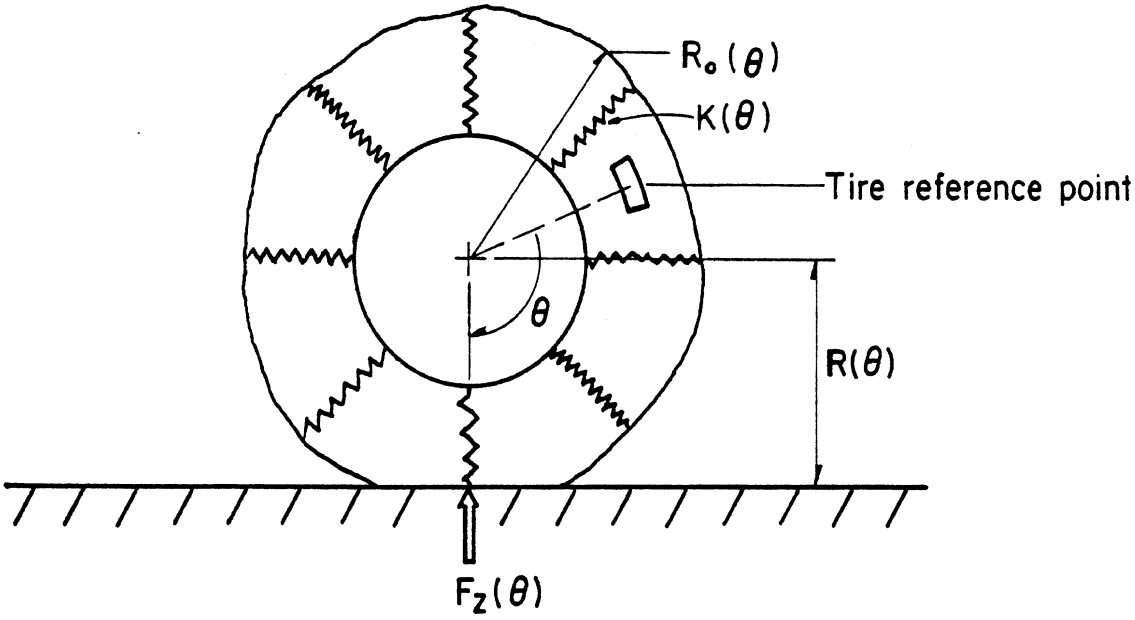

Figure 11. Model of a Tire with Runout and Stiffness Variations.

$$\tilde{F}_z = \tilde{K}(\bar{R}_o - \bar{R}) + \bar{K}(\tilde{R}_o - \tilde{R}) + \tilde{K}(\tilde{R}_o - \tilde{R}) \tag{3.4}$$

The last term in this equation is a variation times a variation which is second order in size and can be neglected with little error in the equation. Thus, in its final form, the variational equation becomes:

$$\tilde{F}_z = \tilde{K}(\bar{R}_o - \bar{R}) + \bar{K}(\tilde{R}_o - \tilde{R}) \tag{3.5}$$

The steady-state value of $(\bar{R}_o - \bar{R})$ is the static deflection at load which is a constant equivalent to $\bar{F}_z/\bar{K}$. Because it is a constant, it will be represented in the equations that follow by the symbol D_s.

Equation (3.5) quantifies the way in which the radial force variations are dependent on the stiffness and runout properties of the tire. The interest here is in understanding what radial force variations would be expected when the tire is tested on a fixed spindle machine (i.e., when $\tilde{R}=0$). Then we have:

$$\tilde{F}'_z = \tilde{K} \cdot D_s + \bar{K} \cdot \tilde{R}_o \tag{3.6}$$

where: $\tilde{F}'_z$ = force variation when the rolling radius is constant.

That is, the radial force variation on a fixed spindle machine will consist of two contributing factors, one arising from the radial stiffness variation and one arising from the free radial runout variation. The contribution arising from radial stiffness variation is dependent on the static deflection at load ($D_s = \bar{F}/\bar{K}$); whereas the radial runout contribution is dependent on the nominal stiffness of the tire. The first term is thus obviously sensitive to both the load and pressure conditions, while the second is primarily a function of the pressure.

A tire can also be tested to measure a loaded radial runout parameter. In that case, the radial force variation is held to zero by varying the radius, $\tilde{R}$. This mode can be described by using Equation (3.5) as follows:

$$0 = \tilde{K} \cdot D_s + \bar{K} \cdot \tilde{R}_o - \bar{K} \cdot \tilde{R}' \tag{3.7}$$

where: $\tilde{R}'$ = radius variation when the radial force is held constant. Combining Equations (3.6) and (3.7), then,

$$\overline{K} \cdot \tilde{R}' = \tilde{K} \cdot D_s + \overline{K} \cdot \tilde{R}_o = \tilde{F}'_z \tag{3.8}$$

That is to say, the loaded radial runout measurement is directly related to the radial force variation by a constant which is the nominal stiffness of the tire. Thus it is a more direct measure of nonuniformity indicative of the radial force variation to be expected.

Summarizing the results of this analysis:

1) Radial force variation arises as the sum of two effects—one which is the product of radial stiffness variations with the static deflection, and one which is the product of the free radial runout variations with the nominal value of the radial stiffness.

2) Radial force variation is directly proportional to loaded radial runout with a proportionality factor which is the nominal radial stiffness of the tire.

The implication of these results is that a loaded radial runout measurement, in itself, should be sufficient to predict radial force variations; whereas, a measure of free radial runout variation must be combined with a measure of radial stiffness variation to completely predict the radial force variation.

3.2.1 Typical Magnitudes. Extensive testing was performed on the MTS Tire Uniformity Test Machine in which various measures of radial nonuniformity and radial force variations were obtained. Forty tires were tested covering the categories of tubeless radials, tubeless bias ply, tube-type radials, and tube-type bias ply, and representing the products of six different tire manufacturers. (Note: Although 40 tires were tested, in the data plots that follow all 40 tires are not always included due to "bad" or lost data points.) The tires were also selected from an inventory of 140 tires to represent various extremes of nonuniformity conditions.

The results reported in this section were obtained with the tires mounted on precision wheels having a nominal accuracy in their radial dimensions of 0.001 inch.

Where possible, all measurements were compiled in terms of composite values and harmonic components. The composite value of a nonuniformity is intended to represent the peak-to-peak magnitude of the variation represented. Composites are accurate and meaningful when the variation of interest is free of electrical noise and dynamic vibrations in the equipment. This is generally true of low-speed measurements, but not so with high-speed measurements (above 10 mph equivalent road speed). Harmonic magnitudies are expressed in terms of the amplitude of their sine wave representation. In some quarters, where peak-to-peak values are used exclusively, this is thought of as a half-amplitude value. The radial force variations observed on the test tires generally followed the characteristic patterns expected. That is, the harmonic magnitudes were only a fractional component of the total load on the tire, and the magnitudes decreased with the harmonic number. The observations are summaried in Table 2 below which lists the half-amplitudes (half of the peak-to-peak) for all the tires, tested at the full load/pressure condition and a speed of 5 mph.

Table 2. Magnitudes of Radial Force Variations.

Harmonic No.	Mean (lb)	Maximum (lb)
1	49.0	135.0
2	18.4	41.4
3	12.2	27.0
4	12.2	29.7
5	8.6	19.0
6	6.1	15.2
7	3.8	10.5
8	3.1	6.3
9	1.8	3.9
10	1.4	4.5

In general, the radial force variations decrease about 30% in magnitude with each step in harmonic, which is in agreement with others [9].

3.2.2 Correlation with Runouts. As was described in Section 2.3, free radial runout measurements were made on the tire tread band, the data being processed into harmonic information directly comparable to the force variations. The loaded radial runout was measured and processed in the same way. In this section, the relationships between these measures of runout and the radial force variations are discussed.

a) Loaded Radial Runout - The relationships of the radial force variations to loaded radial runout for tubeless and tube-type tires are shown in Appendix A, Figure A.1. The multiple plots cover the relationships for the composite and the individual harmonics. In every case, a nominally linear relationship is indicated as would be expected from Equation (3.8). Good correlation exists out through the fifth harmonic. For the sixth and higher harmonics, the force levels are getting so small that the correlation is being seriously affected by the scatter arising from quantization in the digital sampling process. By the seventh harmonic, only discrete levels of runout are being seen due to this effect.

Radial and bias tires use a different pressure at their rated load condition, hence their effective stiffnesses may differ. A comparison of these two groups is provided in Table 3 showing the linear regression equations, correlation coefficients, and standard errors. The slope of the linear regression relationships define the effective stiffness of the tire by which dimensional nonuniformities equate with force variations. The stiffness is dependent on the harmonic and generally increases with harmonic. In the first harmonic, the effective stiffness is 5,600 lb/in for tubeless tires and 4,800 lb/in for tube-type tires; values which are nominally equivalent to the spring rate that would be measured in a static test. The spring rates increase with harmonic, reaching values between 8,700 lb/in (for bias type) and 12,000 lb/in (for radial) by the fifth harmonic.

b) Free Radial Runout on the Centerline - A simple and popular measure of nonuniformity in a truck tire is the runout on the centerline

Table 3 Regression Equations Relating
Loaded Radial Runout to
Radial Force Variations at 5430 Lb. Load

Measure	Radial Tires at 90 psi	Bias Tires at 85 psi
Composite	LRR_c=-11.6+.2568 FZ_c R^2 =.949 SE=-4.2	LRR_c=-4.25+.1975 FZ_c R^2 =.947 SE=3.0
1st Harmonic	LRR_1=.10+.1783 FZ_1 R^2 =.976 SE=1.2	LRR_1=-.25+.206 FZ_1 R^2 =.977 SE=1.1
2nd Harmonic	LRR_2=-.58+.1685 FZ_2 R^2 =.963 SE=.37	LRR_2=-.24+.1834 FZ_2 R^2 =.949 SE=.42
3rd Harmonic	LRR_3=-.14+.1584 FZ_3 R^2 =.846 SE=.54	LRR_3=-.22+.1677 FZ_3 R^2 =.852 SE=.22
4th Harmonic	LRR_4=-.36+.1430 FZ_4 R^2 =.880 SE=.38	LRR_4=.22+.1014 FZ_4 R^2 =.885 SE=.22
5th Harmonic	LRR_5=.08+.0826 FZ_5 R^2 =.809 SE=.18	LRR_5=0.0+.1153 FZ_5 R^2 =.738 SE=.35
6th Harmonic	LRR_6=.14+.0743 FZ_6 R^2 =.476 SE=.26	LRR_6=-.03+.098 FZ_6 R^2 =.737 SE=.23
7th Harmonic	LRR_7=.12+.059 FZ_7 R^2 =.510 SE=.17	LRR_7=.07+.061 FZ_7 R^2 =.377 SE=.15
8th Harmonic	LRR_8=.15+.0190 FZ_8 R^2 =.058 SE=.14	LRR_8=.17-.002 FZ_8 R^2 =.001 SE=.08
9th Harmonic	LRR_9=.08+.0364 FZ_9 R^2 =.162 SE=.08	LRR_9=.07+.030 FZ_9 R^2 =.104 SE=.08
10th Harmonic	LRR_{10}=.06+.0147 FZ_{10} R^2 =.056 SE=.07	LRR_{10}=.09+.010 FZ_{10} R^2 =.010 SE=.07

of the tread (FRROC). This simple dimensional measurement, however is not a highly accurate predictor of the radial force variation. Figure A.2, Appendix A, shows the plots for the tubeless tires tested, while the comparison of radial and bias tires is provided by the regression equations listed in Table 4.

The fairly high degree of scatter in these relationships is due to two factors. First, the runout on the centerline is not as closely linked to tire force behavior as those on the shoulders where the greater load is carried. Second, the force variation is a result not only of the runout, but also stiffness variations, and the stiffness variation is not reflected in the runout measurement. Thus it is concluded that the measurement of Free Radial Runout on the Centerline is not an effective predictor of radial force variations in a tire.

c) Two-Point (Shoulder) Radial Runout - The relationships of radial force variation to the two-point radial runout on the shoulder of tubeless tires are shown in Figure A.3, Appendix A. Note that the runouts on the two shoulders are vector quantities when reduced to harmonics. That is, for each shoulder there is a first harmonic having an amplitude and phase angle to be combined with that of the opposite shoulder. The average for the two shoulders is obtained by adding the two vectors and halving the amplitude of the resultant. This process is equivalent to averaging runout values around the tire prior to transformation into harmonic values. That the shoulder runout measurement is more relevant to force generation is indicated by the reduced scatter, at least at the first harmonic level.

The regression equations for the two-point runouts for radial and bias tires are given in Table 5. Significant correlation is only observed at the first harmonic level, and even then, the R-square of 0.6 - 0.7 would suggest that two-point radial runout is not a very accurate predictor of radial force variation.

d) Three-Point Radial Runout - The three-point radial runout is another possible combination of the free radial runouts that can be measured. The three-point runout is obtained by averaging the two shoulder measurements with the centerline measurement. (Note: The vector averaging

Table 4 Regression Equations Relating Free Radial Runout on the Centerline to Radial Force Variations at 5430 Lb. Load

Measure	Radial Tires at 90 psi	Bias Tires at 85 psi
Composite	$FRROC_c = 32.2 + .327\ FZ_c$ $R^2 = .665$ SE=16.3	$FRROC_c = 33.5 + .238\ FZ_c$ $R^2 = .343$ SE=21.3
1st Harmonic	$FRROC_1 = 7.2 + .230\ FZ_1$ $R^2 = .526$ SE=7.8	$FRROC_1 = 10.9 + .261\ FZ_1$ $R^2 = .489$ SE=9.0
2nd Harmonic	$FRROC_2 = 6.1 + .011\ FZ_2$ $R^2 = .007$ SE=3.4	$FRROC_2 = 4.6 + .119\ FZ_2$ $R^2 = .173$ SE=2.5
3rd Harmonic	$FRROC_3 = 2.5 + .074\ FZ_3$ $R^2 = .197$ SE=1.2	$FRROC_3 = 3.0 + .242\ FZ_3$ $R^2 = .104$ SE=4.5
4th Harmonic	$FRROC_4 = 1.6 + .173\ FZ_4$ $R^2 = .291$ SE=1.9	$FRROC_4 = 1.1 + .246\ FZ_4$ $R^2 = .392$ SE=1.9
5th Harmonic	$FRROC_5 = 1.1 + .175\ FZ_5$ $R^2 = .198$ SE=1.6	$FRROC_5 = 1.7 + .114\ FZ_5$ $R^2 = .123$ SE=1.5
6th Harmonic	$FRROC_6 = 2.1 + .168\ FZ_6$ $R^2 = .128$ SE=1.4	$FRROC_6 = .81 + .281\ FZ_6$ $R^2 = .445$ SE=1.2
7th Harmonic	$FRROC_7 = .38 + .327\ FZ_7$ $R^2 = .465$ SE=1.0	$FRROC_7 = .95 + .322\ FZ_7$ $R^2 = .274$ SE=1.0
8th Harmonic	$FRROC_8 = 1.9 + .101\ FZ_8$ $R^2 = .025$ SE=1.1	$FRROC_8 = 1.2 + .339\ FZ_8$ $R^2 = .808$ SE=1.4
9th Harmonic	$FRROC_9 = 1.1 + .127\ FZ_9$ $R^2 = .066$ SE=.47	$FRROC_9 = 1.6 - .164\ FZ_9$ $R^2 = .035$ SE=.75
10th Harmonic	$FRROC_{10} = 1.3 + .370\ FZ_{10}$ $R^2 = .193$ SE=.84	$FRROC_{10} = 1.7 - .238\ FZ_{10}$ $R^2 = .069$ SE=.63

Table 5 Regression Equations Relating
2-Point Radial Runout to Radial Force Variations
at 5430 Lb. Load

Measure	Radial Tires at 90 psi	Bias Tires at 85 psi
Composite	N/A	$FRRO2P_C = 17. + .155\ FZ_C$ $R^2 = .377$ SE=12.9
1st Harmonic	$FRRO2P_1 = .49 + .272\ FZ_1$ $R^2 = .602$ SE=8.0	$FRRO2P_1 = 1.8 + .187\ FZ_1$ $R^2 = .697$ SE=4.2
2nd Harmonic	$FRRO2P_2 = 3.7 + .071\ FZ_2$ $R^2 = .414$ SE=2.3	$FRRO2P_2 = 1.5 + .149\ FZ_2$ $R^2 = .374$ SE=1.9
3rd Harmonic	$FRRO2P_3 = 1.3 + .195\ FZ_3$ $R^2 = .553$ SE=1.4	$FRRO2P_3 = 1.5 + .113\ FZ_3$ $R^2 = .457$ SE=.78
4th Harmonic	$FRRO2P_4 = .60 + .190\ FZ_4$ $R^2 = .534$ SE=1.3	$FRRO2P_4 = .54 + .168\ FZ_4$ $R^2 = .448$ SE=1.1
5th Harmonic	$FRRO2P_5 = 1.5 + .074\ FZ_5$ $R^2 = .140$ SE=.82	$FRRO2P_5 = .78 + .126\ FZ_5$ $R^2 = .396$ SE=.79
6th Harmonic	$FRRO2P_6 = .37 + .252\ FZ_6$ $R^2 = .588$ SE=.69	$FRRO2P_6 = .47 + .160\ FZ_6$ $R^2 = .466$ SE=.67
7th Harmonic	$FRRO2P_7 = 1.0 + .085\ FZ_7$ $R^2 = .137$ SE=.64	$FRRO2P_7 = 1.1 + .061\ FZ_7$ $R^2 = .013$ SE=1.0
8th Harmonic	$FRRO2P_8 = .71 + .255\ FZ_8$ $R^2 = .279$ SE=.74	$FRRO2P_8 = 1.2 - .010\ FZ_8$ $R^2 = .000$ SE=1.0
9th Harmonic	$FRRO2P_9 = .73 + .051\ FZ_9$ $R^2 = .021$ SE=.35	$FRRO2P_9 = .48 + .161\ FZ_9$ $R^2 = .121$ SE=.37
10th Harmonic	$FRRO2P_{10} = .40 + .460\ FZ_{10}$ $R^2 = .414$ SE=.60	$FRRO2P_{10} = .75 - .002\ FZ_{10}$ $R^2 = .000$ SE=.37

process is equivalent to that described in the preceding paragraph.) The relationships to radial force variation for tubeless tires are shown in Figure A.4, Appendix A. The comparison of radial and bias tires is provided in the linear regression equations of Table 6. The three-point runout is a slightly better predictor of force variation (R-square values near 0.7 or greater) than the two-point.

e) Free Lateral Runout - Although lateral runout measurements are perpendicular to the radial force direction, there are conceptual models of the tire/wheel assembly that suggest there might be some relationship between these variables. A regression test between the radial force variation and lateral runout was tried, but no significant correlation was observed.

In all the correlations described above, no significant differences between tubeless and tube-type, or radial and bias ply were observed. In individual regressions, the slopes and correlation coefficients differed slightly, but those differences are generally in the range of statistical scatter in the testing. At best, perhaps, the only significant difference is the slightly higher effective stiffness of radial tires in the relationship between radial force variation and loaded radial runout. The higher stiffness is the logical result of the radial tires having a higher inflation pressure.

3.2.3 Effect of Load/Pressure Conditions. The effects of load and pressure can be examined along two dimensions—1) how does radial force variation change with load and pressure and 2) how does its relationships to runout nonuniformities change with load and pressure?

The radial force variations at 100% inflation pressure, and two different load conditions are plotted for the tubeless tires in Figure A.5. (Note: Due to the need to abbreviate the experimental program, the matrix of load/pressure conditions were not tested on the tube-type tires.) The forces are highly correlated (R-square values above 0.9) out through the sixth harmonic. Further, except for a certain amount of statistical scatter, the slopes of the relationships fall very close to unity, indicating that the force variations are effectively constant with load.

Table 6 Regression Equations Relating
3-Point Radial Runout to Radial Force Variations
at 5430 Lb. Load

Measure	Radial Tires at 90 psi	Bias Tires at 85 psi
Composite	$FRRO3P_C = 9.2 + .326\ FZ_C$ $R^2 = .670$ SE=16.1	$FRRO3P_C = 20.2 + .192\ FZ_C$ $R^2 = .600$ SE=10.1
1st Harmonic	$FRRO3P_1 = .40 + .281\ FZ_1$ $R^2 = .675$ SE=7.0	$FRRO3P_1 = 3.9 + .291\ FZ_1$ $R^2 = .764$ SE=4.1
2nd Harmonic	$FRRO3P_2 = 3.8 + .056\ FZ_2$ $R^2 = .300$ SE=2.4	$FRRO3P_2 = .83 + .186\ FZ_2$ $R^2 = .603$ SE=1.5
3rd Harmonic	$FRRO3P_3 = 1.4 + .149\ FZ_3$ $R^2 = .489$ SE=1.2	$FRRO3P_3 = .31 + .205\ FZ_3$ $R^2 = .654$ SE=.94
4th Harmonic	$FRRO3P_4 = .40 + .200\ FZ_4$ $R^2 = .654$ SE=1.0	$FRRO3P_4 = .37 + .198\ FZ_4$ $R^2 = .529$ SE=1.1
5th Harmonic	$FRRO3P_5 = .85 + .124\ FZ_5$ $R^2 = .173$ SE=1.2	$FRRO3P_5 = .63 + .145\ FZ_5$ $R^2 = .462$ SE=0.8
6th Harmonic	$FRRP3P_6 = .44 + .273\ FZ_6$ $R^2 = .583$ SE=.76	$FRRO3P_6 = .30 + .221\ FZ_6$ $R^2 = .680$ SE=0.6
7th Harmonic	$FRRO3P_7 = .68 + .174\ FZ_7$ $R^2 = .450$ SE=.57	$FRRO3P_7 = .96 + .113\ FZ_7$ $R^2 = .079$ SE=.73
8th Harmonic	$FRRO3P_8 = .79 + .249\ FZ_8$ $R^2 = .352$ SE=.61	$FRRO3P_8 = .88 + .144\ FZ_8$ $R^2 = .024$ SE=1.1
9th Harmonic	$FRRO3P_9 = .44 + .158\ FZ_9$ $R^2 = .109$ SE=.45	$FRRO3P_9 = .63 + .073\ FZ_9$ $R^2 = .020$ SE=.44
10th Harmonic	$FRRO3P_{10} = .50 + .494\ FZ_{10}$ $R^2 = .624$ SE=.42	$FRRO3P_{10} = .66 + .022\ FZ_{10}$ $R^2 = .000$ SE=.46

Comparable plots for measurements at 75% load and two different pressure conditions are shown in Figure A.6. Again, good correlations are generally observed in the lower harmonic range, although the slopes of the relationships are not unity. Rather, the slopes indicate that the radial force variation decreases with pressure on both the radial and bias-ply tires. Not surprisingly, at 75% pressure, the radial force variations are only about 75% of the magnitude observed at 100% pressure.

3.2.4 Effect of Speed. The ultimate interest in measuring the radial force variations produced by a tire or a tire/wheel assembly is to obtain an indication of the excitation forces that will be imposed on a truck at high-speed operation on the road. The surrogate measure for that effect in the laboratory is the measure of the radial force variations on a fixed spindle at high speed. Though the test machine was subject to errors when used at high speed because of the resonances, still some picture of the influence of speed on the radial force variations is possible. The machine resonances effectively result in frequency sensitivity in the gain of the measurement process. Precise measurement and correction for that gain error proved time consuming and subject to error because of the overall complexity of the phenomenon. Therefore, the data at different speeds was not corrected, but should be evaluated with the knowledge that the resonant gain changes are an integral part of the reported observations. Figure A.7 shows the relationships between radial force variations at 5 and 60 mph for the entire collection of tires tested. Only the first and second harmonic are shown because the measurements at 60 mph were always truncated above the second harmonic due to machine dynamic limitations. Simple linear relationships are evident, indicative of the fact that radial force variations have consistent behavior with changes in speed. The first harmonic variations increase by about 25% in going from 5 to 60 mph, while the second harmonic increases roughly by 40%. A factor which undoubtedly contributes to this phenomenon is the frequency-sensitive gain of the test machine. Unfortunately, the gain errors under actual operating conditions could not be measured to ascertain whether they were solely responsible for the increase in measured radial force variations. The dynamic characterization with the nonrolling tire, as was typified

in Figure 5.c, does not fully account for the 25% and 40% factors. However, it is not known how much the dynamic gain will change with a rolling wheel. Also, the accuracy with which the gain changes can be determined is limited by the fact that the 5 mph measurements correspond to temporal frequencies of 0.6 and 1.2 Hz for the first and second harmonic, respectively, which are in the range that is heavily filtered, and hence involves the additional errors associated with filter compensation.

3.3 Lateral Force Variations

The lateral force variations present in a tire are not readily explained by simple engineering models. The fact that a wheel has lateral runout is not, in itself, a basis for expecting lateral force variations. The best illustration of this comes from the simple model of a rigid disc wheel mounted on an axle such that it wobbles as it rolls. The wobble constitutes lateral runout. When it rolls, the wheel produces radial inputs due to its varying radius, along with inputs in the aligning moment and overturning moment directions. Yet, even though the rim rolls along a very circuitous path, the center of the wheel follows a straight path, and hence there is no lateral force variation.

The lateral force produced by a tire is transmitted to the wheel through the sidewalls. Thus any nonuniformity must be intimately related to this force path. To the extent that the sidewalls act like a membrane, the tensile forces distributed throughout the sidewall account for a portion of the lateral force. Because of their thickness, however, additional components of lateral force will arise from the bending in the sidewalls and shoulder areas. In straight running with a perfectly symmetric tire, the lateral forces in the opposite sidewalls balance out. Yet for real tires, the idealized symmetry can never be achieved. Thus lateral force variations will occur. Inasmuch as they arise from more than one mechanism, and those mechanisms are not directly reflected in the runout properties, the development of simple models against which to compare experimental measurements is not possible.

Unlike the radial direction, there is no lateral equivalent of a loaded runout measurement used in practice. If there were, it might be expected that a good correlation to that measure would be obtained. Yet, a loaded lateral runout measurement requires more complex hardware than for measurement of lateral force variation, hence, there is no motive for developing a loaded lateral runout test.

In a functional sense, there is little guidance to suggest to what operating variables the lateral force variation will be sensitive. Because the force path goes through the tire sidewall, it is perhaps reasonable to expect sensitivity to the nominal deflection of the tire (hence load and pressure), but no reason to expect sensitivity to speed.

3.3.1 Typical Magnitudes. The lateral force variations measured on the 40 test tires follow patterns similar to the radial force variations. Specifically, the largest magnitudes are normally observed in the first harmonic, with each higher harmonic proportionately lower than the previous. Characteristically, the magnitudes of the lateral force variations are less than half that of the radial force variations. The half-amplitude values from 5-mph tests on the precision wheel are shown in Table 7, below.

Table 7. Magnitudes of Lateral Force Variations.

Harmonic No.	Mean (lb)	Maximum (lb)
1	18.8	67.0
2	8.8	27.7
3	3.9	8.0
4	2.3	6.1
5	1.7	4.6
6	1.0	3.3
7	0.6	1.7
8	0.7	1.7
9	0.6	1.5
10	0.5	1.3

3.3.2 Correlation with Lateral Runout. Only one runout measure appropriate to the lateral direction is in common use—the free lateral runout. Free lateral runout is generally measured on the scuff rib on the sidewalls, which presents a flat surface for measurement. The runout is characterized by the sum of the readings on both sides of the tire.

The relationships between lateral force variations and lateral runouts are given in Figure A.8. As rationalized in the preceding discussion, no significant correlation exists for any of the harmonics. Thus, with respect to force nonuniformities, the free lateral runout measurement is of little utility.

3.3.3 Effects of Load/Pressure Conditions. The lateral force variations were measured on tires at the four load/pressure conditions described in Section 3.2.3. The effects of load and pressure can be illustrated by comparing the force variations generated under the different conditions. Figures A.9 and A.10 show those relationships as a function of load differences and pressure differences, respectively. At different load conditions, the lateral force variations are well correlated out through the seventh harmonic for the radial tires. The slopes of the lines through the data, however, are not unity; but rather, indicate that the lateral force variation decreases with increasing load. The correlation with bias-ply tires is not as good. With the poorer correlation it is more difficult to state with confidence the exact effect of load.

In Figure A.10, good correlation of the lateral force variations at different pressures is seen for the radial tires; and the magnitude is unaffected by pressure variations. The data for the bias-ply tires is not as consistent. Although most of the tires are unaffected by the pressure change, several of the tires changed erratically.

3.3.4 Effects of Speed. The influence of speed on the lateral force variations can be seen by comparing the force magnitudes observed at the 5 and 60 mph test speeds. Only the first two harmonics can be compared because only two harmonics are available at the 60 mph test speed. Figure A.11 shows these results for both the tubeless and tube-type tires.

No significant difference between the two types of tires is indicated. Though the plots would suggest that the force variation increases with speed, the plots include effects from dynamic gain changes with speed, and cross-coupled radial force variations. The first harmonic increases by about 15 percent between 5 and 60 mph, while the second harmonic increases about 35 percent. The dynamic properties of the machine in the lateral direction do not include resonant effects of a magnitude necessary to account for the 15 and 35 percent gain factors. However, the cross-coupling from other channels, especially the radial direction, could be sources accounting for the speed effects. Thus, at this point, it is not possible to make concrete statements as to how the lateral force variation changes with speed.

3.4 Tractive Force Variations

Tractive force variations in tires arise from variations in both the stiffness and runout properties. These effects combined as variations in the radius of the tire under load (the loaded radial runout) can be sources of tractive force variations. Consider the nonuniform tire as was shown in Figure 11 having a variation in its loaded radius. As the tire rolls, the high points in the radius resist rolling, creating a tractive force as they are forced to pass through the contact area. Whether a discrete feature on the tread or a general eccentricity in the wheel, this effect will be present. The magnitude of the tractive force thus created would not be expected to vary directly with the speed at which the wheel is rotating.

On the other hand, it is hypothesized that the variation in radius may also cause the rotational speed of the tire to vary as it rolls, given that the ground speed is held constant. If that is true, the tire/wheel assembly will experience accelerations and decelerations in the course of a revolution. The actual acceleration magnitude, however, will be speed sensitive—the higher the speed, the higher the acceleration. Because of its rotational inertia, tractive forces must be generated at the tire contact patch to produce the acceleration/deceleration phenomena.

Thus, tractive force variations are likely to relate to the radial uniformity parameters of the tire. Inasmuch as the several mechanisms of tractive force generation have different relationships to speed, the influence of speed on tractive force variations may be complex to characterize.

3.4.1 Typical Magnitudes. Tractive force variations are strongly dependent on speed, hence, reported magnitudes should be qualified by speed. The complete 10 harmonics were available at 5 mph, hence data will be given for that condition. The half-amplitudes for the tires tested are summarized in Table 8, below.

Table 8. Magnitudes of Tractive Force Variations.

Harmonic No.	Mean (lb)	Maxiumum (lb)
1	2.9	7.4
2	1.7	3.6
3	2.0	3.6
4	2.6	5.2
5	2.5	4.8
6	2.4	5.9
7	1.6	3.2
8	2.2	5.4
9	1.3	3.5
10	1.1	2.3

Note in the table above that the tractive force magnitudes at 5 mph are quite low, and near the threshold of measurement error. Though it is difficult to make precise comparisons, it can be stated with some confidence that the tractive force variations at low speed do not strongly decrease with harmonic number.

3.4.2 Correlation with Runouts. The only runout parameters which have any potential to correlate with tractive force variations are the radial runouts. Figure A.12 shows the relationship of tractive force variation at 5 mph to the loaded radial runout. A slight correlation is evident at the first harmonic level, but the two are virtually uncorrelated at higher harmonics.

3.4.3 Effects of Load/Pressure Conditions. Because of the low magnitudes of the tractive force variations at 5 mph, measurement errors make it difficult to extract the effects of load and pressure on each of the ten harmonics. As an alternative, the data for two harmonics at 60 mph are examined. Figure A.13 shows the tractive force variations at two loads and one pressure, and Figure A.14 shows the effects of two pressures at one load. In either case, the correlations are not good. Looking through the scatter, pressure does not appear to have much influence on tractive force variations. However, at two loads, as seen in Figure A.13, a large inexplicable difference appears. In both the first and second harmonics, the force variation increased markedly when the load is decreased. Whether this is a result of dynamic effects within the machine, or is an indication of actual tire behavior is not known.

3.4.4 Effects of Speed. The relationship between tractive force variations at 5 and 60 mph are shown in Figure A.15. As evident in the plots, the tractive forces grow dramatically with speed, increasing in some cases by factors of 5 to 10 times. Perhaps the important observation is that, despite such speed sensitivity, the tractive force variations at even the high speed are much lower than the radial force variations, only infrequently exceeding 30 pounds magnitude in the first harmonic. Even then, because it is a high-speed condition, some of the force must be discounted due to the exaggerated gain arising from dynamics.

3.5 Imbalance

Mass imbalance in a tire (or any other component of a tire/wheel assembly) produces a force as the wheel rotates. The magnitude of the force is easily predicted from physical laws and is quantified by the equation:

$$F = \frac{W \cdot R \cdot \omega^2}{6176}$$

where

$W \cdot R$ = the imbalance (weight x radius) in in-oz

ω = rotational speed of the wheel (rad/sec)

The force rotates with the wheel thus producing a force excitation in both the radial and tractive directions. The force is observed and measured on the tire test machine in a "balance test" when the wheel is spinning freely in space. Knowing the speed and force, the imbalance magnitude and its direction is computed. (Tests were performed to validate the computer algorithm; i.e., weight was installed at the specified location to demonstrate that the measured imbalance was eliminated.) The imbalance magnitude and direction was recorded and used for data correction in other test conditions.

When the mass imbalance is not located in the wheel plane, aligning and overturning moments are also produced, yielding what is known as "dynamic imbalance." The aligning moment effects are observed on the test machine, however, due to the poor quality of this data (arising from cross-coupling and dynamic errors) no effort was made to utilize it.

The magnitude of the cyclic force produced by imbalance is dependent on the amount of imbalance "W • R," and the speed of rotation. Rotational speed and translational speed are related through the rolling circumference of the tire, which for the 10.00x20 and 11x22.5 sizes is 10.58 feet. Thus the cyclic force arising from a 100 in-oz imbalance on these tire/wheel assemblies is 37.12 lb at 55 mph acting equally in the radial and tractive force directions.

CHAPTER 4

INFLUENCE OF NONUNIFORMITIES IN RIMS, WHEELS, AND HUBS

4.1 Introduction

The tire, as discussed in the previous chapter, is only one source of nonuniformity that may be responsible for force variations in a truck wheel. All rotating components are potential sources to the extent that they can influence the balance or runout properties of the wheel assembly. The hubs and wheels themselves are the major items in this category of other rotating components. Truck wheels are of two generic types—1) disc wheels that mount to studs on a hub, comparable to most passenger car wheels; and 2) rims that mount to a cast spoke wheel. For this latter configuration, the tire mounts to a rim which fits to machined surfaces on the cast spoke wheel and is retained by clamps secured to the wheel studs.

The overall wheel assemblies may also be of either the single- or dual-wheel types. The disc wheels or rims are common for both the single and dual arrangements; however, the hub or cast spoke wheels differ in each case. The hubs used with disc wheels may have different wheel-centering features (Budd or Center-Pilot). Cast spoke wheels may vary in the number of spokes, or have different rim-locating geometry.

Thus, when all the variables of truck wheel design are taken into account, there are many potential sources of nonuniformities in the hardware. Those that contribute to the force variations in the rolling wheel are of greatest interest. The experiments with tire and wheel combinations in this research have provided unique data from which to examine these phenomena. The following discussion reports the findings from that work. The emphasis here is in understanding the mechanisms by which nonuniformities in the wheel components cause force variations so that tire and wheel contributions can be compared on the same scale. Only a few selected samples of each type of hardware were tested. Thus, the relative magnitudes of nonuniformity reported here are not necessarily representative of the broad population of actual hardware.

4.2 Radial Force Variation

The radial force variations produced by tire/wheel assemblies might logically be expected to exhibit the same behavior as observed with the tires on the precision wheels. By and large, this is the case. The loaded radial runout measure proves to be the closest correlate of radial force variation for the overall assembly. Figure B.1 shows the relationship of radial force variation to loaded radial runout in the first few harmonics for a variety of tire/wheel combinations. The data points cover single- and dual-wheel arrangements for both disc and cast spoke wheels. Because the relationship depends on the radial stiffness of the tire/wheel assembly, the single and dual wheels exhibit different relationships. Beyond this, however, the relationship is unaffected by the other variables of tire-type and wheel-type.

The relationship between the radial force variations of the tire/wheel assembly and the various measures of free radial runout (radial runout on the centerline, and two- and three-point runouts) is similar to that observed with the tire alone, as discussed in the previous chapter.

Based on the observation that radial force variation and radial runout are closely related, it may be expected that any nonuniformity in a rotating wheel component that contributes to radial runout of the assembly is a source of radial force variation. That influence can be seen more explicitly by comparing the radial force variations attributable to the wheel with the runout properties of the wheel. The radial force variations attributable to the wheel can be determined by use of the vector-averaging process described previously. The method is implemented by installing the wheel on the hub and measuring the bead seat runout (BSRR) as installed. Then a tire is installed on the assembly without disturbing the wheel/hub relationship. The assembly is tested, then the tire is deflated and rotated to a new position (normally 90 degrees from the original orientation). The assembly is again tested, and this procedure is repeated twice again. The results of the four tests are then averaged to remove the tire contribution, leaving a radial force variation that can be attributed to the wheel/hub assembly.

That procedure was followed on a number of single tire/wheel assemblies. The radial force variations attributable to the wheel are compared to the radial runouts on the bead seat in Figure B.2. Good correlation is obtained in the first harmonic, but the correlation deteriorates in the higher harmonics as would be expected. In the first harmonic, the slope of the relationship corresponds to 3.3 pounds of radial force variation per 0.001 inch of bead seat radial runout. The mechanisms by which the wheel runout leads to radial force variation is somewhat overestimated by the assumption that the wheel runout operates directly against the tire stiffness, in which case force values more on the order of 5 pounds per 0.001 inch would be expected. The reduced level of the effective stiffness observed is probably due in part to the additional compliance contributed by the wheel and the fact that the tire helps to suppress or absorb the runout present in the wheel. To some extent, the absorbing process is reflected in the relationship between the bead seat radial runout and the loaded radial runout attributable to the wheel. These two are correlated in the first harmonic (though not as well—R-squared value of 0.85) with a slope that indicates the loaded radial runout will only be about 92 percent of the runout observed at the bead seat.

For purposes of completeness here, it should be noted that no significant correlation exists between the radial force variations of the wheel and the lateral runout measured at the bead seat. Likewise, there is no significant correlation between the bead seat lateral runout and other radial force properties.

Dual Wheel Combinations - Also of possible interest is the way in which the radial force variations in a dual-wheel assembly arise from the variations in the individual wheels. From the understanding developed thus far, one would expect that the radial force variation of the assembly is the simple vector addition of the contributions from each wheel. Figure 13 illustrates from actual measurements that vector addition occurs. The arrow on the plot represents the force variation for the inside wheel when it is measured alone. When the outside wheel is mounted in different

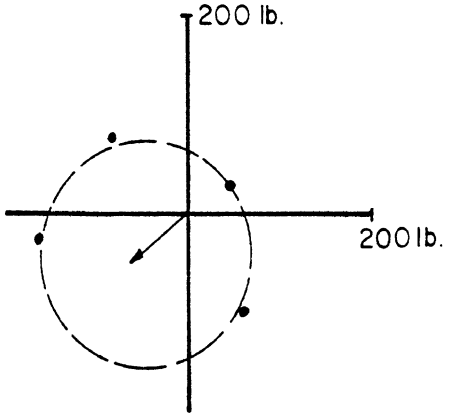

GENERAL 74/201 - 1st Harmonic

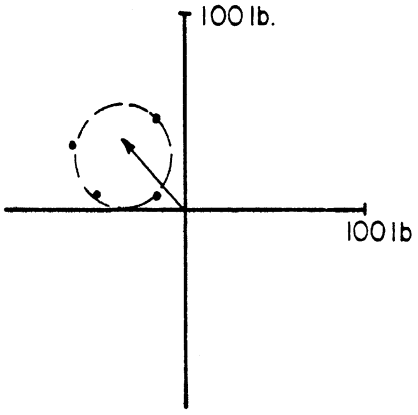

GENERAL 74/201 - 2nd Harmonic

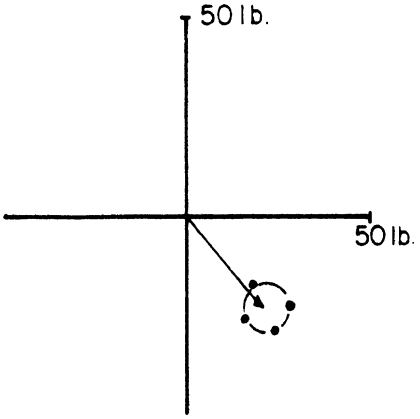

GENERAL 74/201 - 3rd Harmonic

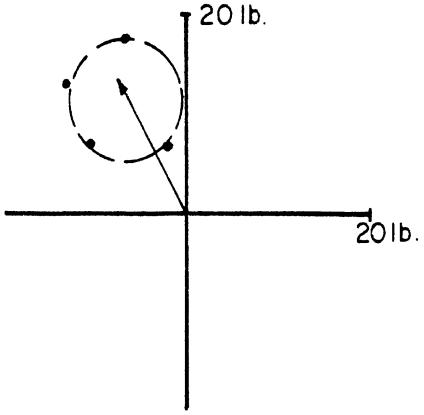

GENERAL 74/201 - 4th Harmonic

Figure 13. Radial Force Variations on a Dual- (Disc) Wheel Set when the Outside Wheel is Mounted with Different Orientations.

positions, the data points show the composite value measured. (Note that the outside wheel positions were 1/5 of a revolution apart, even though only four data points are shown.) The figure clearly shows the vector addition process in this series of tests, even though some error is evident. In this case, the inside wheel has a first harmonic radial force variation of 75 lb, while the outside wheel is 115 lb. Depending on the orientation with which they are mounted, the first harmonic for the total assembly may be anywhere from 40 lb (115-75) to 190 lb (115+75).

In general, the data seen in Figure 13 demonstrate that the vector addition process prevails when two wheels are mounted in a dual-wheel set. However, the process is not easily demonstrated for any arbitrary wheel set because wheel mounting variations may be large enough to obscure the "circle" representing the outside wheel. The data in Figure 13 were obtained using a disc wheel set for which the inside wheel could be locked in place while the outer wheel was moved to different orientations. In similar tests with cast spoke wheels, movement of the inner wheel with each repositioning of the outside wheel caused so much data scatter that the vector addition process could not be demonstrated. Nevertheless, it can be argued that vector addition is still taking place, although the mounting variations are a significant contributor to the force variation present in each wheel.

4.3 Lateral Force Variations

In the previous examination of tires, no dimensional uniformity measure was an effective predictor of lateral force variations. The same remains true for the tire/wheel assembly. Figure B.3 shows the relationship of lateral force variations to lateral runouts in single tire/wheel assemblies. (No equivalent data are shown for dual-wheel assemblies because of the difficulty of obtaining lateral runout measurements on both wheels.) Included in these data are examples of good and bad mounting practice. In general, the bad mounting examples yield the cases of high first harmonic runout, but have no direct influence on the second and higher harmonics. The absence of a clear relationship between the lateral force and lateral runout when the wheels are carelessly mounted is proof of the statement in

the previous chapter that a wobbly wheel is not a direct source of lateral force variation.

The data were also checked to see if there was any relationship between lateral runout of the wheel and the radial force variation. No correlation was observed.

4.4 Tractive Force Variations

Tractive force variations in tire/wheel assemblies arise from radial stiffness and runout nonuniformities in the overall assembly. The relationships to loaded radial runout are shown in Figure B.4. Although a rough correlation appears inexplicably in the second harmonic for single wheels, in general, no correlations occur in all other cases.

4.5 Sources of Nonuniformities

The radial and tractive force variations show such strong links to dimensional variations that the natural question is—What are the sources of those variations? Obviously, they are products of the way in which the components mechanically interface; but one must ask which are the critical factors. The overall variations in a tire/wheel assembly can be broken down into the following sources:

-Tire variations
-Bead-seating effects
-Wheel (or rim) variations
-Wheel-mounting effects
-Hub (or cast spoke wheel) variations

The tire, wheel, and hub variations are the products of the dimensional deviations in the manufacture of each component. The bead-seating and wheel-mounting effects are the result of the way in which one component interfaces with another. The tire, wheel, and hub nonuniformities are independent factors that, with proper methods, can be measured separately. The bead-seating and wheel-mounting effects are interactive and dependent on the combination of two components. Thus they can only be measured in those paired combinations.

The tire variations have been fairly well documented as to their magnitudes and qualities in the previous chapter. The remaining four effects are integral to the data on tire/wheel combinations that have been presented in this chapter, but have not been separated out yet. Thus these separate sources of variations will now be addressed.

a) Bead Seating - When a tire is mounted on a wheel, a certain amount of force variation may arise due to the fact that the tire must be seated onto the bead under high load. The magnitude of this variation might be expected to be specific to the tire bead contour (hence the tire manufacturer), as well as the wheel bead seat contour. When the tire is mounted on the wheel, the assembly has force variations which are the vector resultant from both the tire and the wheel (as mounted on a hub). In general, when the tire is mounted on the wheel, the force variations will not quite match that vector resultant because of the bead-seating influences. Should the tire be deflated, unseated, then reinflated, the overall force variations might be expected to vary slightly due to the change in the bead-seating effect. Alternately, if the tire is deflated, rotated to a new position on the wheel, and reinflated, the same effect will occur. Though the tire and wheel vector components are known, the variation for the assembly will differ from the vector resultant for the tire and wheel due to bead-seating variations. Theoretically, the bead-seating influence can be determined by testing a tire at multiple positions on a wheel/hub assembly. Because the measurements are made relative to the tire, the simple vector average of all tests is the tire force variation. The radius of the "best fit" circle through the data points is the magnitude of the wheel force variation. The data points will not fall exactly on the circle, but will evidence some random error, that error being the "bead-seating" effect. It was possible to extract a "bead-seating" error for some of the tests on commercial wheels by this process, although in many cases it was not possible due to the fact that the pattern for the wheel data did not appear like a circle. The process is quite tenuous, nevertheless, the data obtained are listed in Table 9. The reader is

Table 9. Magnitudes of 5 mph Force Variations Attributable to Bead-Seating Effects for Tires on Commercial Wheels.

Harmonic No.	Radial Force Variation (lb)		Lateral Force Variation (lb)		Tractive Force Variation (lb)	
	Mean	Max.	Mean	Max.	Mean	Max.
1	.253	.62	.064	.15	.036	.19
2	.099	.20	.040	.18	.056	.33
3	.090	.15	.014	.03	.011	.05
4*	-	-	-	-	-	-
5	.061	.12	.007	.02	.020	.09
6	.021	.08	.001	.02	.007	.04
7	.014	.05	.003	.01	.003	.01

*4th harmonic data not valid.

cautioned in using this data to recognize that the results obtained are likely to be conservative estimates of force variations attributable to bead-seating effects. Those cases where bead-seating variations are large will naturally confound the efforts to fit a circle to the data and are thus not included here. Therefore, the analysis process has a bias to underestimate bead-seating errors. Even though the true magnitude of bead-seating errors cannot be stated with confidence from this data, it would appear that they are quite small.

b) Wheel/Hub Variations - The variations associated with the mounting of a wheel on a hub (or alternatively a rim on a cast spoke wheel) individually are much more difficult to define and quantify. Theoretically, the variations can be determined by testing a wheel at multiple orientations on a hub and separating the wheel, hub, and mounting influences in a fashion analogous to that described above for the tire/wheel combination. Although a number of commercial wheel/hub assemblies were included in the tests, because of their variety no statistically significant sample of any one type was obtained. (For example, of the four hubs used in the tests, no two were alike; rather, the four were single and dual configurations of disc and cast spoke hubs. Similarly, only two undocumented samples of the four wheel types—tubeless discs, tubeless rims, tube-type discs, and tube-type rims—were tested.) Inasmuch as the sample sizes do not warrant a statistical analysis of each group, only the statistics for the overall sample are presented. Even then, the data are limited to the single-wheel configuration because of the complexity of separating effects on dual-wheel assemblies; and of all tests, only those in which a circle could be fitted were usable. The force variation magnitudes observed for the wheel/hub assemblies are listed in Table 10.

c) Wheel-Mounting Effects - The potential influences of wheel mounting are undoubtedly one of the effects most interesting to the industry. The separate characterization of force variations attributable to wheel-mounting variations is a task analogous to that of the bead-seating effects between the tire and the wheel. In order to separate out a force that can be attributed to mounting variation, the data obtained must fit the vector

Table 10. Magnitudes of Force Variation Attributable to Wheel/Hub Assemblies.

Harmonic No.	Radial Force Variation (lb)		Lateral Force Variation (lb)		Tractive Force Variation (lb)	
	Mean	Max.	Mean	Max.	Mean	Max.
1	41.5	135	2.64	4.83	6.49	31.3
2	6.47	14.3	1.53	3.35	1.57	7.24
3	4.83	10.0	0.79	1.42	0.60	2.00
4*	-	-	-	-	-	-
5	4.80	17.9	0.43	1.02	0.60	1.38
6	0.78	2.83	0.45	1.00	0.36	1.75
7	0.54	1.17	0.14	0.31	0.27	0.80

*4th harmonic data not valid.

addition model. When the mounting variations (which are random) are large, however, the "circle" representing the wheel cannot be found, and the analysis is confounded. Those data being excluded from the analysis lead to a biased picture of the magnitude of mounting effects. That being the case, perhaps the best picture of mounting variations is obtained by simply looking at the raw data for force variations when both "good" and "bad" mounting practices are used. Mounting practice is only a significant factor with cast spoke wheels. "Good" practice with cast spoke wheels is a progressive tightening of the lug nuts in a star pattern with care taken to minimize lateral runout; whereas, "bad" practice is equivalent to assembling the wheel to the point that all clamps and lug nuts are in place, then tightening one nut prior to all others. Table 11 shows those variations for single- and dual-wheel configurations. For single wheels there is virtually no influence from mounting procedure, and even then, only the lateral force variation shows any increase with bad mounting. The really significant effects show up on the dual-wheel configurations with a substantial increase in the radial force variation when bad mounting practice is used. In these tests, the "bad" practice was truly bad (pulling the rim up on one clamp before tightening the others), so the magnitudes shown in Table 11 are the upper limits of the mounting effects.

Table 11 Average Magnitudes of Force Variations on Cast Spoke Wheels with Good and Bad Mounting Practices

SINGLE WHEELS

Direction	Practice	1st Har.	2nd Har.	3rd Har.	4th Har.
FZ	Good	95.13 lb	35.88 lb	18.18 lb	9.17 lb
	Bad	91.51	35.94	17.80	8.99
FY	Good	29.91	6.73	5.73	1.61
	Bad	37.64	7.13	5.75	1.56
FX	Good	4.96	3.45	2.97	1.57
	Bad	4.85	3.46	2.85	1.66

DUAL WHEELS

Direction	Practice	1st Har.	2nd Har.	3rd Har.	4th Har.
FZ	Good	124.5 lb	31.16 lb	20.56 lb	23.18 lb
	Bad	289.4	34.11	19.75	23.13
FY	Good	26.5	7.03	5.83	5.80
	Bad	28.1	6.65	6.02	4.62
FX	Good	4.45	3.45	3.18	3.33
	Bad	11.20	4.05	3.18	3.24

CHAPTER 5

CONCLUSIONS

The findings obtained from conduct of the Phase I research program fall in two categories—those reflecting advancements in the technical understanding of how tire/wheel nonuniformities influence truck ride vibrations, and findings specific to how tire/wheel nonuniformities contribute to force variations. Though the ambitious objectives set at the beginning of the project have not all been achieved, nevertheless, substantial progress has been made in the direction of understanding truck tire/wheel nonuniformities and their influence on truck ride. Drawing on both the Phase I and Phase II [2] findings, the status of technical development can be summarized as follows:

1) A proper methodology for measuring nonuniformities in truck tire and wheel components has been established. Specifically, design and performance requirements for test machinery capable of making valid measurements (free from dynamic and cross-coupling errors) are known, test procedures have been established, and data reduction methods have been demonstrated. However, no test machine has yet been built to fully utilize that methodology.

2) The mechanisms by which force variations in the individual tire and wheel components combine to yield a force variation for the overall assembly is understood in many areas. For the radial force direction, which is the source of the largest variations, the "vector addition" model characterizes the combination effect.

3) The mechanisms by which force variations in tire/wheel assemblies dynamically couple to a truck are characterized by the "impedance coupling" concept [7]. The influence of this mechanism was seen in the dynamic problems with the test machine and the concept was employed in development of road simulator test methodology in the Phase II research project.

4) The relative importance of various harmonic force variations as ride excitation sources has been quantified for one typical truck in a

pilot test program [2], thus offering means to assess the relative significance of specific tire and wheel nonuniformities.

From the tire and wheel tests in the Phase I program, specific findings relating tire or wheel nonuniformities to force variations have been made. It should be noted that the testing and analysis could not nearly cover the entire sample of tires, and the tire/wheel samples used were not randomly selected to represent the general population. From these findings, the following primary conclusions are offered. It should, however, be noted that due to machine shortcomings, conclusions applying to other then the radial direction, and at high speed other that the first harmonic, are tentative.

Tire Radial Force Variations

-Radial force variations are generally the largest.

-Low-speed measurements are good predictors of high-speed (60 mph) force variations.

-Radial force variations in a tire are closely related to the loaded radial runout in the range of first through fifth harmonic.

-The two- and three-point radial runouts will only predict force variations in the first harmonic, and then with much lower quality of relationship.

-The radial force variations produced by tires showed no relationship to lateral runout properties.

-Radial force variations in tires are independent of load, but are dependent on (roughly proportional to) pressure.

Tire Lateral Force Variations

-Low-speed measurements are good predictors of high-speed (60 mph) force variations.

-Lateral force variations show no relationship to lateral runout properties.

-Lateral force variation tends to be independent of pressure, while a load sensitivity (force variation diminishing with load) is observed with radial tires.

Tire Tractive Force Variations

-Tractive force variations vary significantly with speed, and were not predictable from low-speed measurements, due to the limited capabilities of the present test machine.

-First harmonic tractive force variations (measured at 5 mph) are loosely correlated with loaded radial runout.

-The high-speed force variations appear to be relatively independent of pressure, but dependent on load (decreasing with increasing load).

-Due to the generally lower magnitude of tractive force variations, tire imbalance is potentially of greater relative significance to this force direction.

Tire/Wheel Assembly Radial Force Variations

-Loaded radial runout is a good predictor of radial force variation for a tire/wheel assembly; and, the runout of a dual-wheel assembly produces a much greater force variation than for a single wheel due to greater stiffness of a dual-wheel set.

-The two- and three-point free radial runouts on a single tire/wheel assembly are only loosely correlated to the first harmonic radial force variation.

-Bead-seat radial runout is a good predictor of first harmonic radial force variations arising from the wheel. Runout on the bead seat appears to be attenuated by the tire, contributing about 3.3 pounds of force variation per 0.001 inch of runout, for the tires included in this study.

-Contributions of the wheel/hub assemblies to first harmonic radial force variations are nominally of the same magnitude as for tires (for the limited samples tested). The wheel/hub contributions diminish in importance for the second through fifth harmonic, and are negligible thereafter.

-Lateral runout in a wheel does not contribute to radial force variation of the assembly.

-Radial force variations of a dual-wheel set are the vector addition of the force variations of the individual wheels.

-Poor mounting practice with dual cast spoke wheels can significantly increase radial force variations. No difference was observed with single wheels.

Tire/Wheel Assembly Lateral Force Variations

-Lateral force variations are unrelated to lateral runout properties.

-Mounting practice with cast spoke wheels did not affect lateral force magnitudes.

Tire/Wheel Assembly Tractive Force Variations

-Tractive force variations appear unrelated to loaded radial runout of the tire/wheel assembly.

-Poor mounting practice with dual cast spoke wheels can significantly increase the first harmonic tractive force variation (as measured at low speed). No effect was observed with single wheels.

Aligning Moment

Data were not evaluated due to the poor quality arising from errors associated with cross-coupling and dynamic effects.

CHAPTER 6

REFERENCES

1. Foster, A.W. "Factors Which Constrain Truck Ride Engineers." Presentation at the MVMA Truck Ride Quality Demonstration, Detroit, Mich., May 23, 1979.

2. Gillespie, T.D. "Influence of Tire/Wheel Nonuniformities on Heavy Truck Ride Quality." Report No. UM-HSRI-82-30, September 1982.

3. Truck Tire/Wheel Systems Research Program, Quarterly Report, January-March 1980, HSRI, Univ. of Mich., April 30, 1980.

4. "Testing Machines for Measuring the Uniformity of Passenger Car Tires." SAE Recommended Practice J332A.

5. MTS Model 860 Tire/Wheel Endurance Test Machine. Brochure No. 114.01-02, MTS Systems Corp., Minneapolis, Minn.

6. "Tentative Performance Specifications - MTS Truck Tire/Wheel Test System." Prepared by HSRI, Univ. of Mich., May 29, 1979.

7. Gillespie, T.D. "The Dynamic Behavior of Nonuniform Tire/Wheel Assemblies." Special Report, in preparation.

8. Gillespie, T.D. "Validation of the MTS Model 860 Tire Test Machine Measurements." Letter Report to MVMA, March 25, 1982.

9. Klamp, W.K., et al. "Higher Orders of Tire Force Variations and Their Significance." SAE Paper No. 720463, 1972, 8 p.

APPENDIX A

PLOTS OF TIRE UNIFORMITY TEST RESULTS

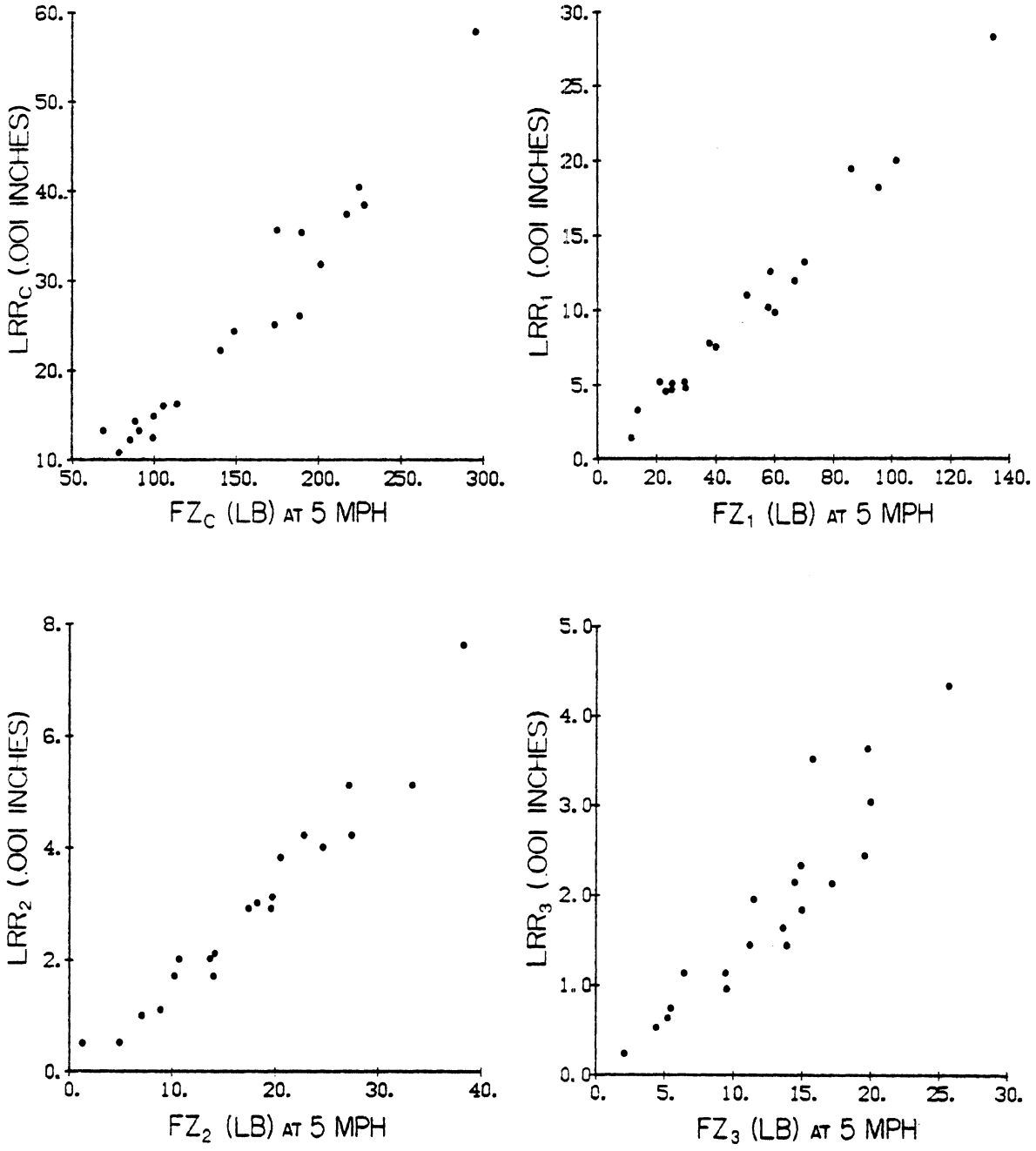

Figure A.1a. Relationship of radial force variations to loaded radial runout for tube-type tires.

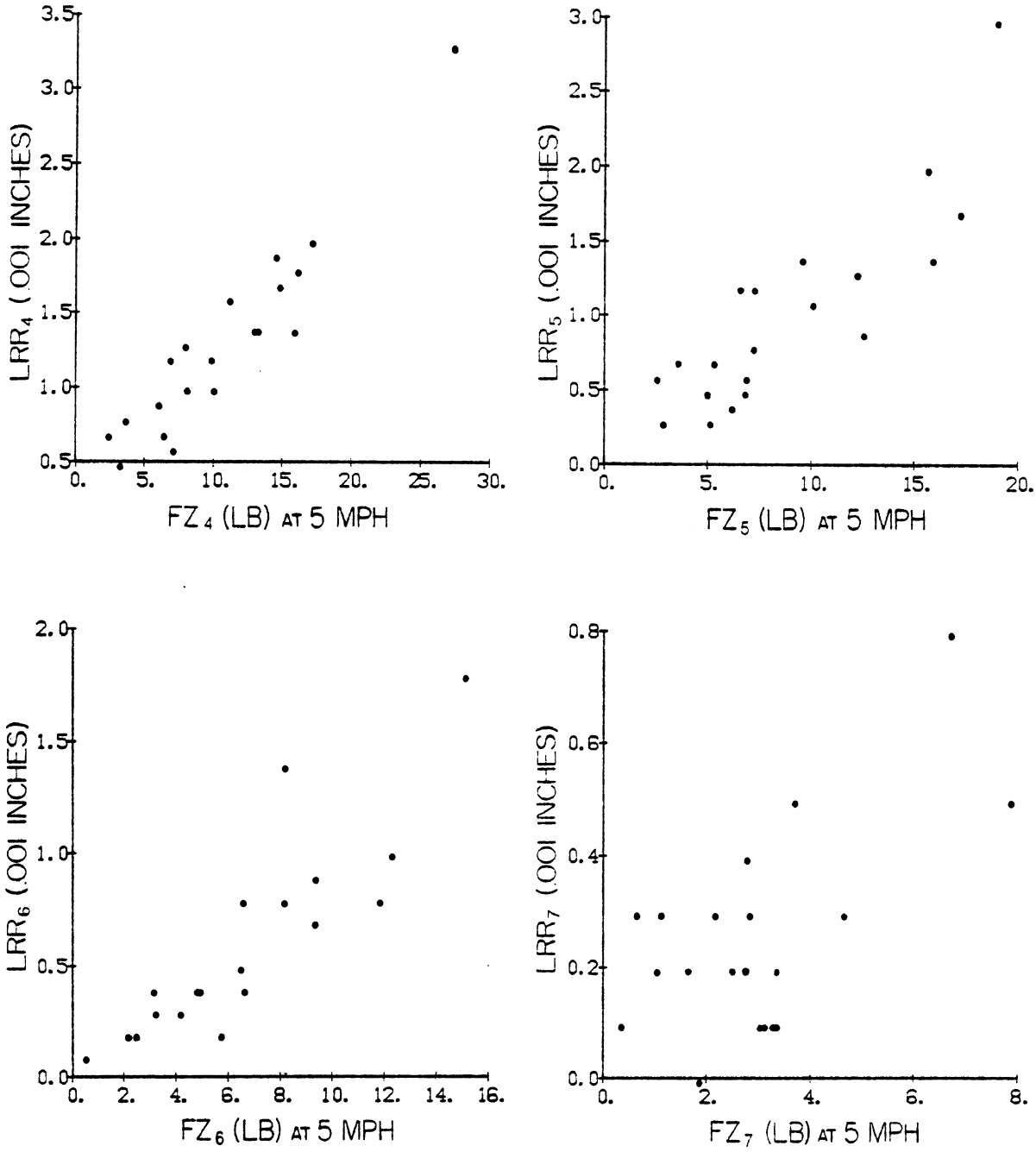

Figure A.1a. (Cont.)

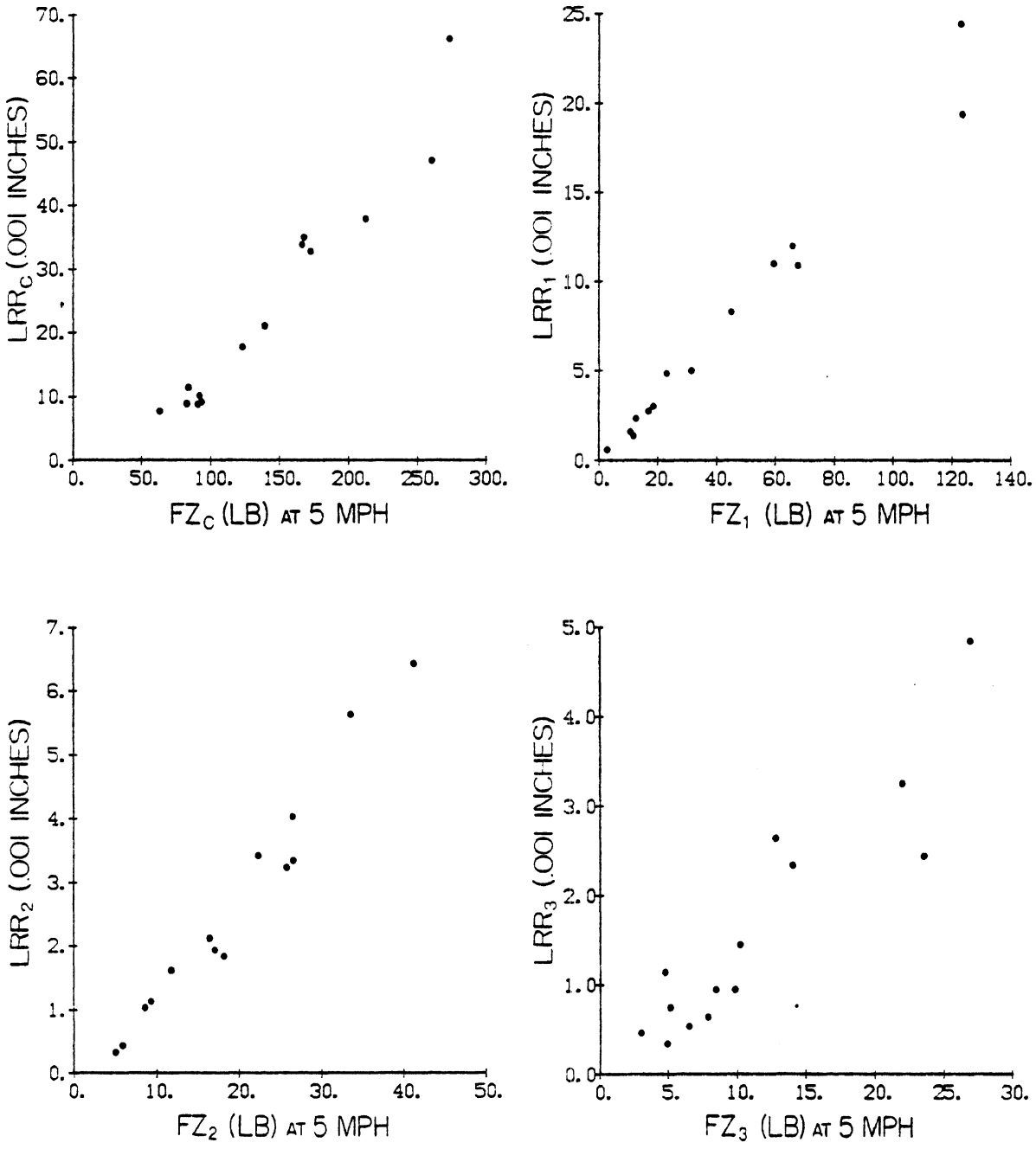

Figure A.1b. Relationship of radial force variations to loaded radial runout for tubeless tires.

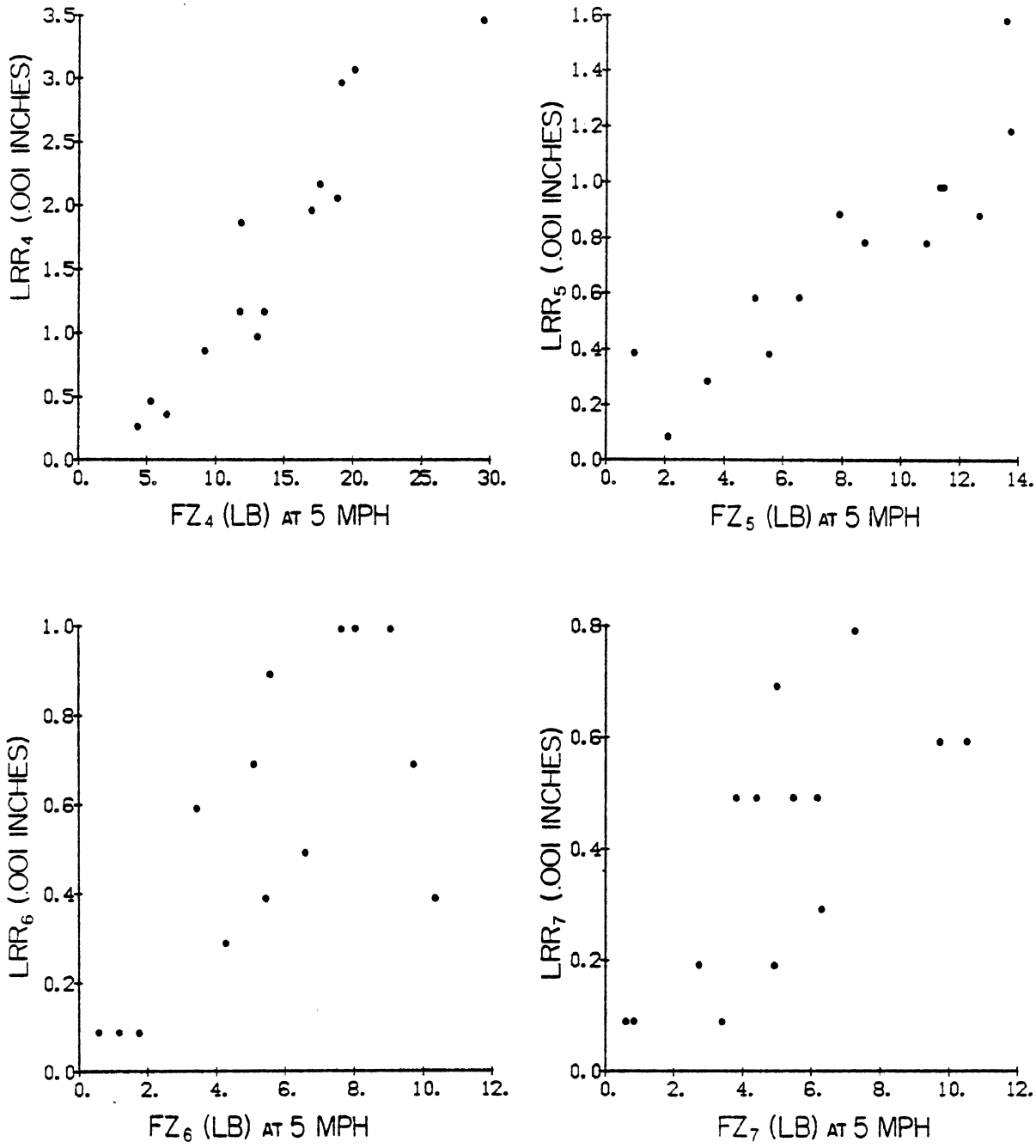

Figure A.1b. (Cont.)

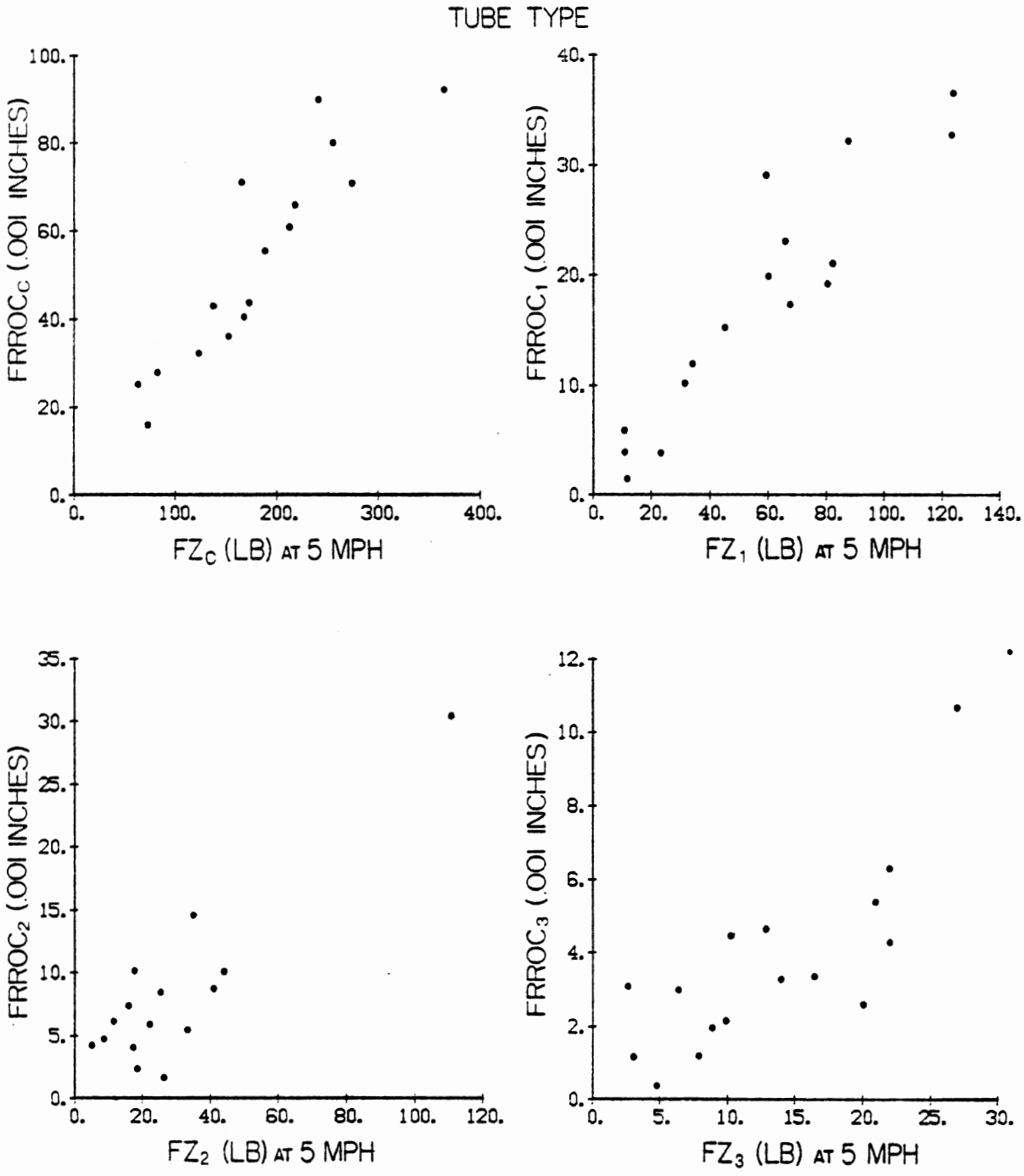

Figure A.2. Relationship of radial force variations to free radial runout on the centerline for tubeless tires.

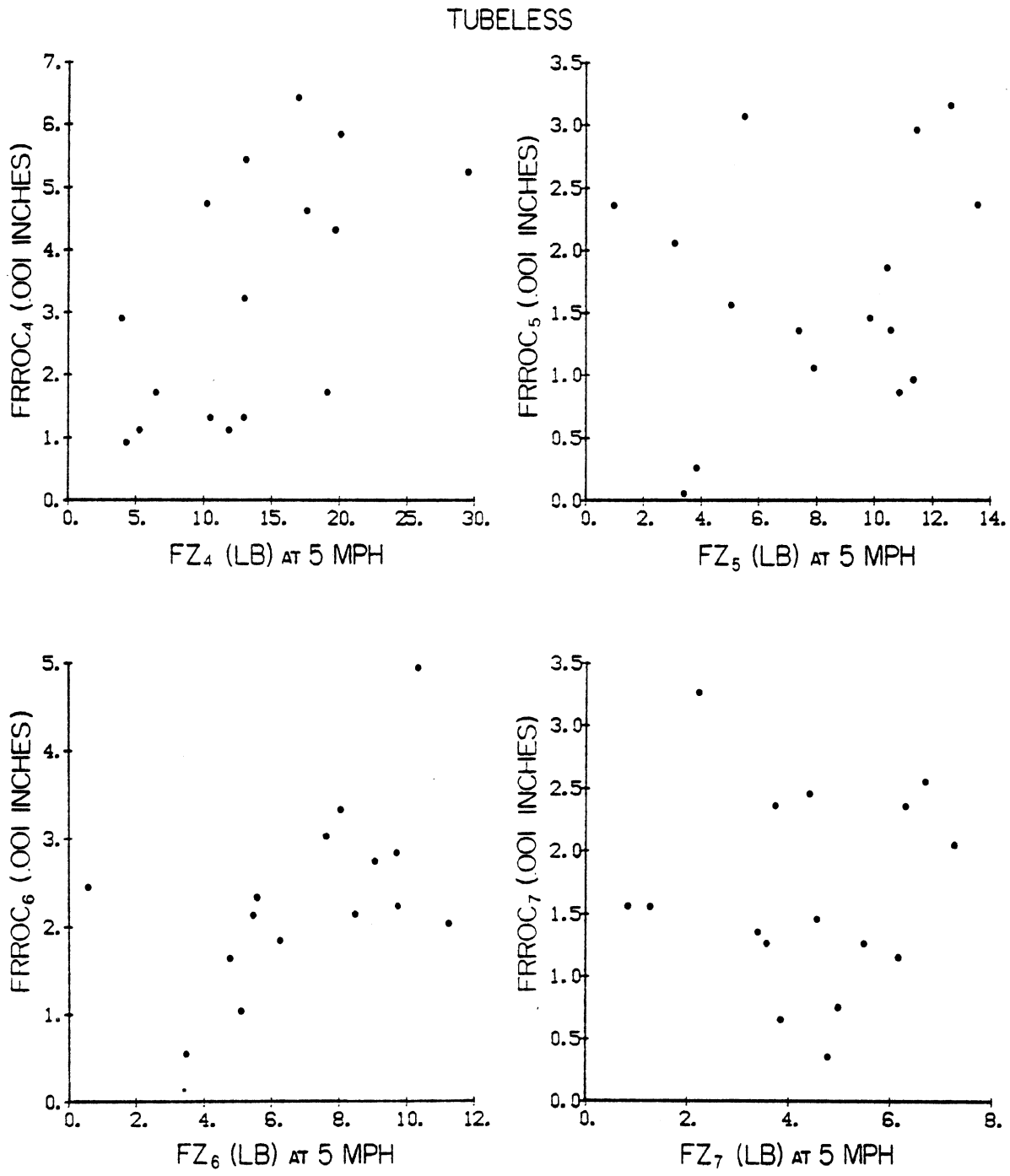

Figure A.2 (Cont.)

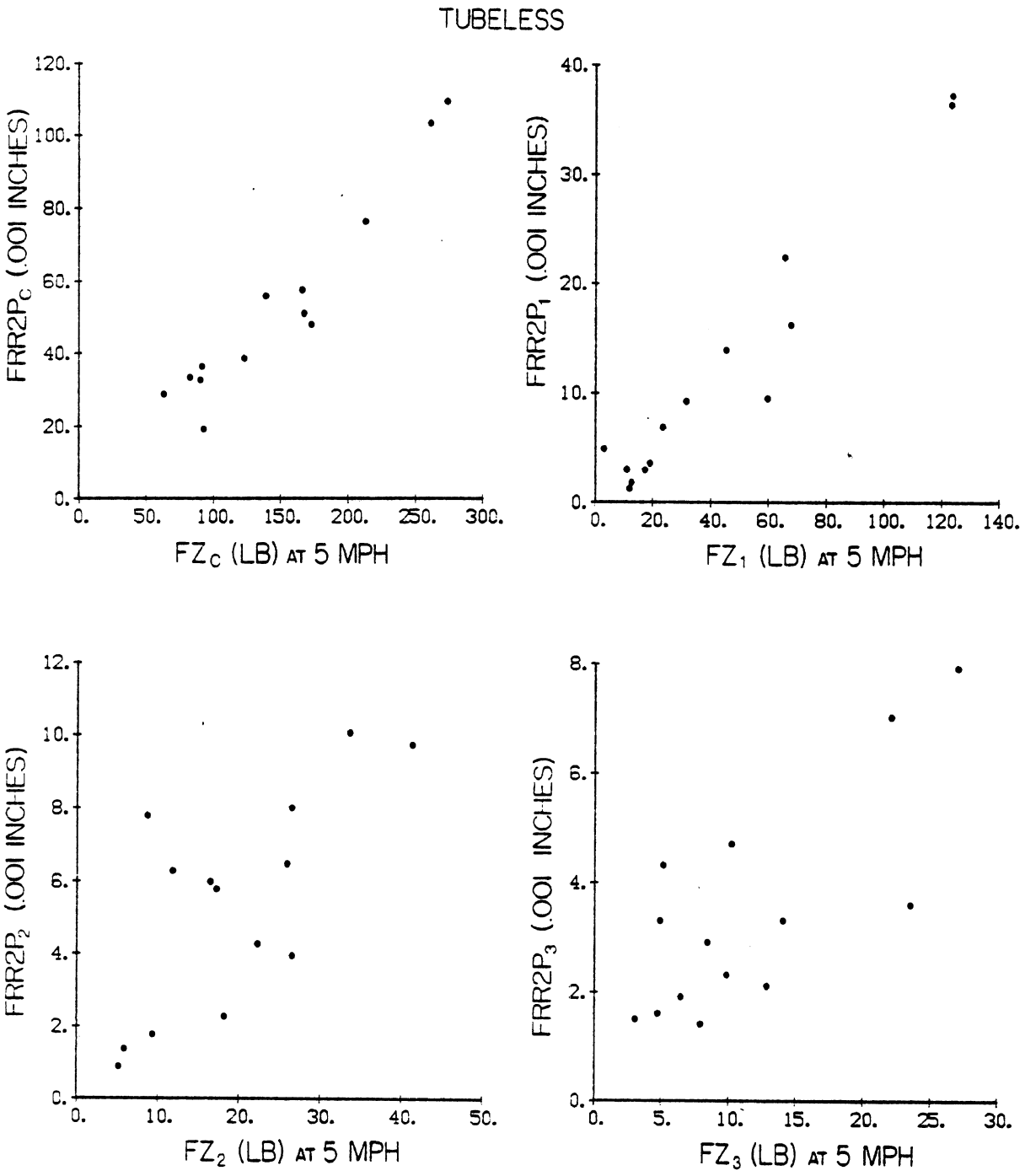

Figure A.3. Relationship of radial force variations to 2-point free radial runout for tubeless tires.

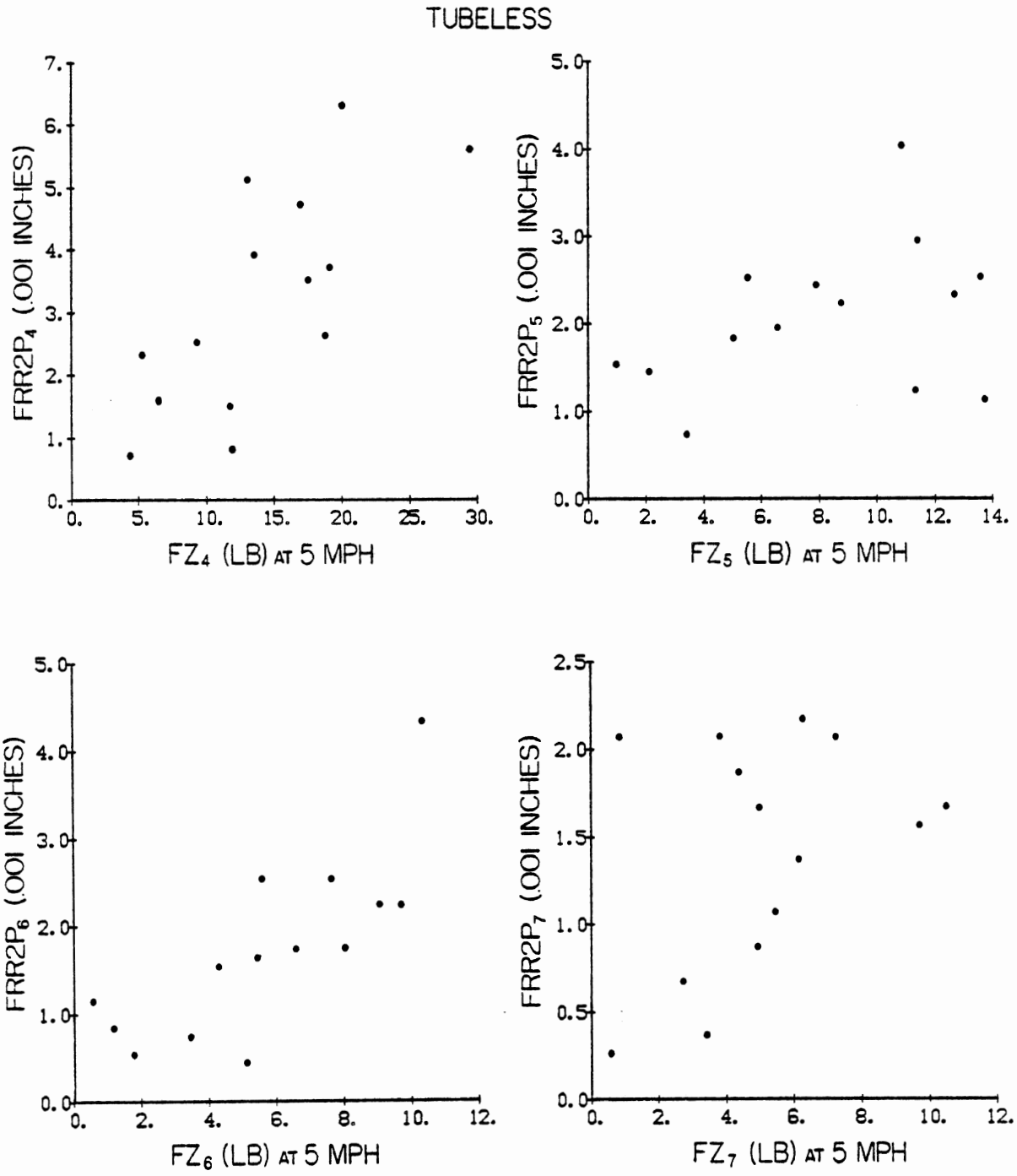

Figure A.3 (Cont.)

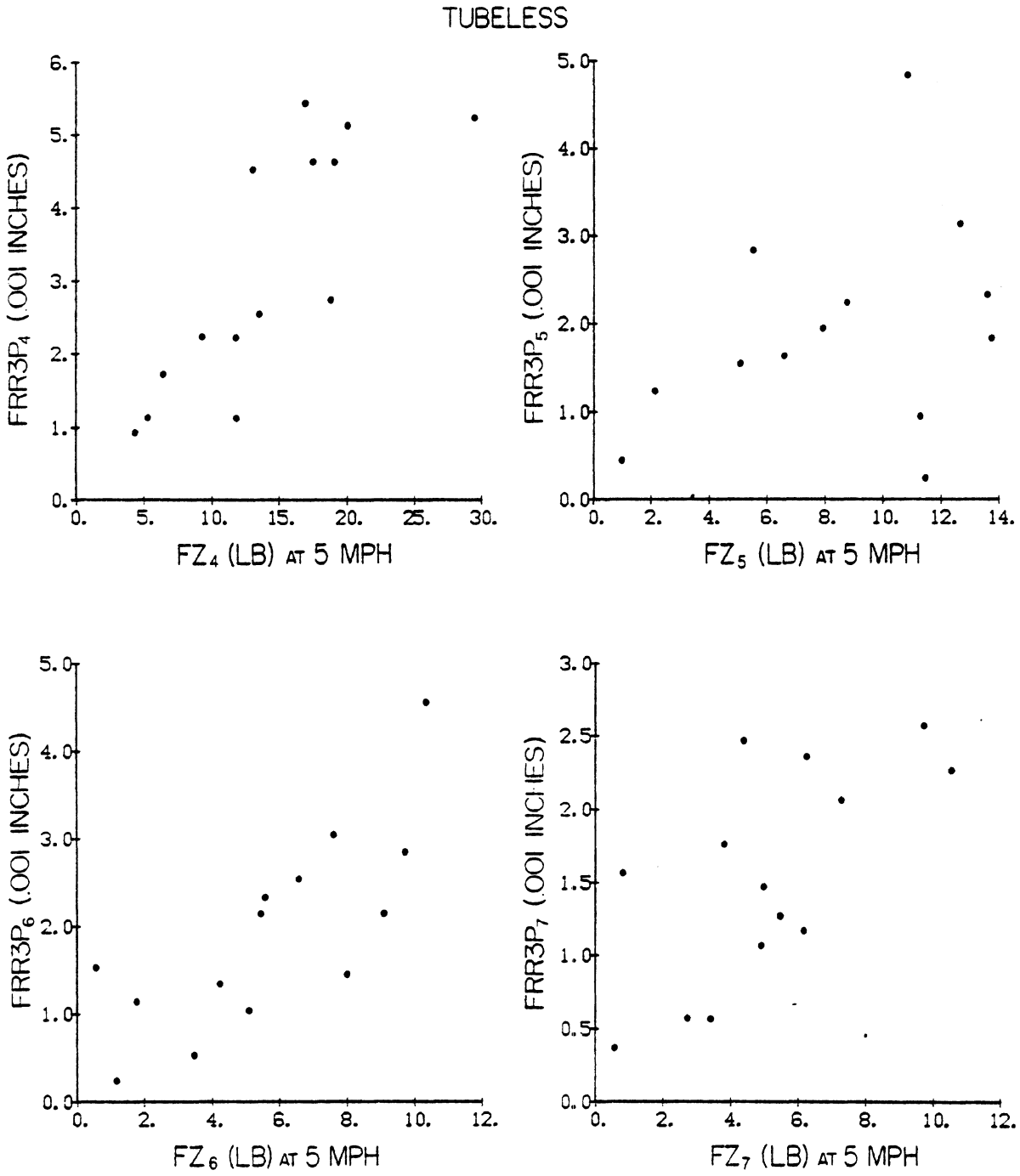

Figure A.4. Relationship of radial force variations to 3-point free radial runout for tubeless tires.

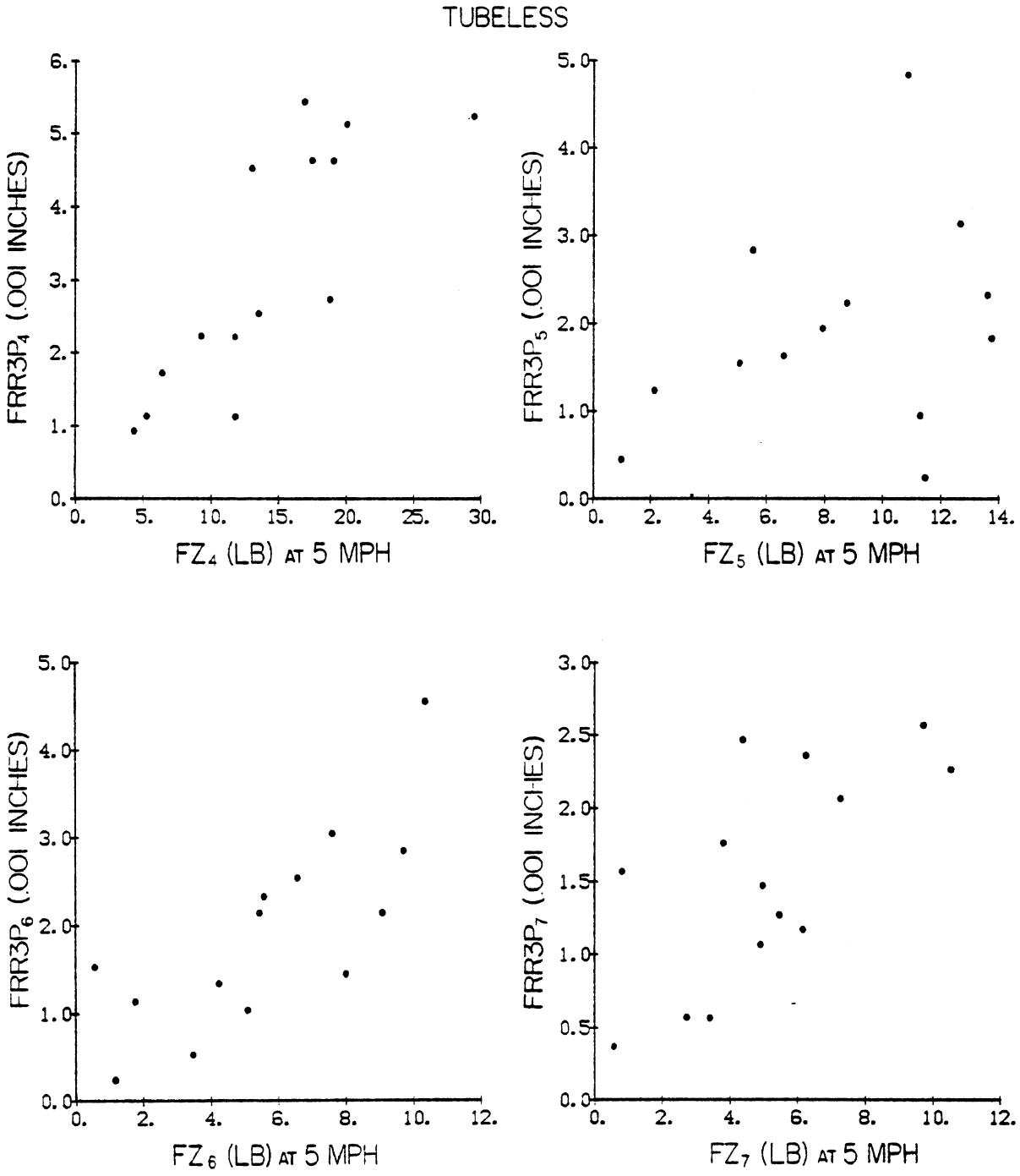

Figure A.4 (Cont.)

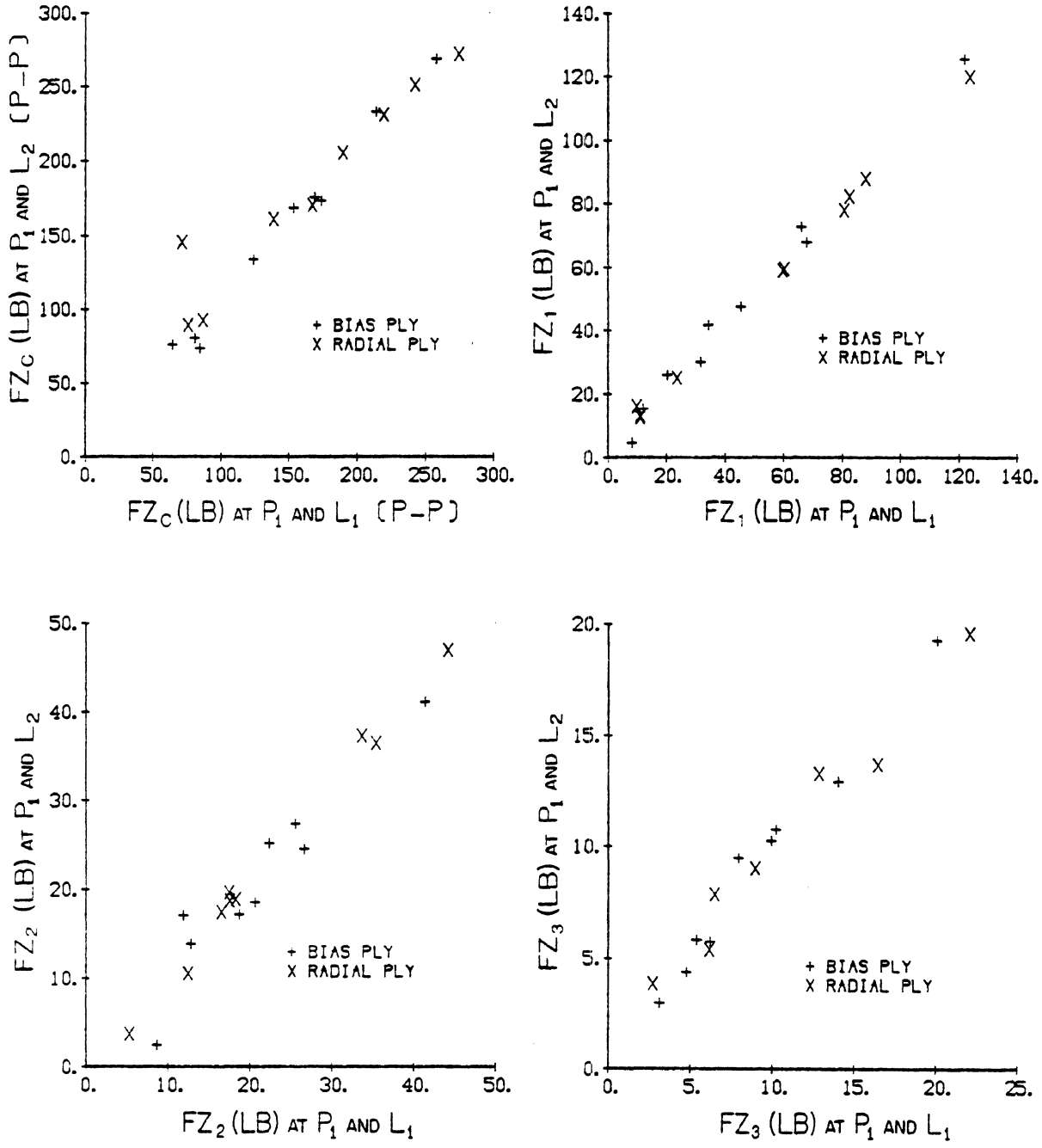

Figure A.5. Effect of load on radial force variations for tubeless tires: L_1 = 5430 lbs, L_2 = 4073 lbs.

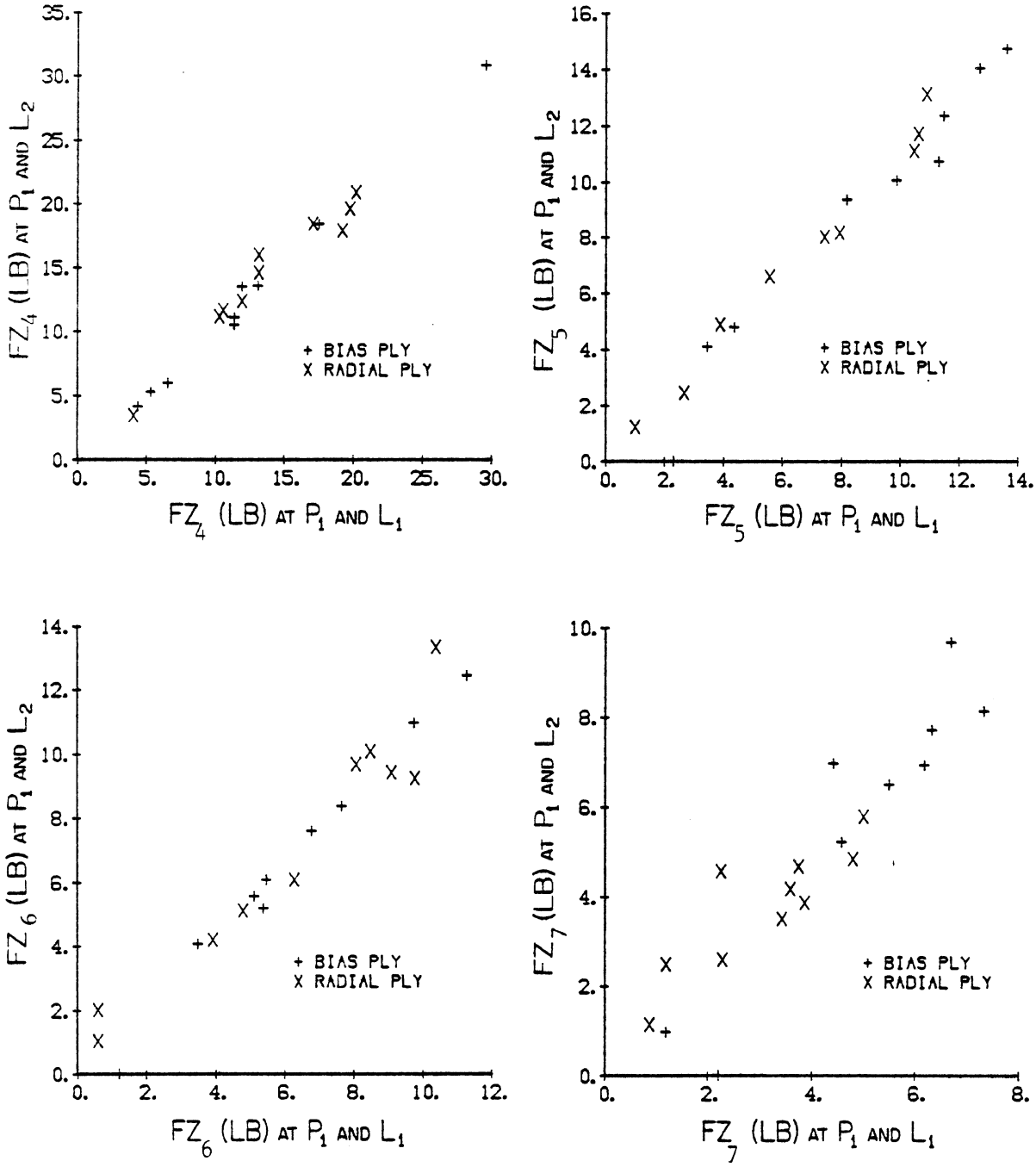

Figure A.5 (Cont.)

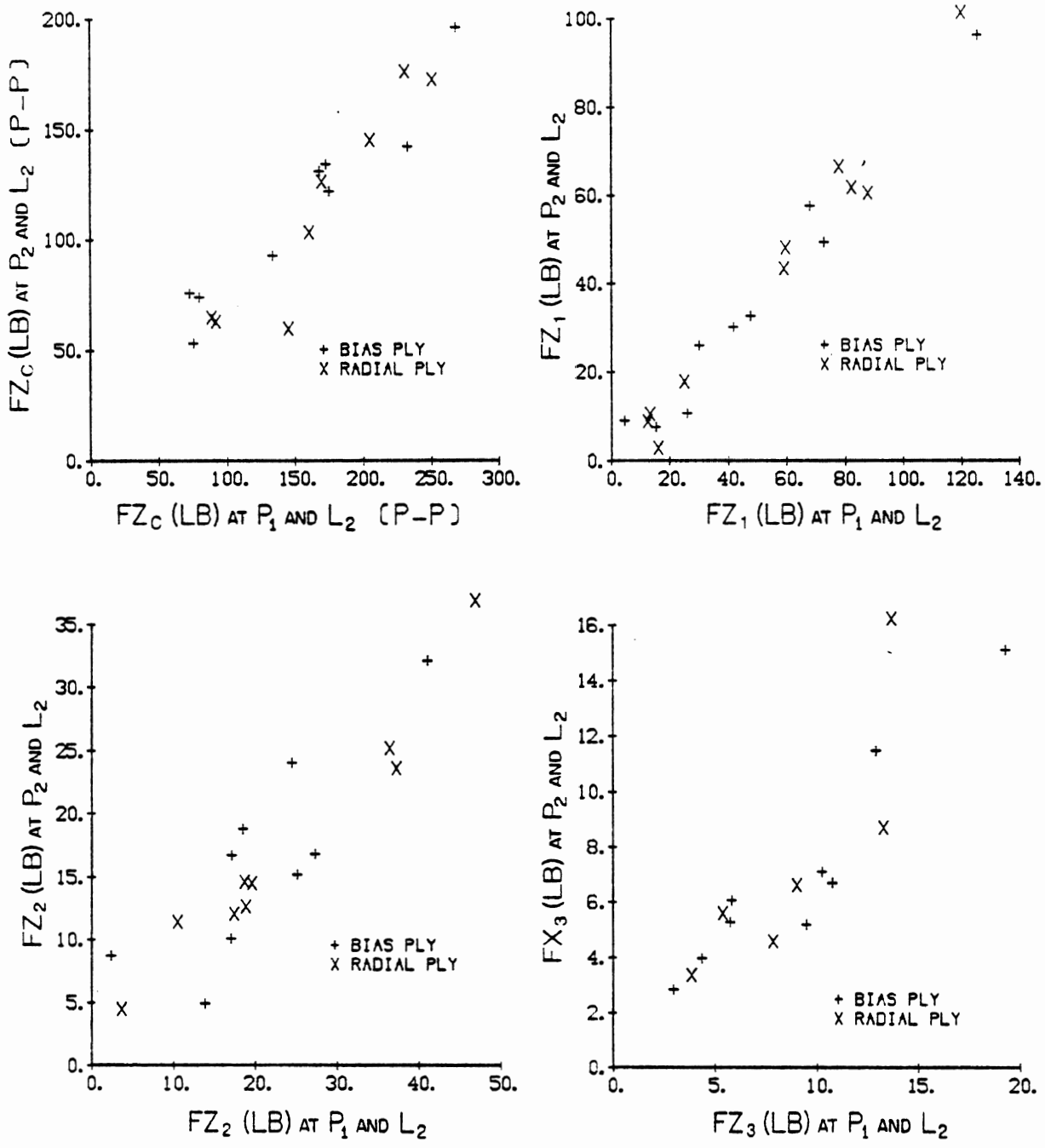

Figure A.6. Effect of pressure on radial force variations for tubeless tires; P_1 = 100%, P_2 = 75% of rated pressure.

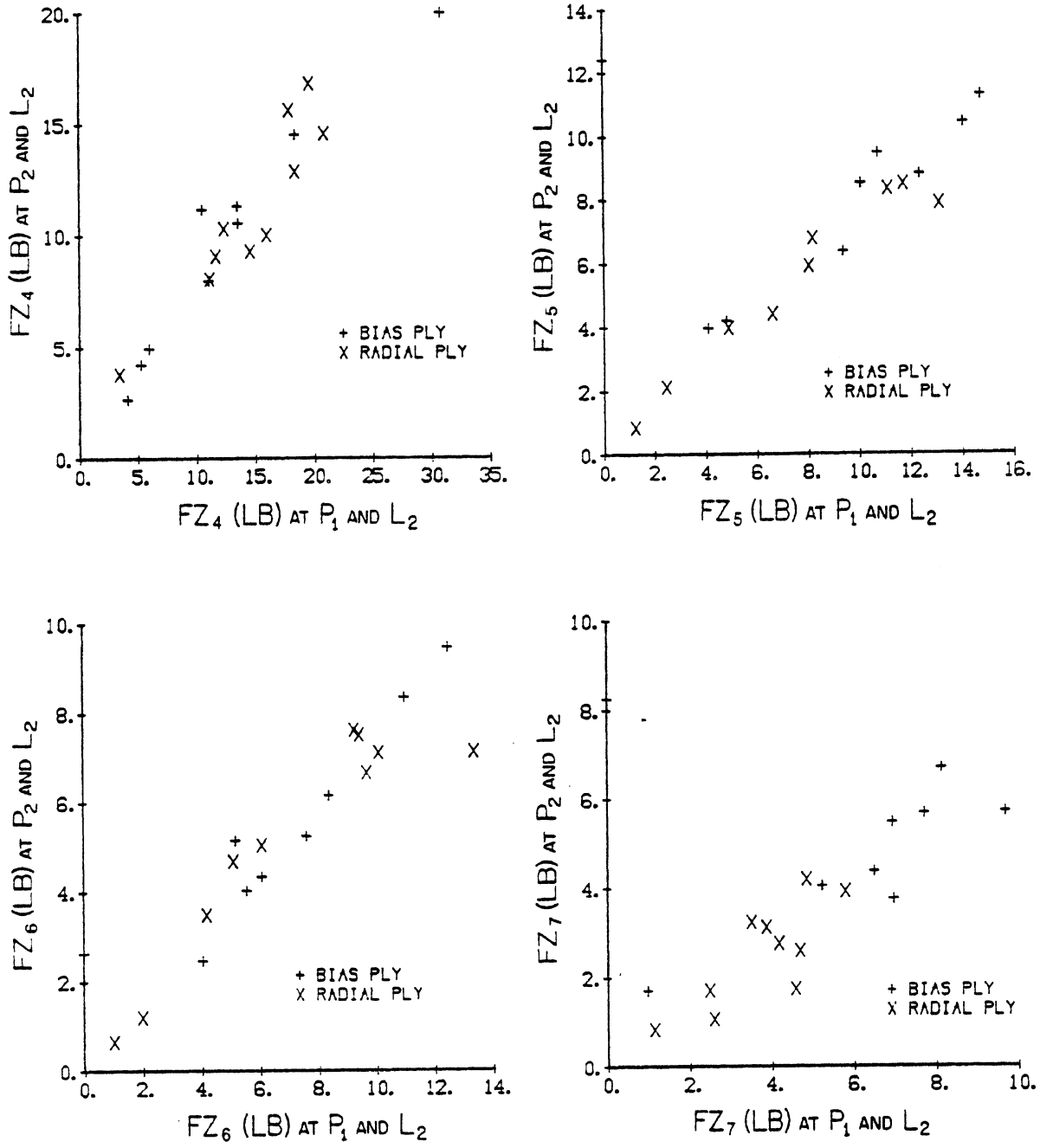

Figure A.6 (Cont.)

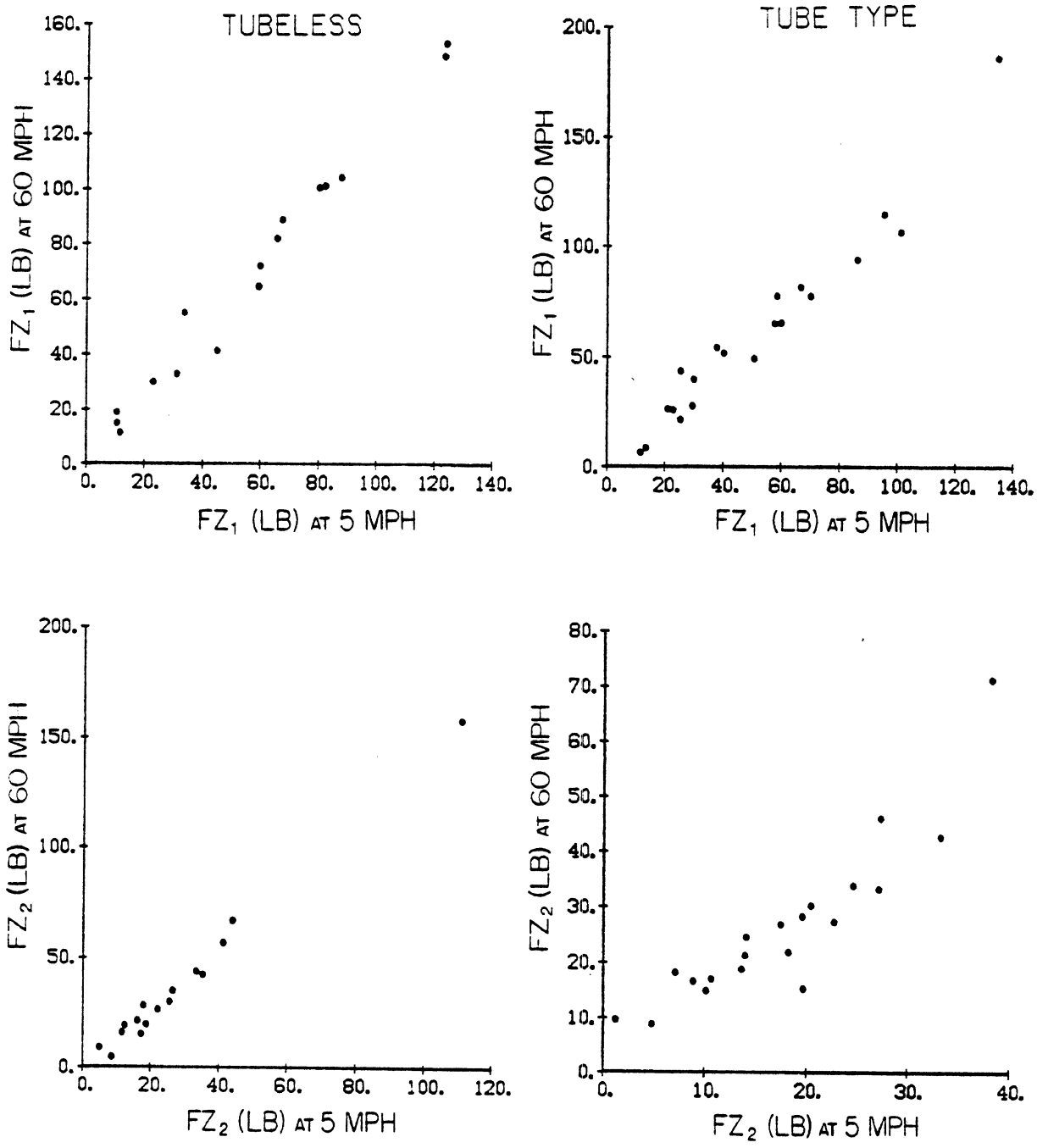

Figure A.7. Effect of speed on radial force variations.

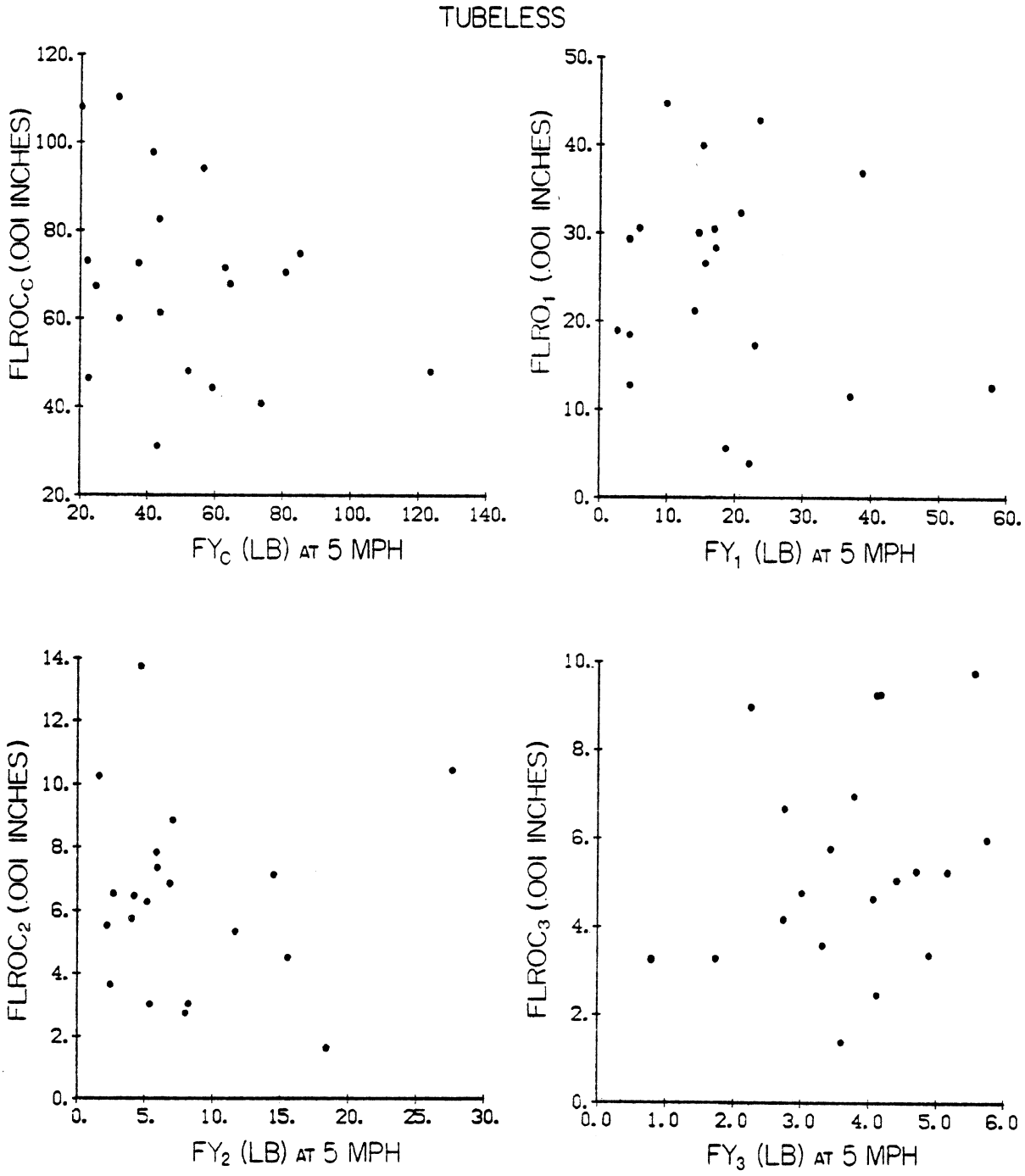

Figure A.8. Relationship of lateral force variation to free lateral runout.

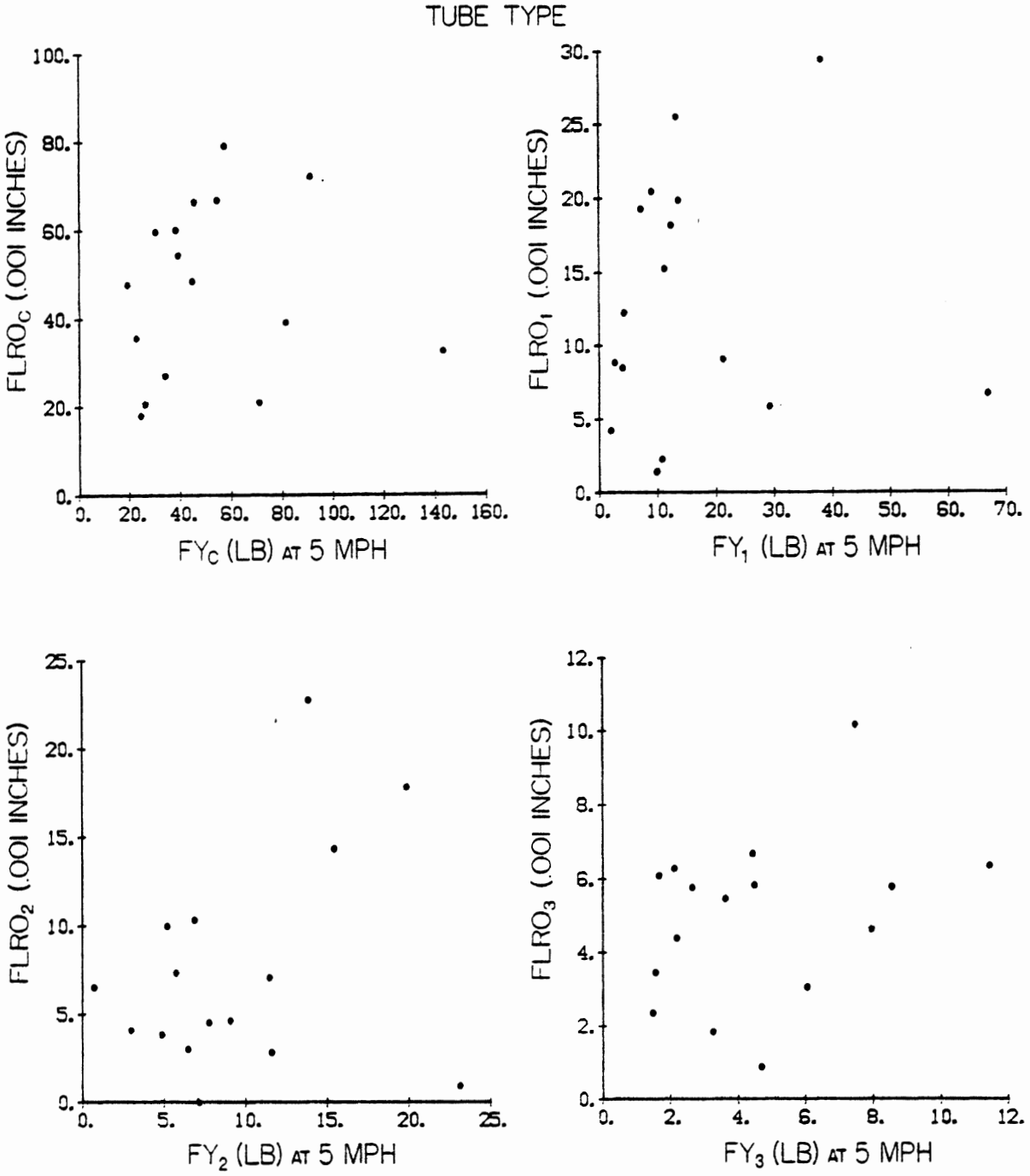

Figure A.8 (Cont.)

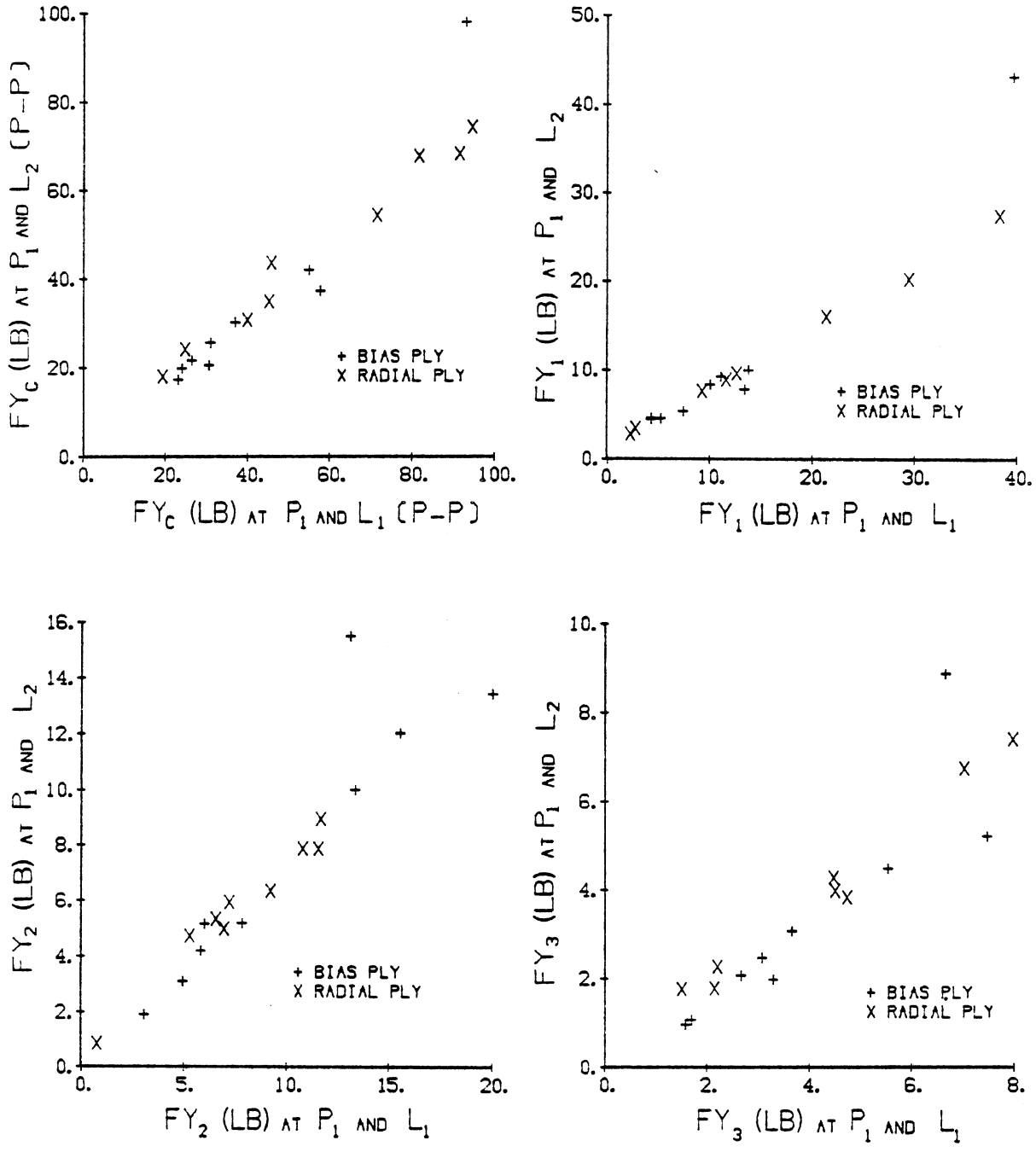

Figure A.9. Effect of load on lateral force variations for tubeless tires; L_1 = 5430 lbs, L_2 = 4073 lbs.

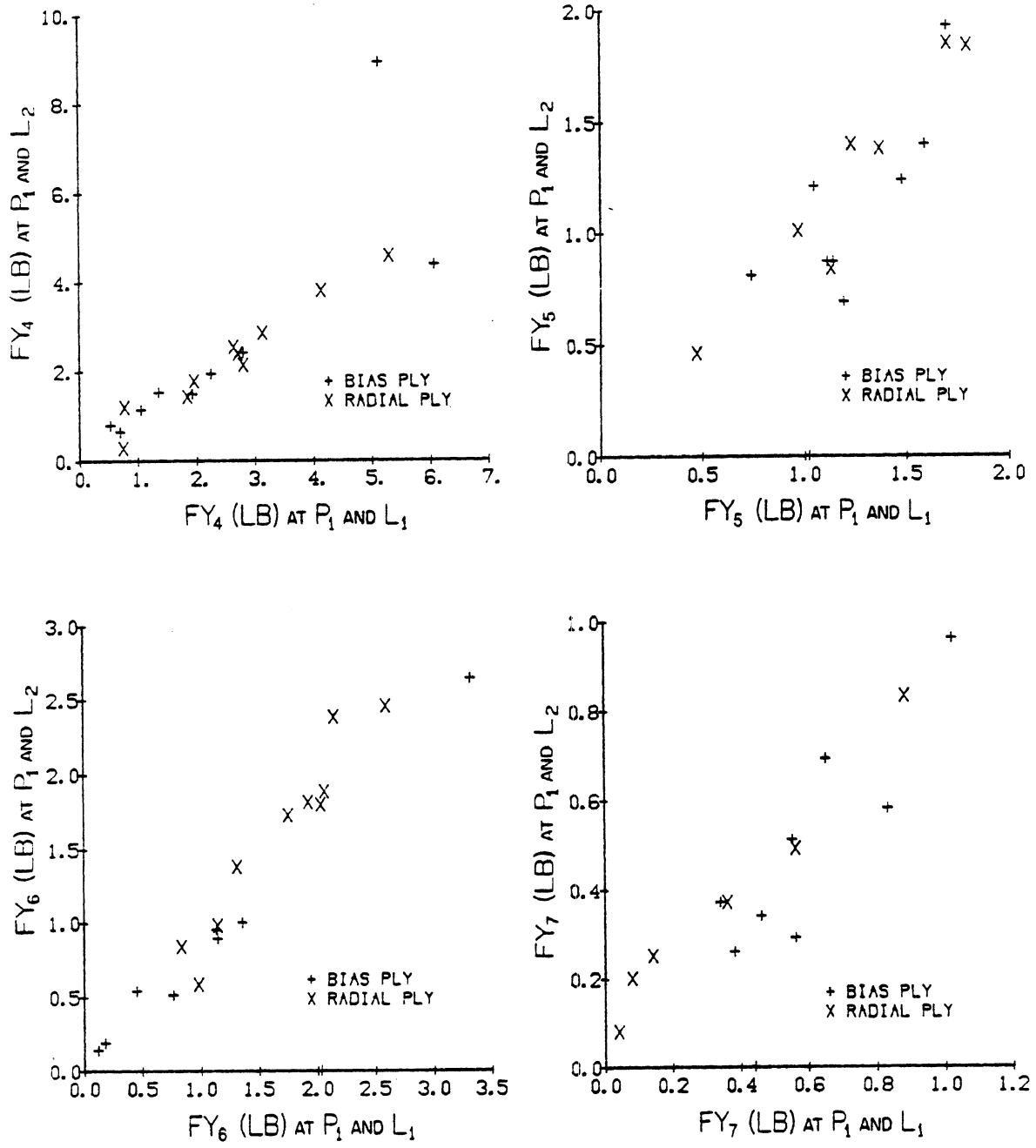

Figure A.9 (Cont.)

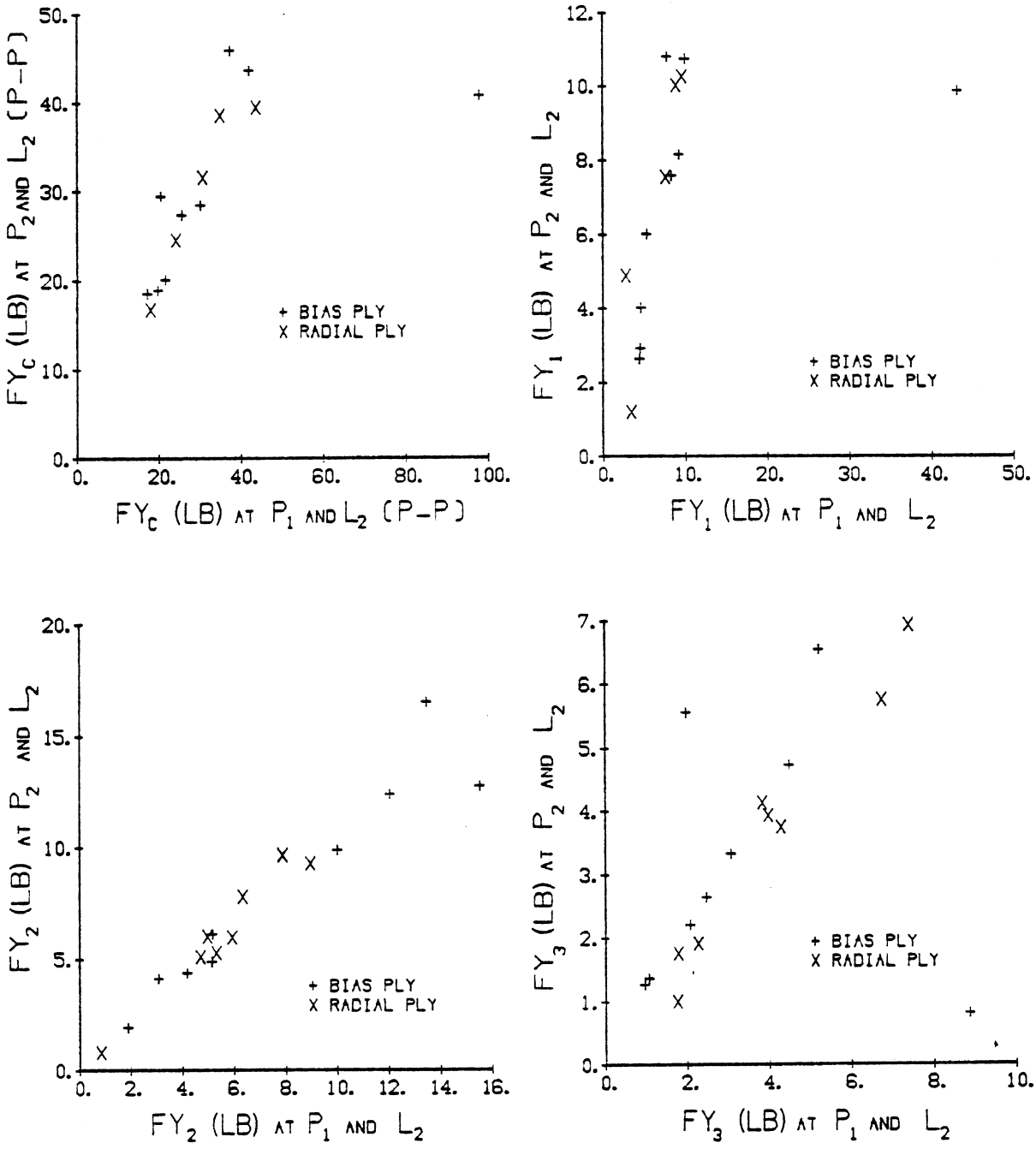

Figure A.10. Effect of pressure on lateral force variations for tubeless tires; P_1 = 100%, P_2 = 75% of rated pressure.

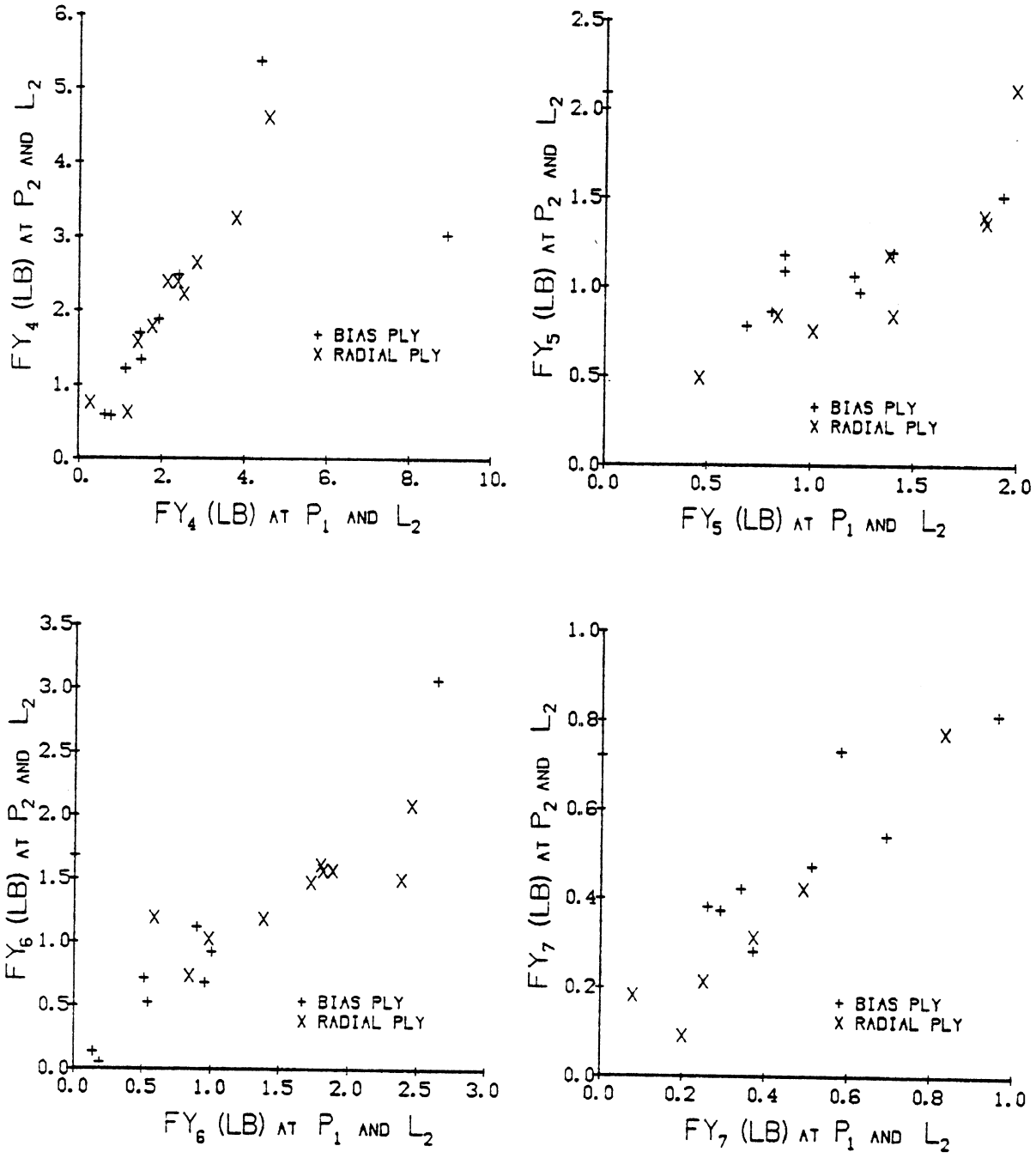

Figure A.10 (Cont.)

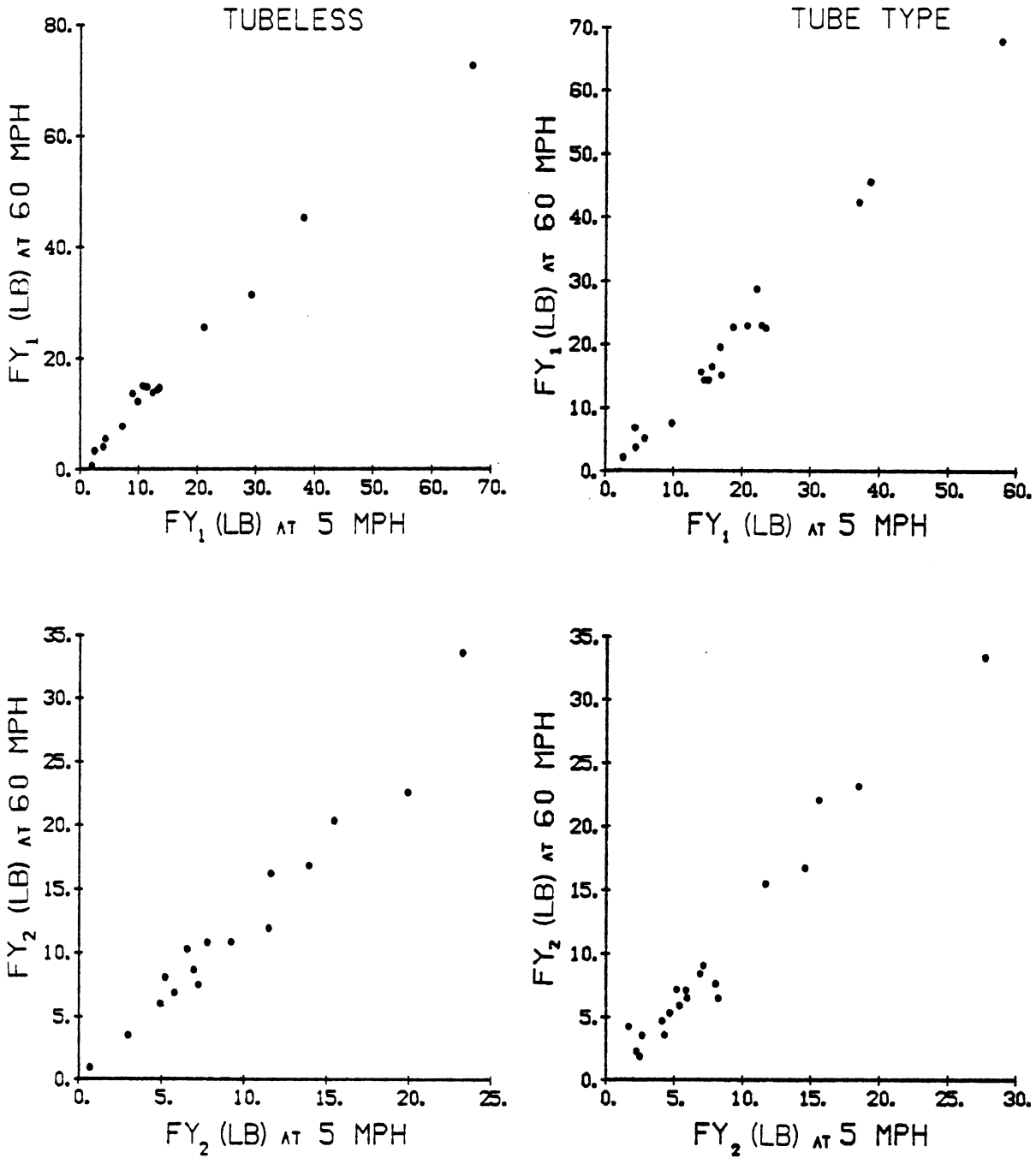

Figure A.11. Effect of speed on lateral force variations.

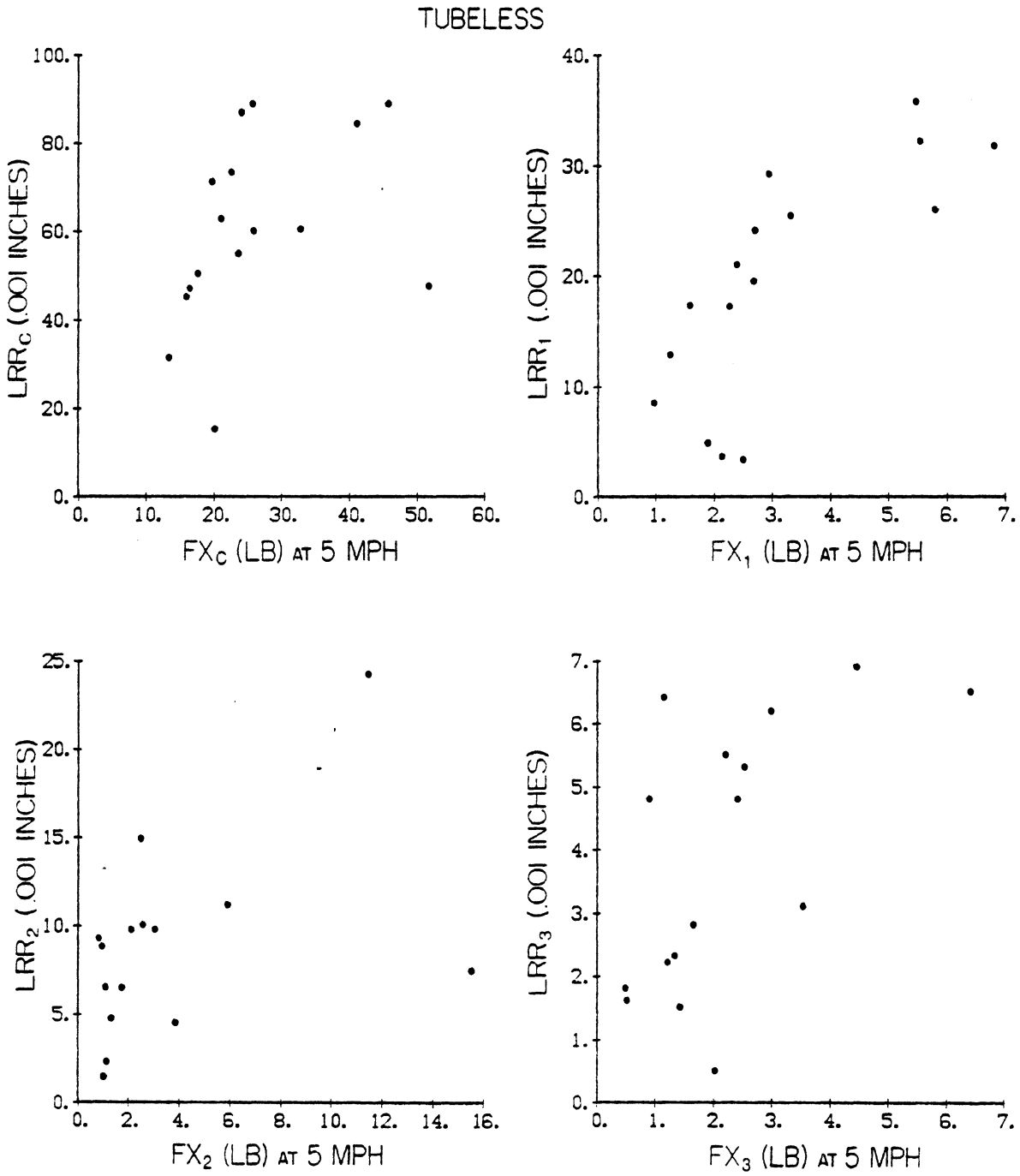

Figure A.12. Relationship of tractive force variations at 5 mph to loaded radial runout.

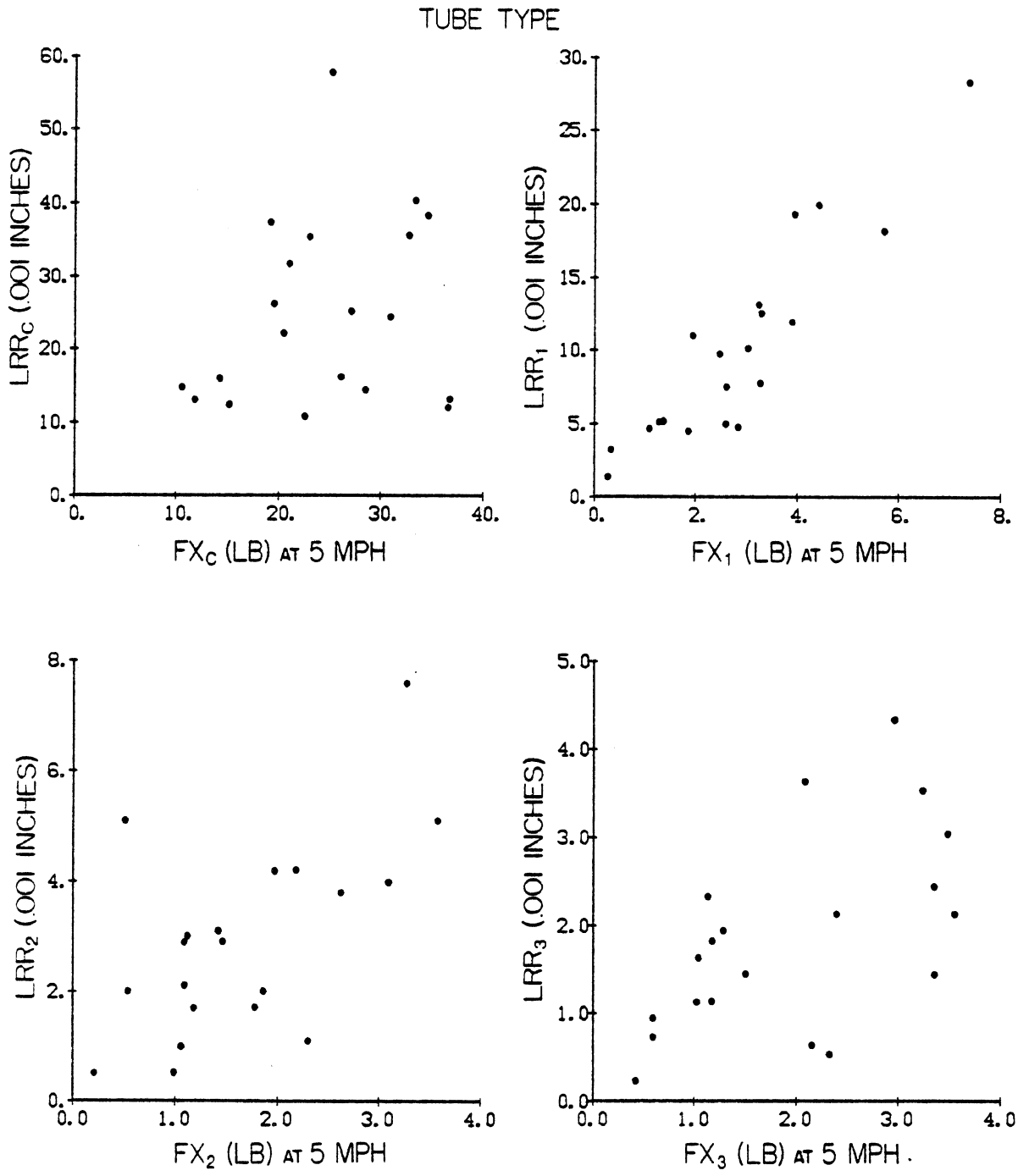

Figure A.12 (Cont.)

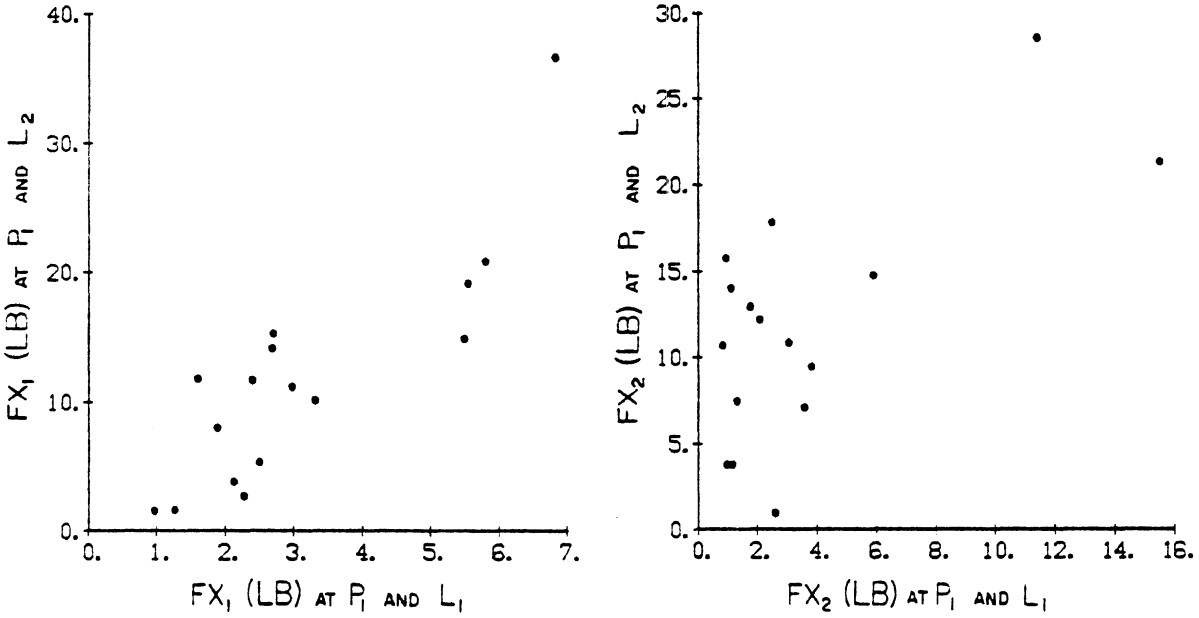

Figure A.13. Effect of load on tractive force variations for tubeless tires; L_1 = 5430 lbs, L_2 = 4073 lbs.

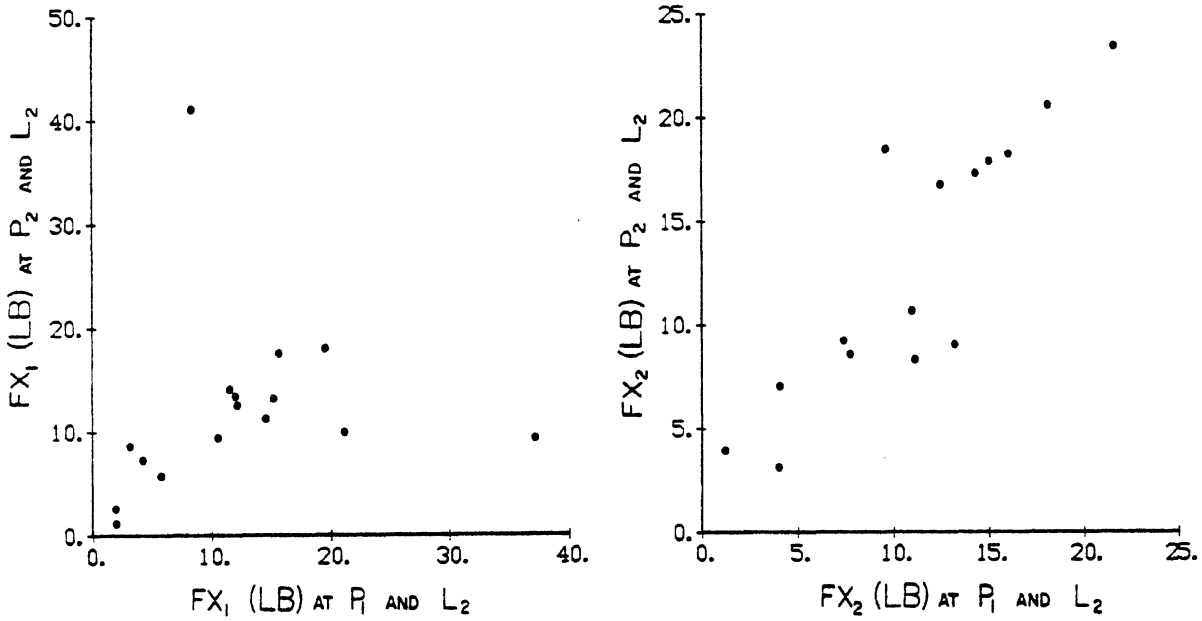

Figure A.14. Effect of pressure on tractive force variations for tubeless tires; P_1 = 100%, P_2 = 75% of rated pressure.

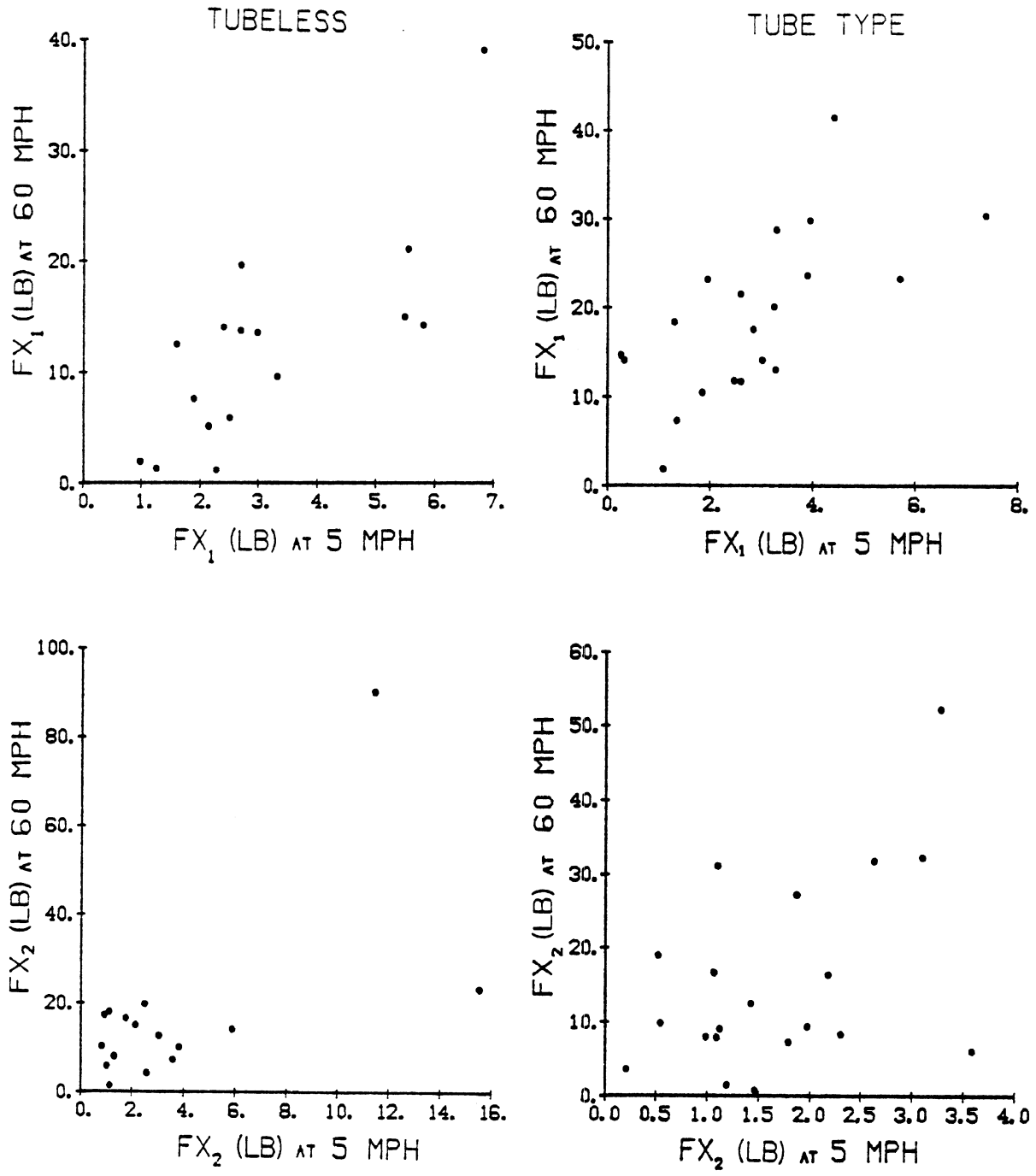

Figure A.15. Effect of speed on tractive force variations.

APPENDIX B

PLOTS OF TIRE/WHEEL ASSEMBLY UNIFORMITY TEST RESULTS

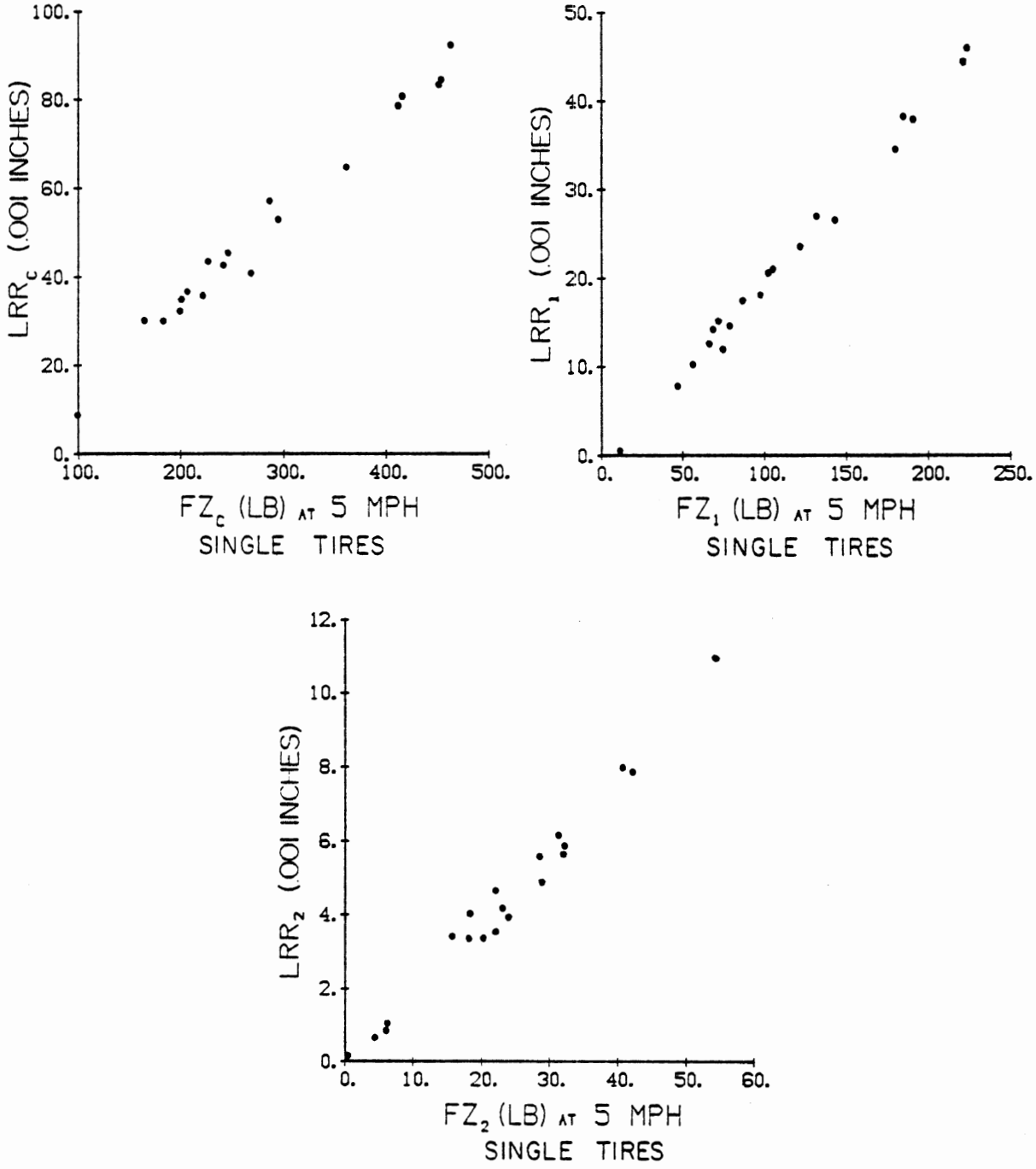

Figure B.1. Relationship of radial force variations to loaded radial runout for single and dual tire/wheel assemblies.

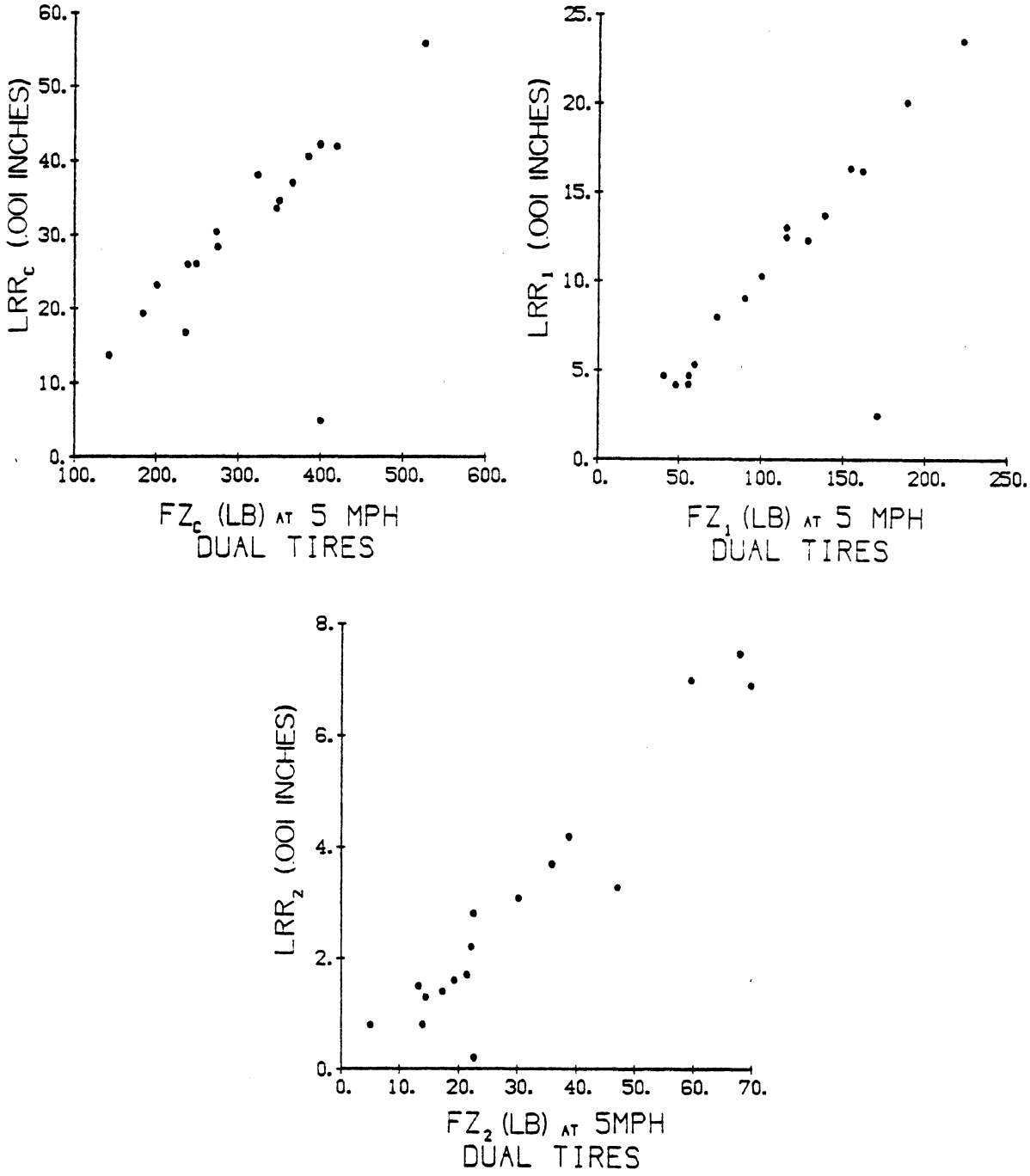

Figure B.1 (Cont.)

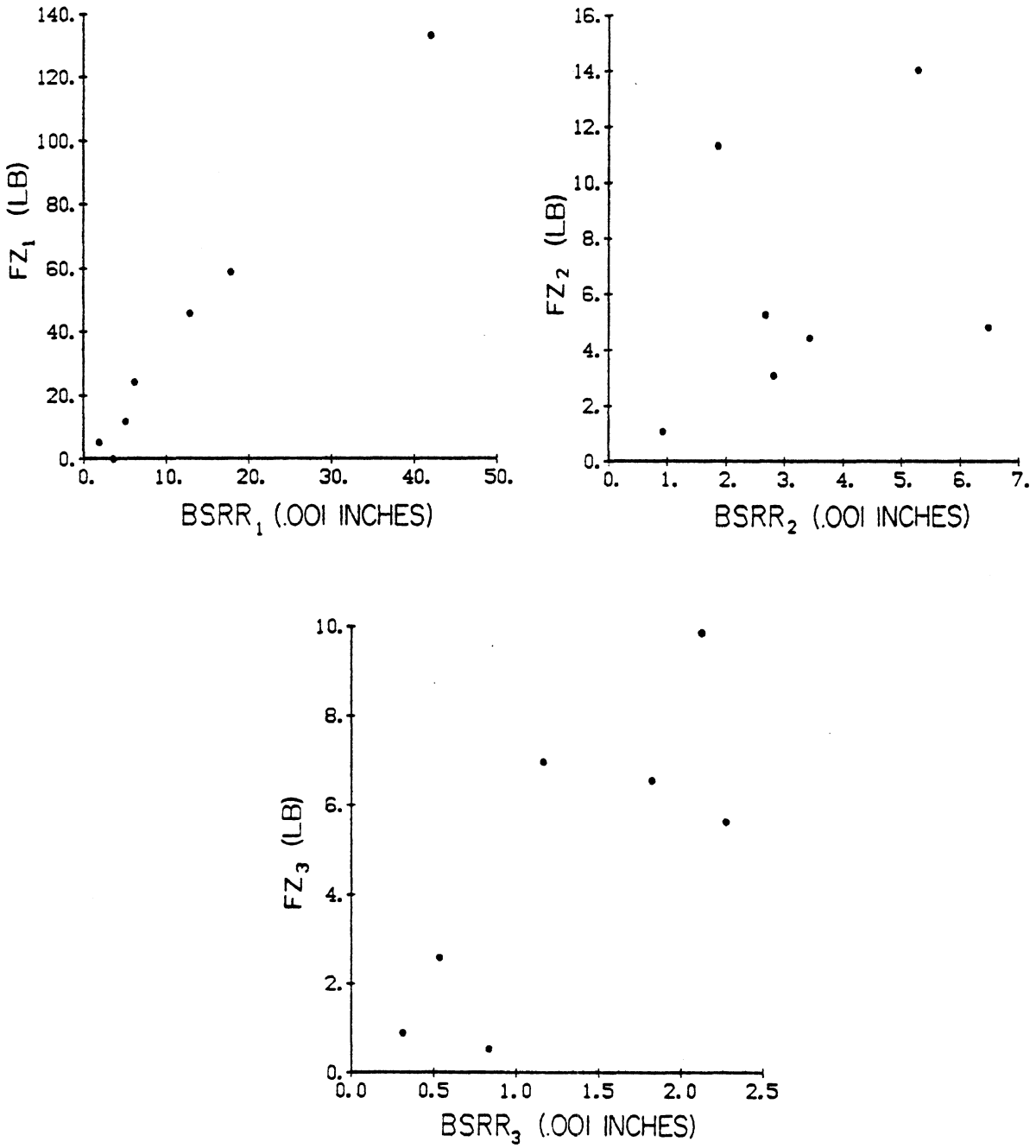

Figure B.2. Relationship of radial force variations attributable to the wheel to bead seat radial runout, on single wheels.

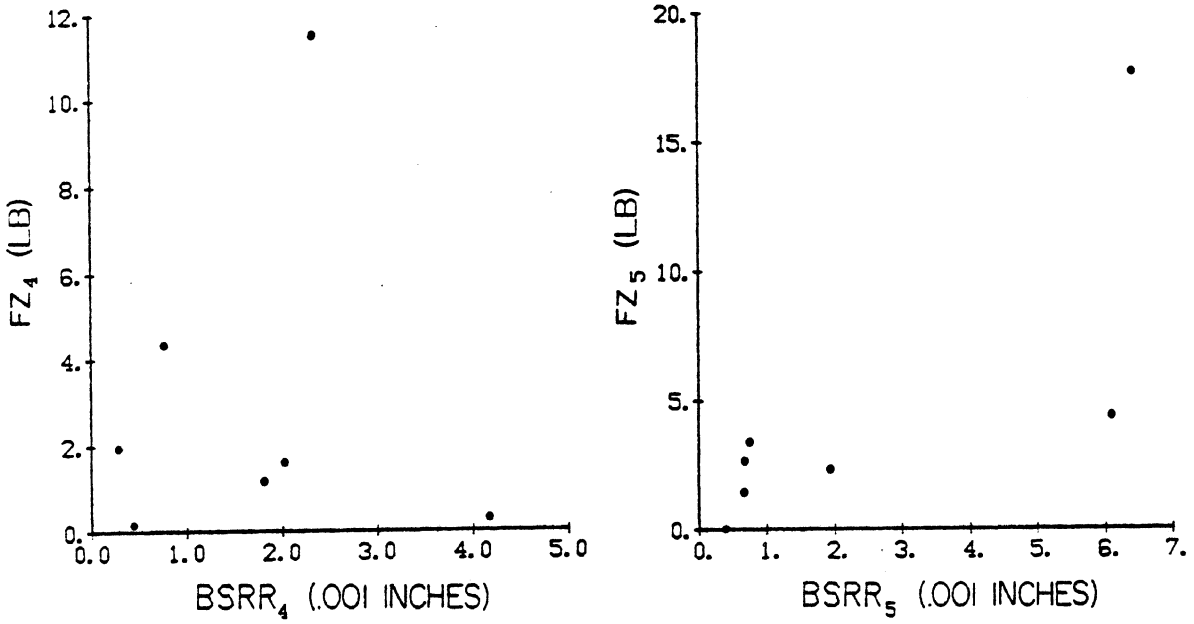

Figure B.2 (Cont.)

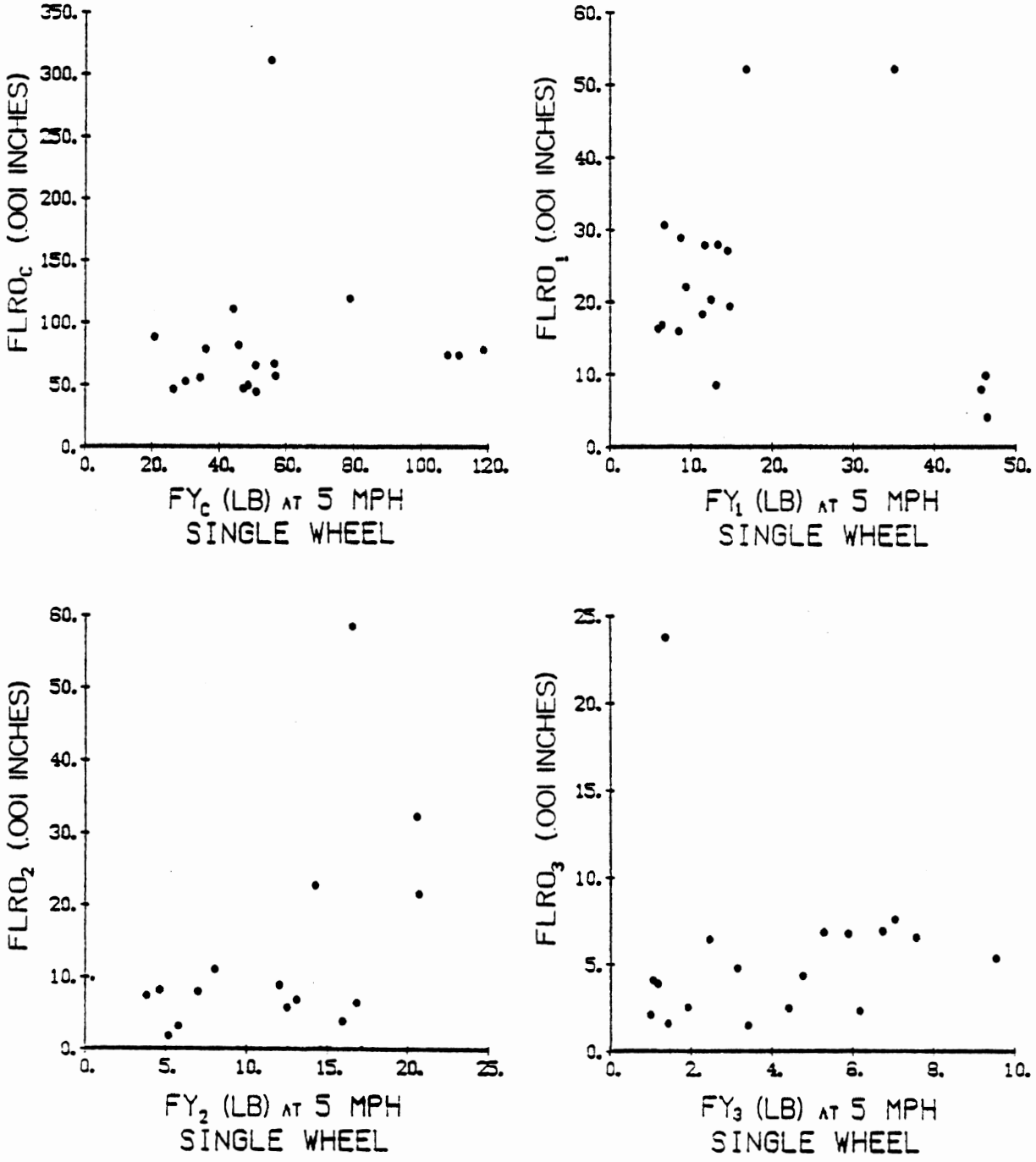

Figure B.3. Relationship of lateral force variations in a tire/wheel assembly to free lateral runout.

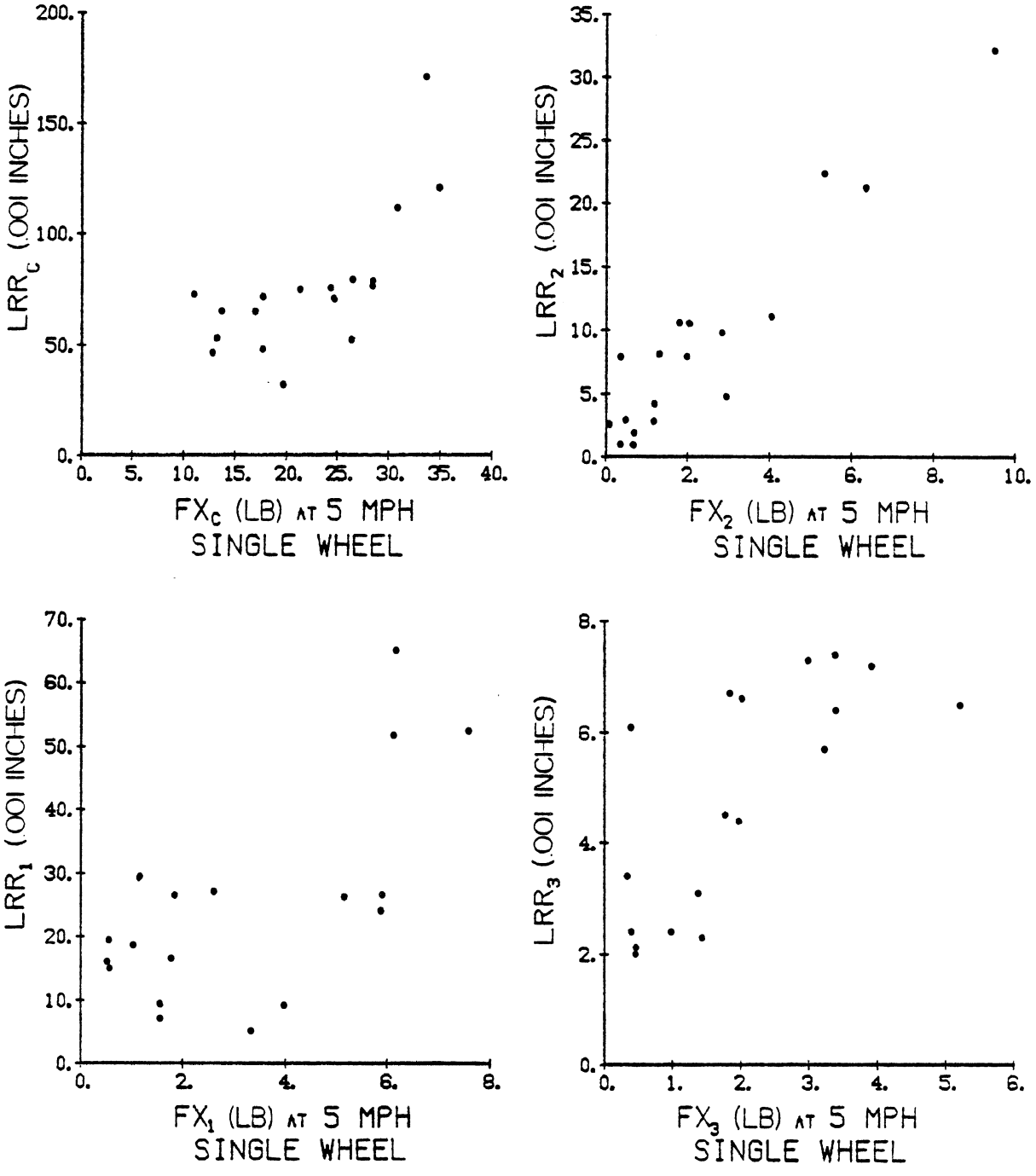

Figure B.4a. Relationship of tractive force variations to loaded radial runout for single wheels.

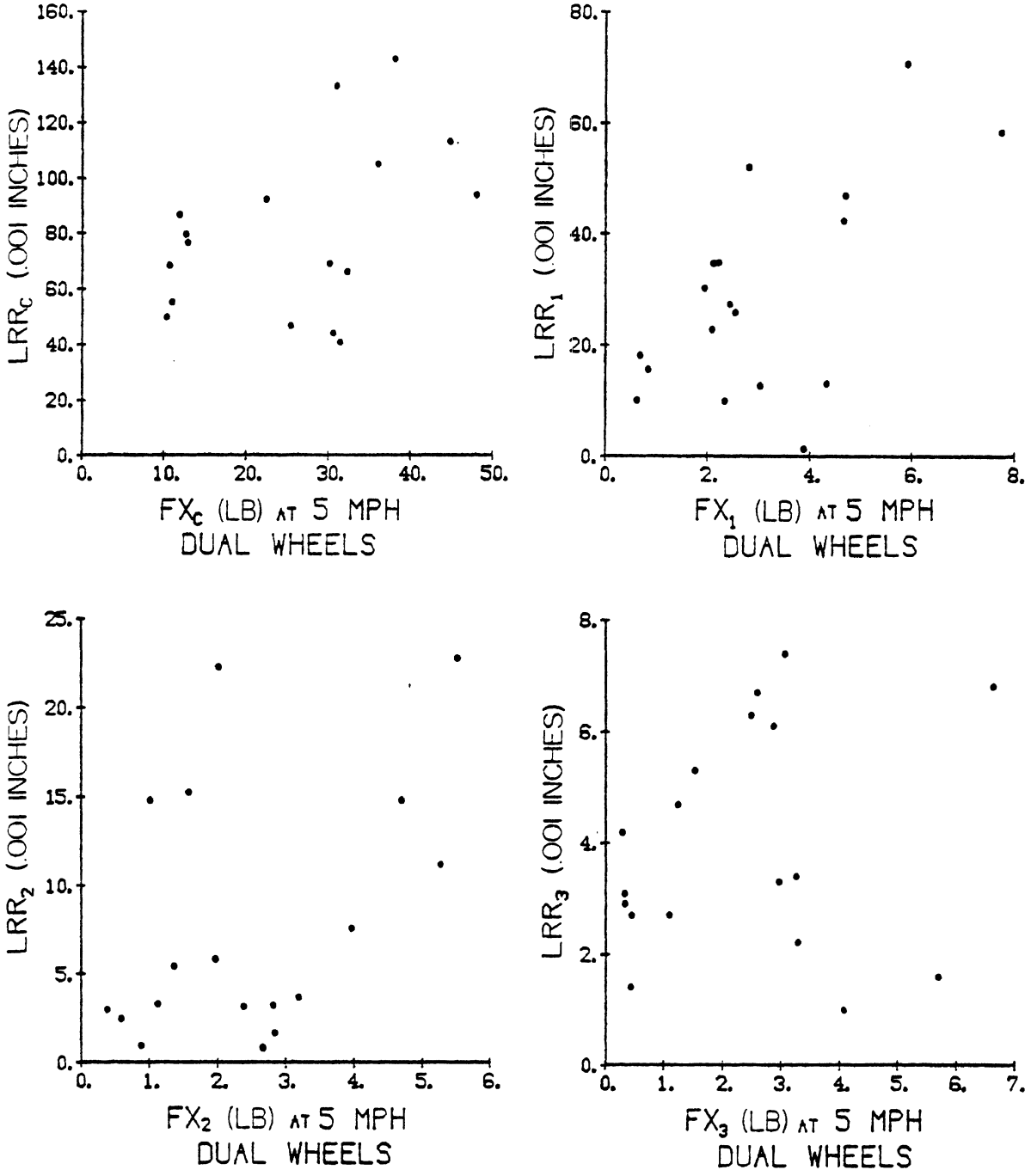

Figure B.4b. Relationship of tractive force variations to loaded radial runout for dual wheels.

APPENDIX C

FLAT-BED TIRE UNIFORMITY TEST RESULTS

Michael Sayers

Introduction

This appendix documents tests of truck tire force variations on a flat-surface machine conducted under the Truck Tire/Wheel Systems Research Program sponsored jointly by the Motor Vehicle Manufacturers Association (MVMA) and the Rubber Manufacturers Assocation (RMA). An objective in the research is to quantify the force and moment variations of free-rolling truck tire/wheel assemblies that result from nonuniformities in the individual components of the assembly. The program is designed around component testing on an MTS Systems Corporation Model 860 (67.23-inch diameter drum type) tire test machine, covering various types of tires and wheel components with different levels of nonuniformities. The periodic force and moment signals are processed by computer to yield amplitudes and phase angles of up to 10 harmonics of the tire/wheel assembly. The measurements are ideally made with the spindle position rigidly fixed so that the forces are not influenced by spindle motion.

The contact patch between the tire and drum is about one-tenth of the tire circumference, hence there is reason to suspect that forces measured on the curved surface of the MTS machine drum will differ from those produced on the flat surface of a road. It is expected that the differences are more significant for the higher harmonics than the lower ones because they correspond to physically shorter wavelengths nearer the size of the contact patch. In order to quantify these differences, 10 truck tires were tested on the UMTRI flat-bed tire test machine.

The tires were tubeless size 11-22.5, and were provided by five manufacturers, each of whom is represented by one radial and one bias-belted type. The tires were selected from a group of 90 tires representing different uniformity quality levels, as measured by the manufacturers prior to shipping. All were tested at their rated pressure (85 psi for bias, 105 psi for the radials) and at 85 percent of their rated loads (85 percent levels were 4612 lbs for bias and 5134 lbs for radial).

The remainder of this appendix details the test equipment, the interaction of various error effects in the measured force signals, and the test method that was developed to compensate for those effects and allow extraction of the tire force variation information. It concludes by presenting the significant final results.

Test Apparatus

The flat-bed tester (see Fig. C.1) is routinely used to obtain precise measurements of the mechanical characteristics of rolling and standing tires. It accommodates passenger-car and truck tires ranging from 24 to 44 inches in diameter and can apply vertical loads of up to 10,000 lbs. The device is designed for low-speed tests at steer angles between ± 90 degrees and camber angles between $\pm$ 20 degrees, and is instrumented to measure the three forces and three moments developed by the tire. For these tests, the flat-bed surface was carefully set up with shims to reduce its unevenness to the minimum practical level ($\sim$ .01 inch) as measured statically. Because the moving table is supported by rollers, spaced one foot apart, it is not possible to remove all variations in the elevation of the table under load. Hence, the force variations measured reflect movement of the bed, as well as the forces generated by tire/wheel nonuniformity. The table also allows a small amount of lateral free play which can act to lower the lateral force generated by the tire.

The tires were mounted on an 8.25 x 22.5-inch precision wheel designed for use on the flat-bed machine. Though precise in its rim contours, this wheel is a multi-piece assembly designed to allow tire mounting while installed on the machine. The assembly tolerances are normally of no significance in low-speed measurement of steady-state tire properties. However, for these tests it was necessary to assemble and carefully shim the clearance spaces with each tire mount.

Test data were acquired by using the analog conditioners for the six load cells on the machine, together with a portable digital data acquisition system. Designed and built in-house, this system consists of

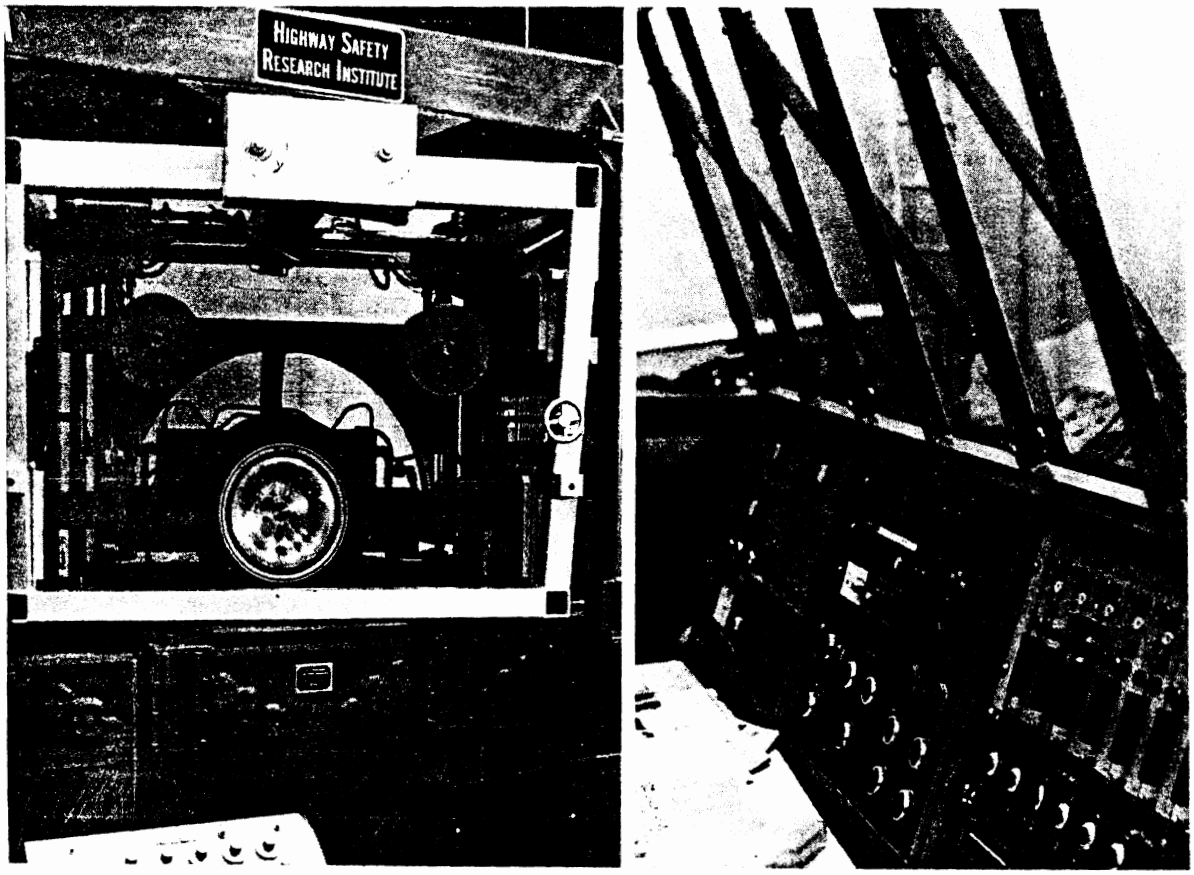

Figure C.1. UMTRI Flat-Bed Tire Test Machine.

a microprocessor (Texas Instruments TM 990), a conditioning unit with adjustable amplifiers, bias controls, voltage supplies (for transducers requiring a calibrated voltage such as potentiometer and load cells), programmable filters, analog-to-digital converters, and digital-to-analog converters. The system has its own CRT display and keyboard control unit, but can be coupled to any computer teriminal. Besides being able to effectively calibrate itself, the system is set by keyboard commands to vary sample frequency, number of channels, and test duration. Data are stored on standard digital tape cartridges (via a Columbia Data Products 300B recorder) for subsequent processing on a larger computer, although the microprocessor is programmed to calculate simple statistics from the data, if asked.

The data acquisition system was set to sample 100 samples/sec, which, at the flat-bed speed of 2.4 ft/sec, usually gives 500 or so samples/revolution. A switch on the frame of the tire test machine is triggered by a point on the flat-bed as it moves by to start the data sampling. Hence, all data records begin at the same location on the flat-bed, regardless of the wheel position. The flat-bed is long enough to obtain about 1-1/2 wheel revolutions, so the data sampling begins after the wheel has rotated about 1/5 revolution to eliminate speed-up effects. A rotary potentiometer is used to sense the angular position of the wheel; hence, force measurements can also be related precisely to the wheel angular position.

Signals from six independent load cells are each passed through a low-pass filter to eliminate a rather large amount of higher frequency noise caused by machine vibrations and electronic sources, and also to prevent aliasing. The filter properties have been measured and found to be nearly identical for all channels, having cut-off frequencies at about 2 Hz. Their transfer functions (gain and phase) from 0-2.4 Hz were recorded and are later used to correct distortion of the amplitudes and phases of the force and moment harmonics.

Data Analysis

The test data on the digital cartridge tapes are transferred to standard 9-track digital tape and analyzed on The University of Michigan computer system. The calculation of harmonics from each set of records is straightforward. First, the wheel rotation signal is scanned to determine the number of data samples in one wheel revolution. Data taken at the end of a revolution are discarded. At each of the remaining sample times, the six load cell measurements are multiplied by a cross-talk matrix, to remove inter-channel influences and provide records of the actual vertical force, lateral force, longitudinal force, and aligning moment. A general-purpose Fast Fourier Transform (FFT) program is employed to transform each of the four records, yielding a series of vectors defined by sinusoidal amplitudes and phases at each rotational harmonic up to 50 Hz, although all but the first 10 are discarded. These 10 harmonics are then corrected for amplitude attenuation and phase lag caused by the low-pass filters used in the data acquisition system. The wheel rotational signal is then used to adjust the phase angles such that the harmonics are references to the tire, rather than to the switch which triggered the data acquisition process during the test. These amplitudes and phases are stored in disk files so that they can be retrieved later.

Sources of Force Variation During Testing

The three forces and aligning moment measured during a test on the flat-bed machine derive from various sources, yet only one—the steady-state tire rolling nonuniformity—is of interest. When possible, the results of other sources are reduced by the design of the test methodology. Many sources of force variation can potentially exist, yet at the same time, they can be relegated into just a few categories, described below.

Tire/Wheel Assemblies. The purpose of this research is to understand and characterize the force variations generated by a truck tire/wheel assembly when installed and rolling free on a moving vehicle. The force variations measured on the vehicle are products of not only the tire properties, but also of the pavement properties and vehicle dynamics. In order

to relate measurements from a test machine to any arbitrary vehicle/road/speed condition, it is best to conduct tests with a rigid flatbed surface and rigidly fixed spindle to ensure that the measured forces are generated only by the free-rolling tire/wheel assembly and are not forces deriving from movements of the test machine. Even when these ideal test conditions cannot be achieved, as is the case with the flat-bed machine, the force variations deriving from tire/wheel nonuniformities can be separated from other forces if they are independent (that is, if the other forces are not induced by the tire/wheel nonuniformities). The force variations caused by the tire/wheel assembly are recognizable as that portion of a force variation that is a deterministic (repeatable) function of the rotation angle of the assembly.

Flat-Bed-Related Forces. A second type of force variation that shows up in the test data is the force variation that is consistently a function of the flat-bed position. Since the flat-bed moves at the same speed test after test, this category also includes force variations that are consistently functions of time. By far, the most significant source of this type of force is the unevenness of the flat-bed. As the tire rolls over the flat-bed, a variation in the vertical force is produced that is proportional to the profile of the flat-bed. Although the flat-bed was shimmed to improve its "flatness," a certain amount of unevenness remains in the vertical direction which causes a force variation. Also, any dynamic deflections which repeat from test to test will appear as a force that is a function of flat-bed position.

A further contribution to this type of force variation is due to the fact that the tire has visco-elastic properties. When the tire is lowered to the flat-bed, such that the spindle reaches a certain height and remains there, the vertical load will rise quickly, then more slowly reach a peak value, and then asymptotically decrease to a lower value. In effect, this is equivalent to the common observation that a non-rolling tire, when loaded, develops a "flat spot." As the flat spot forms, the load gradually decreases. The operator attempts to minimize this effect by lowering the tire to the proper (predetermined) spindle height and starting the test as soon as the

vertical load is within 100 lbs of the desired load. Once the test is complete, the tire is raised to reduce the possibility of forming a flat spot at the end of the test. It is conceivable that during the test some type of repeatable relaxation of the tire occurs, which manifests as a trend in the vertical force history that repeats from test to test and is therefore indistinguishable from the effects of flat-bed unevenness.

Another possible source of consistently repeating force variations is in the response of the servo-controlled hydraulic loading system, which may tend to continue loading the tire during the test duration.

Regardless of the physical mechanisms involved, there is a force variation underlying all of the tests of a tire/wheel assembly that is synchronized with the flat-bed position and adds to the force variation that is a function of wheel angle. Since the force and moment measurements are ultimately reduced to a series of harmonics, each being a vector defined by an amplitude and phase, it is useful now to consider the two sources of force variation for one harmonic. Figure C.2 illustrates how the two components add as vectors to yield the actual measured harmonic vector. Clearly, the measured amplitude depends on the phase angle between the tire/wheel rotation vector and the flat-bed displacement vector. This phase angle is defined by the rotation angle of the tire/wheel assembly when it is lowered to the flat-bed prior to each test.

Figure C.3 illustrates a way by which the influence of the flat-bed-dependent forces can be eliminated from the results. By repeating the test over and over while incrementing the initial rotation angle of the tire/wheel assembly, harmonic values referenced to the tire/wheel assembly will be obtained as shown. When a vector average of the measured harmonics is taken for all of the tests, the flat-bed influence averages away. Figure C.4 also illustrates this averaging process by showing measured vertical force variations for four initial wheel angles when synchronized to the wheel rotation. Each of the records was "wrapped around" on the computer to begin at the same wheel angle, even though the new measurements actually began at the flat-bed position and thus different wheel angles. The raw measurement usually finished at a different force level than when it began, resulting in the discontinuities seen in the figure.

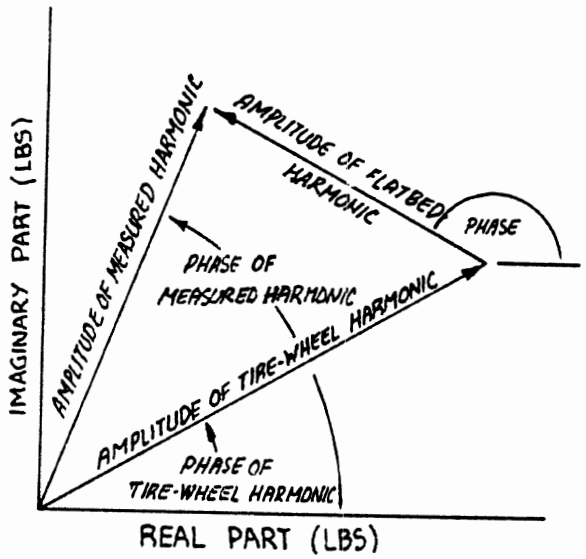

Figure C.2. Vector Addition for One Harmonic of the Tire/Wheel Nonuniformity and Flat-Bed-Related Nonuniformity.

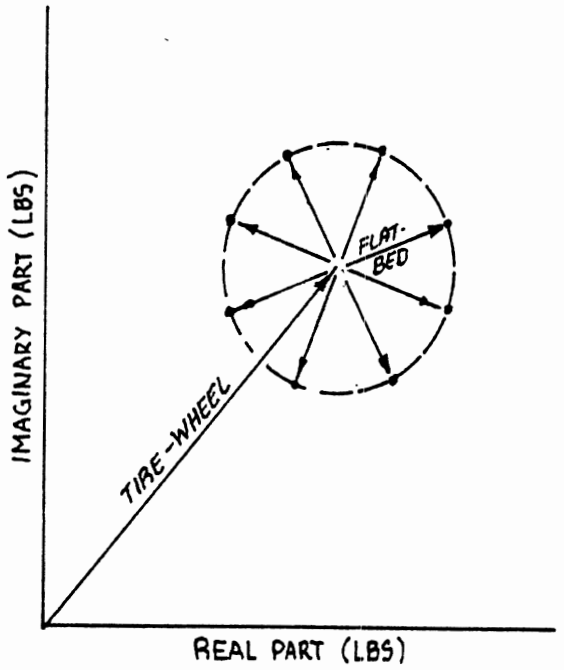

Figure C.3. Cancellation of Flat-Bed Influence for One Harmonic by Repeating Tests with Incremented Initial Angular Position of Wheel.

Since the first 10 tire/wheel harmonics are of interest, each of the first 10 flat-bed-dependent harmonics must be cancelled. This requires a minimum of 20 tests, with the angle between wheel and flat-bed changed by 1/20th of a revolution between each test. To be safe, 24 tests were run at 15-degree increments. For the second harmonic, these would be increments of 30 degrees, for the third harmonic, increments of 45 degrees, and so on up to the twelfth harmonic, when there would be 12 runs at 0 degree and 12 at 180 degrees.

If the 24 vector measurements are not rotated to maintain a constant phase with the wheel rotation (i.e., "wrapped around"), but instead are left relative to flat-bed positon, the vector average will yield the underlying flat-bed effect. Figure C.5 shows the vertical force variations obtained by this process for five tires. The variation is seen to be fairly consistent from tire to tire, although differences do and should exist because the spindle force depends on both flat-bed profile and tire spring rate, as well as the tire circumference.

Random Noise. Not all of the measurement signals can be described by consistent functions of wheel angle or flat-bed position. Other components of the force signals are produced by machine vibrations, "glitches" in the servo-response, or plain electronic noise. In terms of the measured harmonics, a vector is added with an amplitude roughly dependent on the magnitudes of all the individual sources and a phase angle that is completely random relative to wheel angle and flat-bed position. Because the phase angle is random, the contribution of the random sources can be eliminated by ensemble averaging. Since each tire/wheel combination is already tested 24 times in order to distinguish the wheel effects from the flat-bed effects, the random noise contribution is consequently reduced by the averaging process.

Figure C.6 shows actual test measurements (open symbols) for the first harmonic vector. (Only eight of the 24 tests are shown to simplify the illustration.) Note the underlying circular shape, as expected from the additive effects of tire/wheel nonuniformity and flat-bed nonuniformity (as in Figure C.3). The figure also shows calculated points (closed symbols)

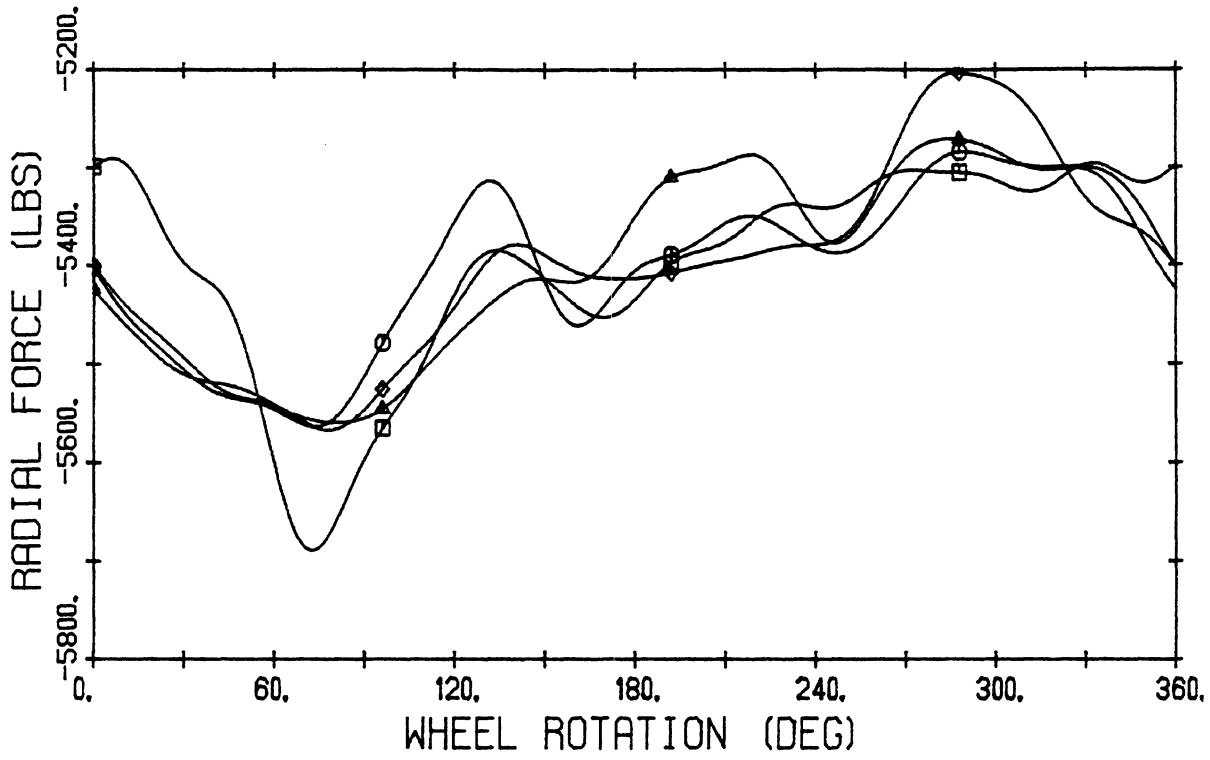

Figure C.4. Radial Force Variations Referenced to Wheel Angular Position.

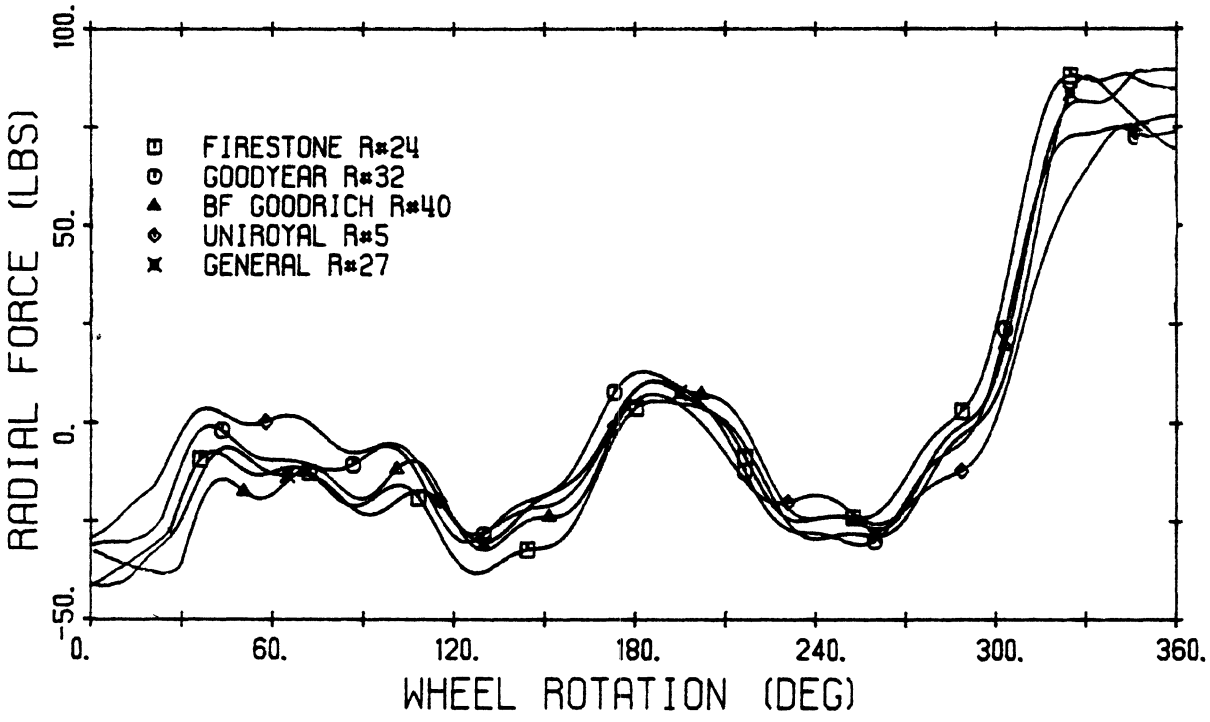

Figure C.5. Flat-Bed Effects that are Removed from Measured Force Variations.

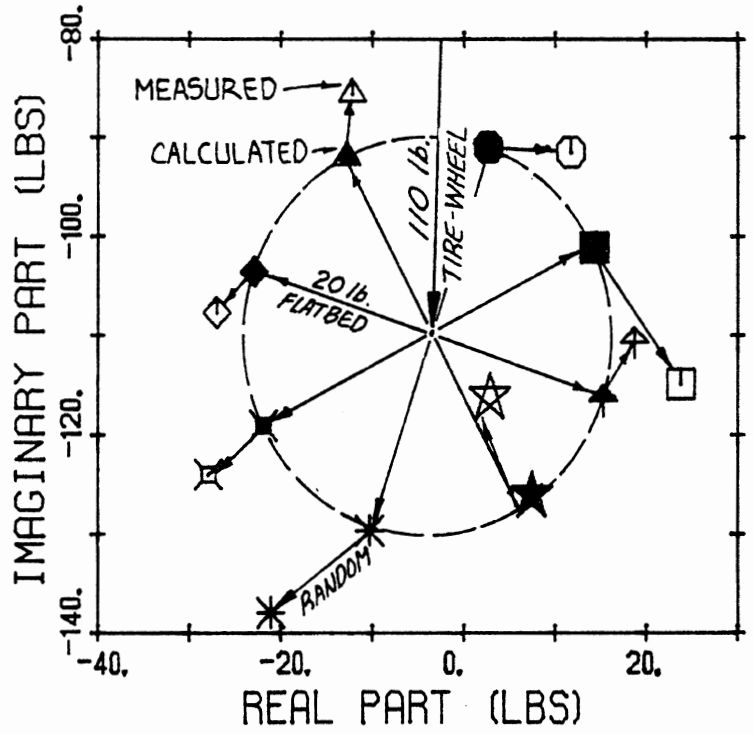

Figure C.6. Eight Individual Measures of the First Radial Force Harmonic. Initial Wheel Angle was Incremented 45° between Tests.

that represent the sums of the average tire/wheel vector and the average flat-bed vector, using the appropriate phase relationship for each test. The differences between these points and the individual measures are the random noise vectors present during each test.

Figure C.7 shows data from the same tests for the second harmonic. Because two periods are present in one revolution, we see two sets of four points spaced about the circle, rather than one set of eight as with the first harmonic.

Wheel and Rim Nonuniformity. Because the tire and wheel rotate together, the force variation that is dependent on the rotation angle is due to both components acting together. But by re-mounting the tire at a different angle relative to the wheel, it becomes possible to separate the effects of each source if they simply add. If the tire is rotated 180 degrees on the rim and the measured harmonic vectors are averaged, either the tire or wheel component will cancel, depending on whether the harmonic phase is referenced to the wheel or the tire. The second harmonic, however, would be shifted 360 degrees and thus no cancellation would occur. In order to effectively separate the tire nonuniformity from the wheel non-uniformity for the first 10 harmonics, at least 20 setups are required. Unfortunately, this involves an unreasonable level of effort in terms of numbers of tests when each setup is tested 20 or more times to eliminate flat-bed effects.

In this project, each tire was mounted three times, varying the mount angle relative to the wheel by increments of 120 degrees. For the second harmonic, these increments are 240 degrees (-120 degrees). Figure C.8 shows the results that should be expected for the first two harmonics when they are plotted as vectors—an equilateral triangle (or three points equally spaced on a circle). When the three measurements have phase angles relative to the tire, the actual tire-only harmonic is the center of this locus. Alternatively, if the phase angles are adjusted such that they reference the wheel angle, the tire effects would average away and the center of the locus would be a wheel-only harmonic.

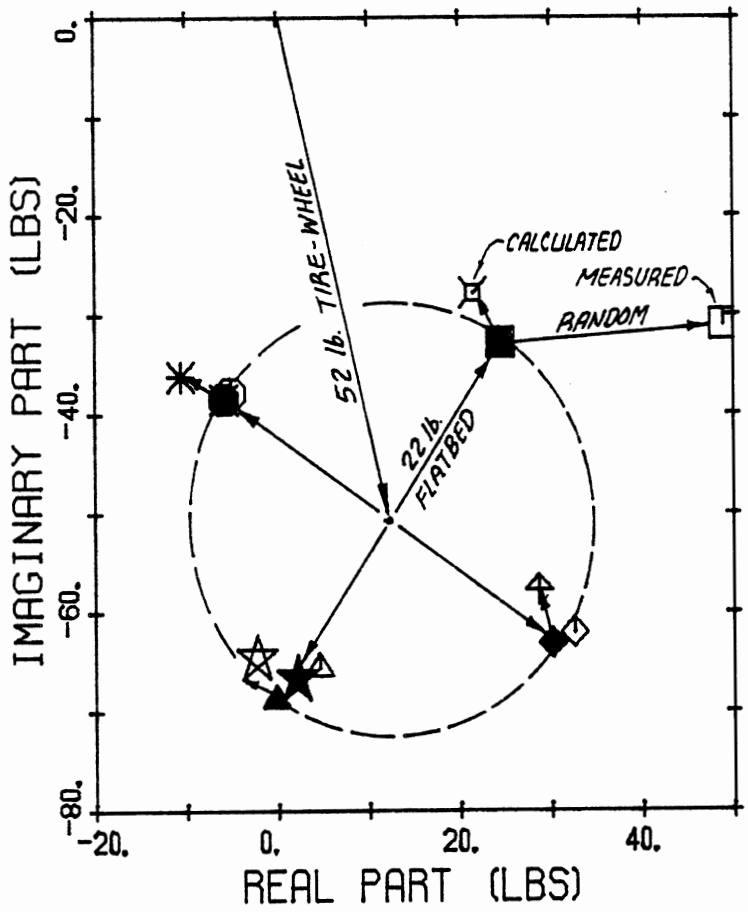

Figure C.7. Eight Measures of the Second Radial Force Harmonic Under the Same Conditions as in Figure C.6.

Mounting Effects. One further mechanism exists which confounds the harmonic measurements—the validity in mounting the tire on the precision rim. Ideally, the tire bead would seat perfectly and uniformly every time, but in actuality, some variation occurs. The irregular seating also adds a component to the force variations which is random in that the phase angles of the harmonics are not related to anything. Once the tire is mounted, this component becomes a consistent contributor to the overall tire/wheel nonuniformity.

Figure C.9 shows the tire mounting effects in the first harmonic for one series of tire tests. The figure represents the results for 24 tests at each of three tire positions on the precision wheel. By averaging all of the 24 tests, first referenced to the tire and then to the wheel, the first harmonic for each is determined. By this process, the flat-bed contributions and the test-to-test random errors have been averaged out of the data shown. For the tire and wheel harmonics thus determined, a calculated value for the 24-test average is obtained (closed symbol). Yet, the average for the measured values (open symbols) do not coincide but reflect an effect on the first harmonic attributable to mounting variations.

Ideally, the tire-only contributions would be much larger than the wheel-only and mounting contributions, but the figure shows that this is not so. As a result, the reliability of the tire-only harmonic is only on the order of 20 lbs. This can be improved by re-mounting the tire a greater number of times so that the mounting irregularities are averaged away.

Figure C.10 shows the same type of data as Figure C.9, but for the second harmonic. In this case, the tire-only harmonic is much larger than the other factors and thus a good measure is obtained with just these three setups.

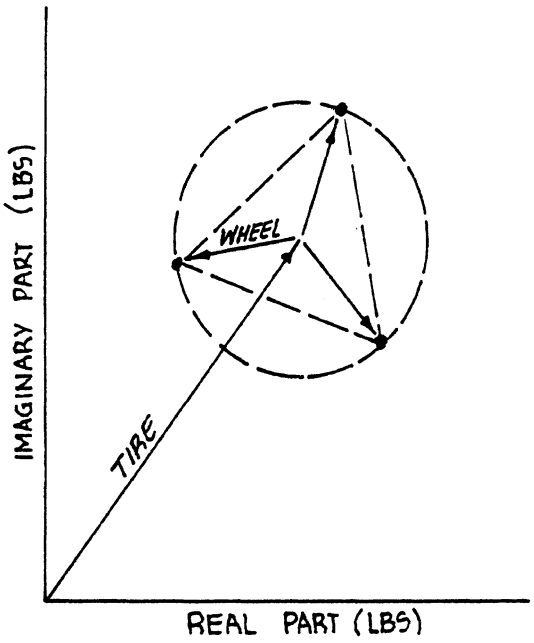

Figure C.8. Vector Addition of Tire and Wheel Nonuniformity at One Harmonic, for Different Angles between Tire and Wheel.

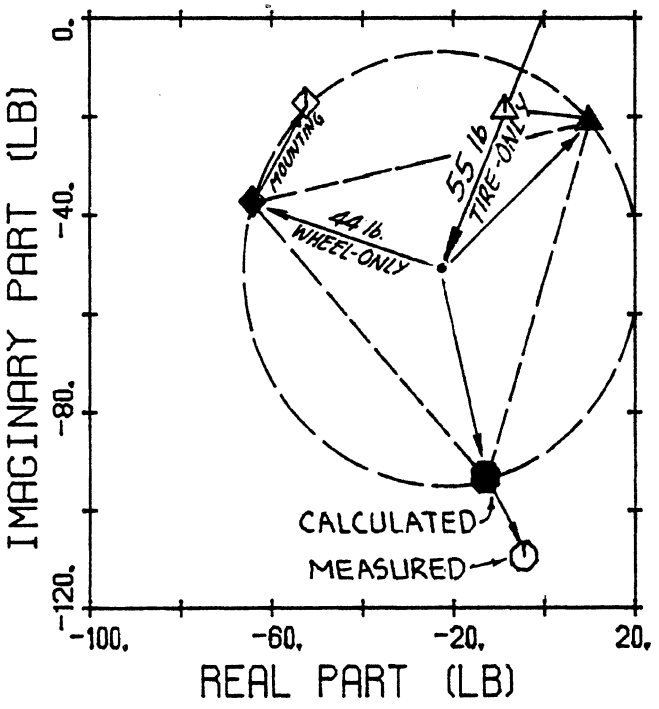

Figure C.9. Measures of the First Radial Force Harmonic for Three Sets of Tests with the Angle between Tire and Wheel Incremented between Sets.

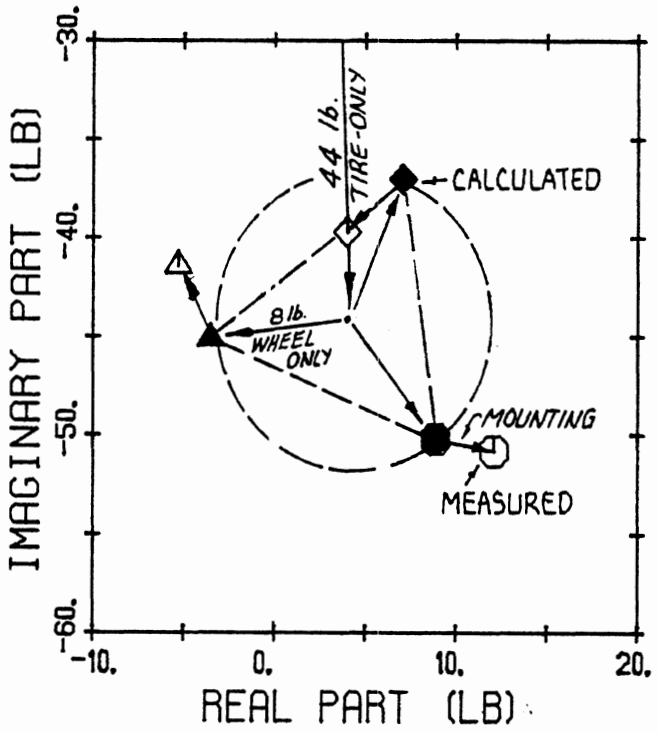

Figure C.10. Measures of the Second Radial Force Harmonic for the Same Three Sets of Tests Used in Figure C.9.

Test Method

Given that a single run on the flat-bed machine yields a measure of force variation caused by the tire, wheel, mounting variations, flat-bed profile, and non-repeatable causes, the tire-only nonuniformity can be gleaned only by correcting for all of the other sources. After taking all measurable steps to minimize these sources, the variations remain large enough that a single test is inadequate to provide an acceptable estimate of the tire-only nonuniformity. The effects are therefore taken out by conducting a number of tests and averaging the measurements.

The non-repeatable random variation is taken out by averaging a number of tests. The flat-bed influence is taken out by repeating the test while varying the relationship between the tire/wheel assembly and the flat-bed surface. Mounting effects are eliminated by re-mounting the tire a number of times during the testing of a tire, and wheel effects are eliminated by changing the angular relationship between tire and wheel when re-mounting the tire.

A single test sequence goes as follows:

1. Rotate wheel to have proper initial angle,
2. lower the wheel onto flat-bed surface,
3. when load is within 100 lbs of test load start flat-bed motion,
4. when flat-bed stops lift wheel,
5. return flat-bed, and
6. type information into the data acquisition computer.

This sequence typically takes less than one minute to execute. Twenty-four tests were conducted for each tire/wheel/mounting setup, allowing the confident removal of force variations due to the flat-bed unevenness and to random noise. Re-mounting the tire, on the other hand, was a more tedious exercise, usually taking one or two hours. The first test data indicated that the wheel and mounting effects contributed little above the first

harmonic, and since the purpose of the research was to validate drum measurements of the higher harmonics, a large number of mounting conditions did not seem justified. All-in-all, each tire was tested 72 times at three angular positions relative to the wheel (120 degrees apart), and at 24 initial angles relative to the flat-bed (15 degrees apart).

Test Results

Ten 11-22.5 tubeless truck tires were tested, provided by five manufacturers. Each manufacturer was represented by one radial and one bias-ply tire. The bias-ply tire test conditions were 4615 lbs at 85 psi, while the radials were 5134 lbs and 105 psi. Figure C.11 summarizes the range of radial force amplitudes found for the first 10 harmonics of all of the tires. (Note that all amplitude values are single-sided, full-scale values. RMS values can be calculated by multiplying these figures by 0.707.) Figures C.12 and C.13 also show the radial force amplitudes as a signature for each tire. These figures show the first-harmonic amplitudes varying from about 15-150 lbs, with amplitude universally decreasing with the order of the harmonic to about .05-0.5 lb at the tenth harmonic. The figures also show little, if any, correlation between amplitudes at different harmonics for any single tire. That is, the magnitude of the first harmonic does not aid in predicting the magnitudes of any of the higher harmonics. As a group, the radial-belted tires seem to have more of their nonuniformities concentrated in the lower harmonics, with smaller amplitudes at the higher harmonics, as compared to the bias-ply tires.

Besides measuring the radial force variations, the lateral force, longitudinal force, and aligning moment were also measured. The harmonics for these forces and moment were typically very small relative to the radial force harmonics. In the case of the lateral force, this may be due to the machine and not a characteristic of the tires. The flat-bed is moved over rollers, which allow a certain amount of free-play in the lateral direction. Hence, the low lateral force amplitudes may be due to induced motion of the bed, even though lateral nonuniformities might be present in the tires.

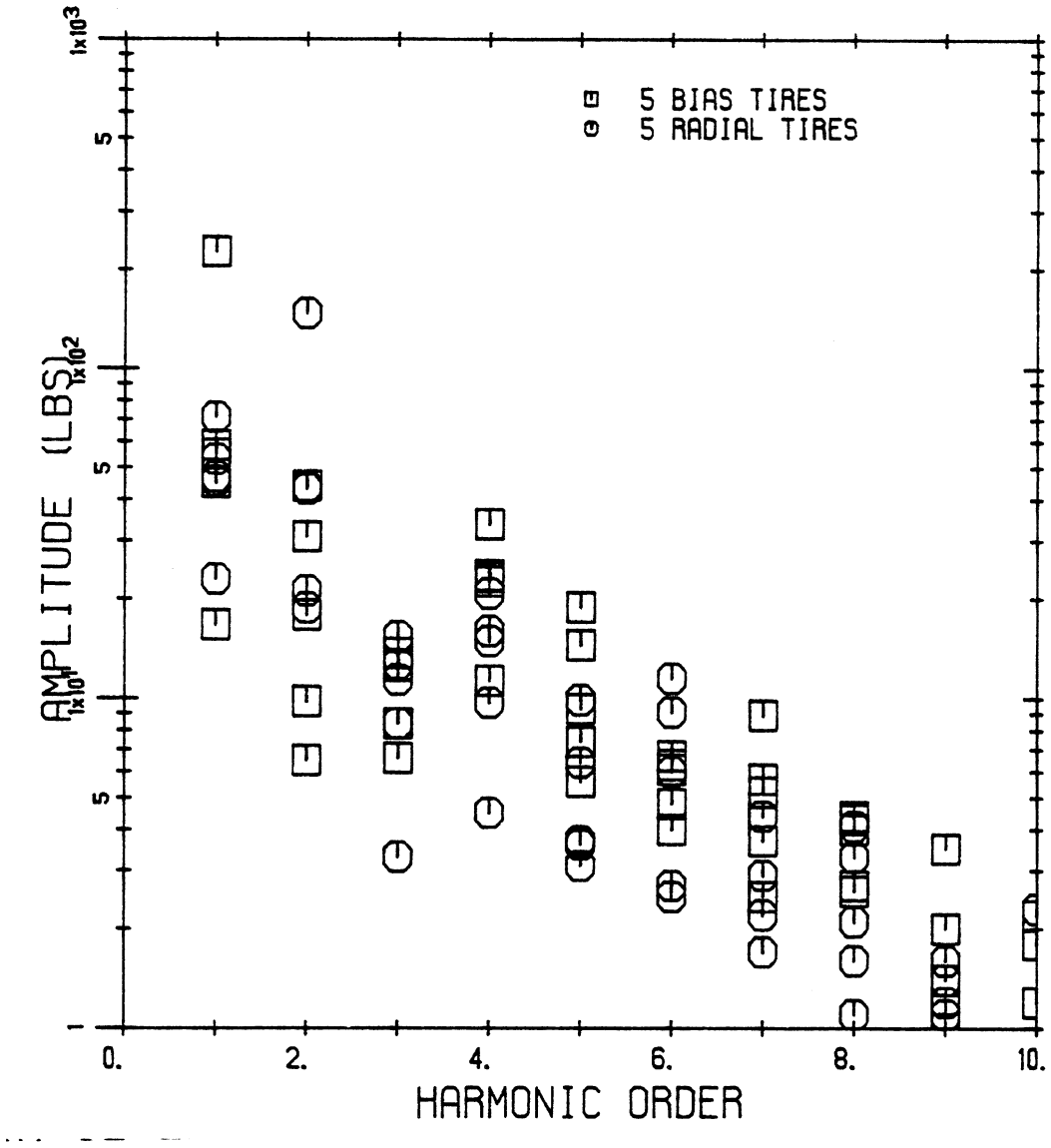

Figure C.11. Summary of the Radial Force Harmonic Amplitudes Measured for Ten Tires.

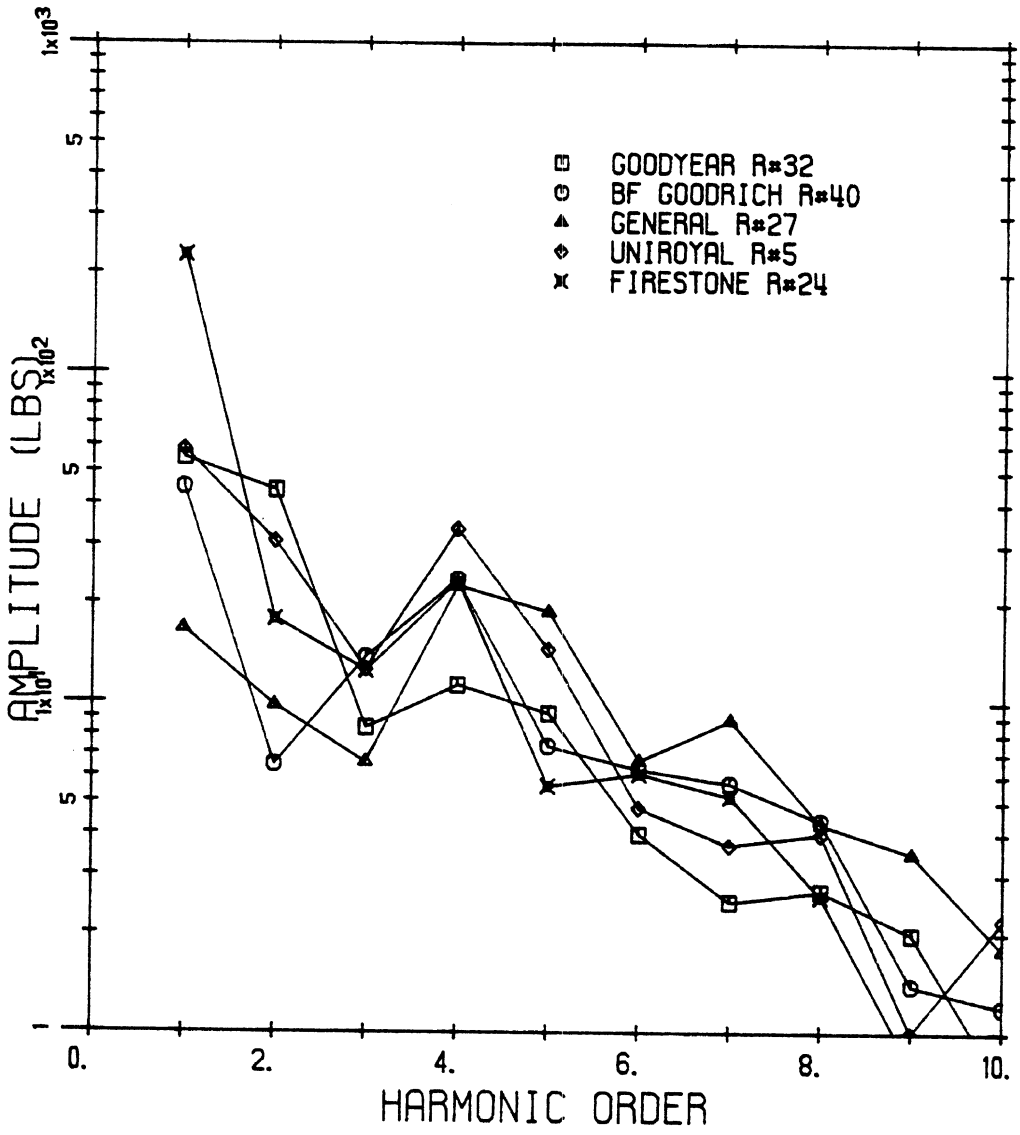

Figure C.12. Summary of the Radial Force Harmonics for Five Bias Tires.

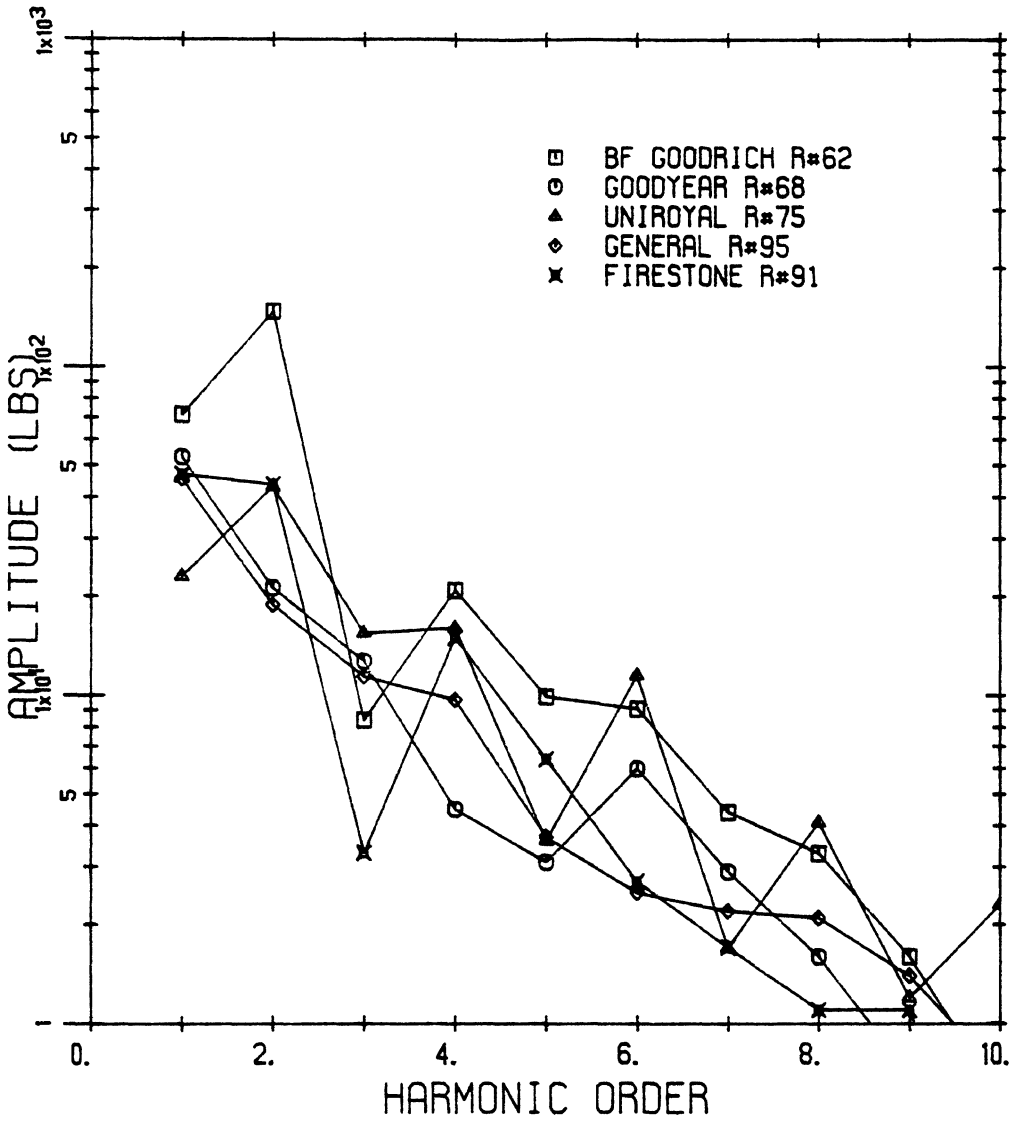

Figure C.13. Summary of the Radial Force Harmonics for Five Radial Tires.

The comparison of the radial force measurements on the flat-bed and the drum machines are shown for each harmonic in Figure C.14. Rather good agreement between the measurements is seen. The error magnitudes are generally the largest in the first harmonic. In part, this is due to the fact that the force variations are largest in the first harmonic. Contributing to this, however, is the fact that the flat-bed, which is designed for constant load testing, does not precisely hold a constant radius and thus measures a first harmonic force magnitude less than that seen by the "stiffer" drum machine. For the second and higher harmonics, good agreement is obtained. It should be noted that because the tire was mounted in only three positions, the wheel effects are not correctly eliminated from these data; consequently, the third, sixth, and ninth harmonics on the flat-bed are a combined tire and wheel force variation which should generally be larger than that of the tire alone measured on the drum machine. Indeed, the flat-bed measures tend to be higher in the third harmonic as would be expected. This is no longer true in the sixth and ninth harmonics because wheel nonuniformities above the fourth harmonic do not show through the tire. For the second through tenth harmonics, a line of equality would reasonably fit the test data within the range of experimental accuracy. Therefore, it is concluded that the measurement on a 67-inch drum is an accurate estimate of the radial force variations produced on a flat surface.

The comparison of results in other force directions are not meaningful, and thus are not given here. The tractive force variations are very small in magnitude, and are very dependent on speed (the same speeds were not used on the flat-bed and the drum machine). Similarly, the lateral force data on the flat-bed is very suspect due to the lateral clearance in the transport mechanism of the table.

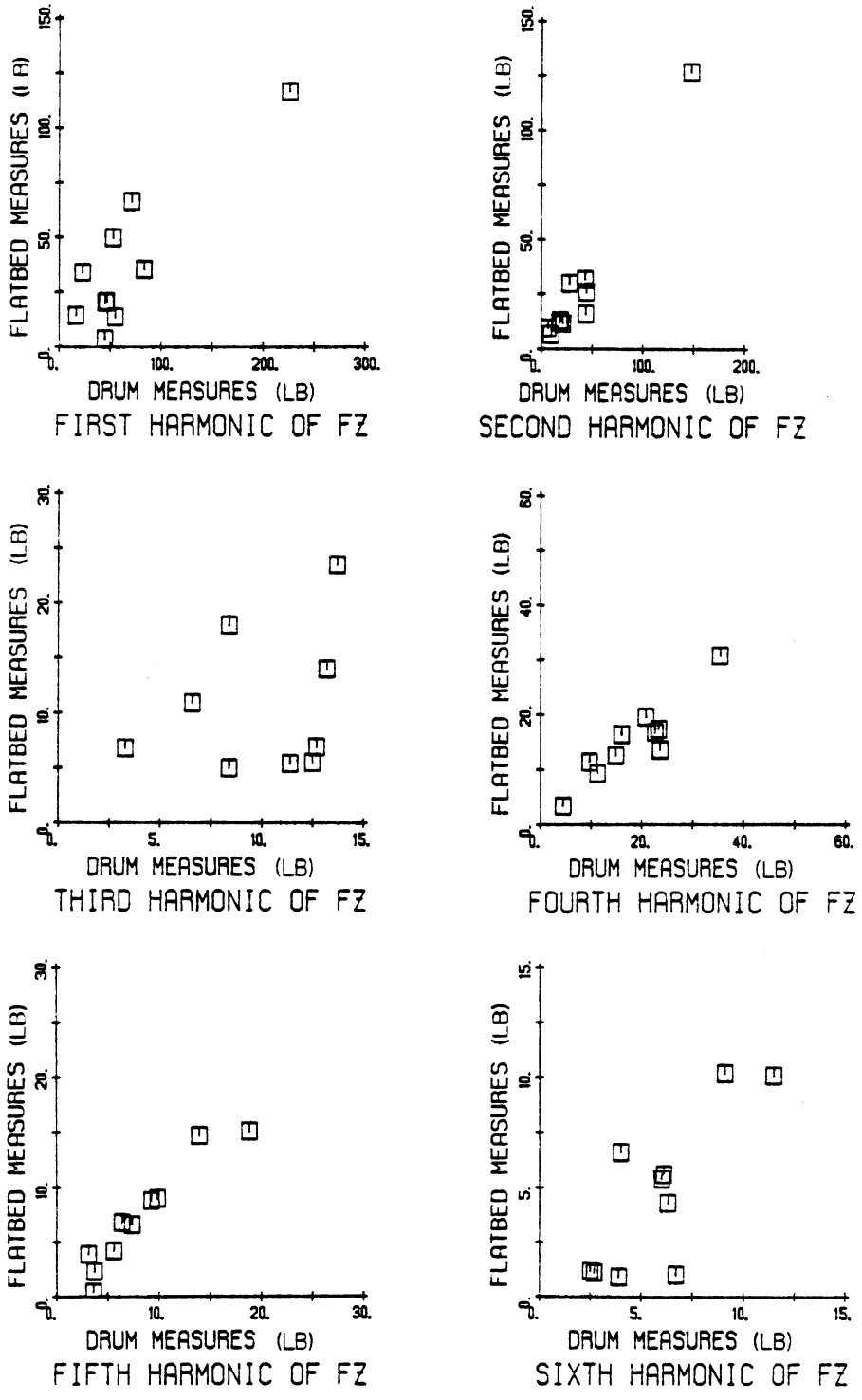

Figure C.14. Comparison of flat-bed and drum measurements of radial force variations.

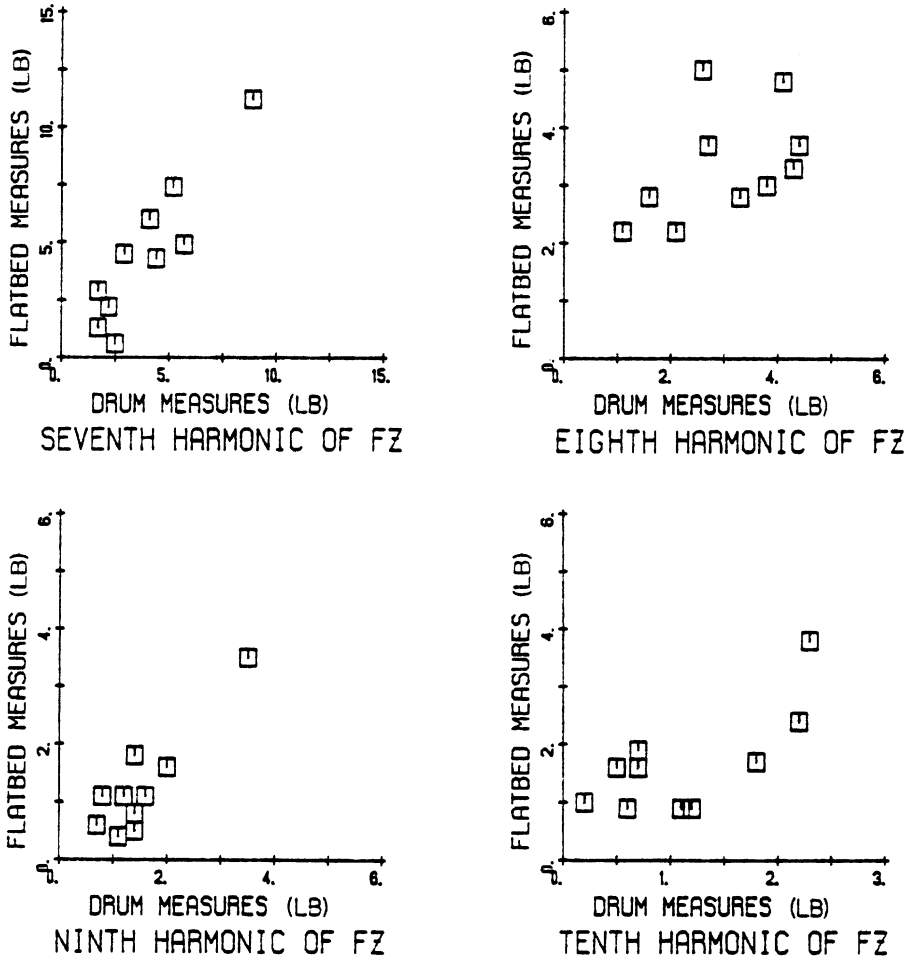

Figure C.14 (Cont.)

APPENDIX D - LIST OF 40 TIRES TESTED

RMA No.	Manufacturer	Tubeless	Tube Type	Bias	Radial	RMA Nonuniformity Category FFROC	RFV_C	RFV_1	LFV_C
40	BF Goodrich	X		X		Lo	Lo	Lo	Lo
56	Uniroyal	X			X	Lo	Lo	Lo	Lo
32	Goodyear	X		X		Lo	Hi	Lo	Lo
58	Goodyear	X			X	Lo	Hi	Lo	Lo
15	General	X		X		Lo	Hi	Hi	Lo
62	BF Goodrich	X			X	Lo	Hi	Hi	Lo
11	Goodyear	X		X		Hi	Lo	Lo	Lo
68	Goodyear	X			X	Hi	Lo	Lo	Lo
39	BF Goodrich	X		X		Hi	Hi	Lo	Lo
75	Uniroyal	X			X	Hi	Hi	Lo	Lo
5	Uniroyal	X		X		Hi	Hi	Hi	Lo
83	Firestone	X			X	Hi	Hi	Hi	Lo
23	Firestone	X		X		Lo	Lo	Lo	Hi
95	General	X			X	Lo	Lo	Lo	Hi
24	Firestone	X		X		Lo	Hi	Hi	Hi
92	BF Goodrich	X			X	Lo	Hi	Hi	Hi
91	Firestone	X			X	Hi	Lo	Lo	Hi
27	General	X		X		Hi	Hi	Hi	Hi
28	Uniroyal	X		X		Hi	Hi	Hi	Hi
85	General	X			X	Hi	Hi	Hi	Hi
1	Armstrong		X	X		Lo	Lo	Lo	Lo
4	BF Goodrich		X	X		Lo	Lo	Lo	Lo
52	Goodyear		X		X	Lo	Lo	Lo	Lo
56	BF Goodrich		X		X	Lo	Lo	Lo	Lo
6	General		X	X		Lo	Hi	Hi	Lo
60	Goodyear		X		X	Lo	Hi	Hi	Lo
15	Armstrong		X	X		Hi	Hi	Hi	Lo
17	Goodyear		X	X		Hi	Hi	Hi	Lo
65	General		X		X	Hi	Hi	Hi	Lo
67	Goodyear		X		X	Hi	Hi	Hi	Lo
18	General		X	X		Lo	Lo	Lo	Hi
20	Goodyear		X	X		Lo	Lo	Lo	Hi
71	BF Goodrich		X		X	Lo	Lo	Lo	Hi
72	Armstrong		X		X	Lo	Lo	Lo	Hi
23	General		X	X		Hi	Hi	Hi	Hi
24	Armstrong		X	X		Hi	Hi	Hi	Hi
74	General		X		X	Hi	Hi	Hi	Hi
75	Armstrong		X		X	Hi	Hi	Hi	Hi
11	BF Goodrich		X	X		Hi	Lo	Lo	Lo
61	BF Goodrich		X		X	Hi	Lo	Lo	Lo